X

# EARTHQUAKE HAZARD STUDIES IN SOUTHEAST MISSOURI

William Stauder, Robert B. Herrmann, Brian J. Mitchell

Saint Louis University
Department of Earth & Atmospheric Sciences
P.O. Box 8099, Laclede Station
Saint Louis, Missouri 63156

USGS CONTRACT NO. 14-08-0001-16708
Supported by the EARTHQUAKE HAZARDS REDUCTION PROGRAM

OPEN-FILE NO. 81-888

EARTHQUAKE HAZARD REDUCTION IN SOUTHEAST MISSOURI

FINAL TECHNICAL REPORT

Contract 14-08-0001-16708

31 January 1981

## 1. Functional Subjects

This research has as its purpose the study of the earthquake hazard in the New Madrid Seismic Zone, and the development of improved ground motion prediction in the midcontinent United States.

The research related to the first of these goals involves the monitoring of the seismicity of the New Madrid Seismic Zone using the data of a sixteen station seismic network. Earthquake hypocenters are routinely determined and published, and research is conducted into the seismicity and focal processes in the region.

In relation to the second goal the research involves source and attenuation/wave propagation studies, and investigations related to the basic understanding of the causes of earthquakes in the midcontinent, and how these may be related to tectonic features.

The functional subjects discussed in Section 2 are

a) the seismic network,

b) the Sharpsburg, Kentucky earthquake of July 27, 1980,

c) the Ridgely Well air gun experiment,

d) program BEAM4 for earthquake location and apparent velocity using curved wave fronts,

e) The Denver earthquakes of 1967-1968.

Section 3 presents a list of publication produced under this contract as well as a general overview of the accomplishments and future research directions.

## 2. Discussion of work performed

### 2a. The Seismic Network

The 16 station USGS regional seismic network in the Mississippi embayment was installed in 1974. Since that time, the original network has been augmented by stations supported by the NRC and by stations installed by TEIC. In addition, a USGS contract was awarded to increase the density of the stations in the zone of dense seismicity. The result has been an improved detection capability.

Another, important, event in the history of the network has been the installation of two USGS minicomputers to aid the analysis of seismic data. Today, much of the routine location of earthquakes is done interactively with the computer. Besides this, a data base of historical earthquakes and regional seismic network earthquake locations has been constructed for easy retrieval. Computer programs for joint-hypocenter location, graphic display of seismic data, and automatic bulletin preparation have been written and are in use. The level of seismic research has been raised because of the computer system and the development and routine use of new analysis techniques is an actuality.

The following section describes the technical aspects of the seismic network.

# A Progress Report: The New Madrid Seismic Telemetry Network

A review of seismic network operations, problems, solutions, and new developments for the period September 1977 through December 1980

by

Sean-Thomas Morrissey
Saint Louis University

## I. Introduction

This report is intended to be a compact review of the current "state of the art" of operating a seismic telemetry network as applied to the New Madrid area, and incidentally, to the Adak, Alaska network because of the author's position as technical director of that network under a joint agreement with CIRES of the University of Colorado. The experiences and opinions expressed herein are necessarily those of the author and as such are limited to his acquaintance with the matter, and should not be construed to contradict or diminish the efforts of others operating telemetry networks under considerably different circumstances.

In the last three years, two main tasks have been undertaken in the New Madrid seismic network operation, namely to improve the station reliability and longevity such that every station should operate for 24-30 months without servicing, and to improve the station density in the research area such that the original station spacing of 40 km is reduced to 10 to 15 km in the areas of more intense earthquake activity. This latter task has included the development and construction of new instrumentation packages that hopefully incorporate the best features of the old units and all the new insights and ideas that have matured over the last six or seven years. Hence it has taken longer than expected, and only half of the new stations are installed. A major reason for the

delay has been the inability to find qualified technical personnel for the field program. We expect to complete the station installation this summer.

The question of station longevity relates heavily to the quality of the data base available for event detection and location. But with a shortage of personnel, we simply cannot be visiting every station several times a year, or even once a year. In fact, most station visits are because of some major failure (lightning, etc.), at which time battery replacement is done if the batteries will not last another six months. A station status chart is maintained on all the physical parameters of each station, such as expected battery depletion. Generally, batteries are replaced before they die, and field trip itineraries are optimized, using information from the status chart, to try to provide service to stations nearing battery depletion. In the Aleutians, this is not possible because of the limited helicopter availability; all the batteries are always replaced, since in some years the stations will have to go without service because of a lack of helicopter support, such as in 1978, and most likely in 1981.

A note is in order on the data acquisition equipment at the seismic data center. Since this equipment is accessible on a daily basis, malfunctions can generally be readily detected and corrected. Nonetheless, even there we are generally uncompromising in designing reliability into the equipment, since the number of major seismic events from New Madrid is rather limited, and a series of significant failures at such a time can compromise what science can be done with the data. (First motion determination of focal mechanisms, for example, require all the data we

can get.)

In the following report sections we will first review the network operations and discuss the various reasons for failures, and then, in section III, review the strengths and weaknesses of each element of the networks and all the new developments pertaining to each.

## II. Summary of network operations

Figure 1 is a table summarizing network performance for the period October 1977 through December 1980 by quarters. The figure is self-explanatory. It should be observed that while some periods had a minimum number of outages, the outage days figure was still high. This is because of the logistics involved. For example, if station CRU (in SW Kentucky) fails in December, it is unlikely to be repaired until March as long as the stations on both sides of it continue to operate. A winter field trip to repair a single station is not practical with limited manpower, nor is it economical.

A review of the various reasons for station outages follows.

1. Battery depletion. As mentioned above, we try to anticipate this with the station status chart, but are not always successful because of the logistics or other unknowns. For example, a lightning damaged radio may draw 5 times its rated current for a month before it is repaired, thereby stealing 4 months of operation from the projected power budget of the batteries. (The converse is also true: blown fuses extend battery life.) The mercury batteries of the electronics package are similarly affected by shorted IC's,

etc., but are generally replaced whenever the buried unit is dug up. We have also had occasion for a single cell of the 3 cell RM23312 units to short internally, or cells of the newer RM42R pack to fail very prematurely.

A weakness of the air cells encountered in the old battery vault housings was wind-blown rain soaking the fibre filters for the carbon electrode air intakes, thus cutting off air and killing the battery until they dried out. At Adak, the barrels formerly used over the batteries would freeze into the tundra, and had to be provided with air vents. Another problem was rodents building nests on the carbons, and sealing off the air supply with mud and/or defecation. The new station housings have eliminated these problems. Now we have ants!

2. Lightning. We have made notable gains in the war against lightning by providing voltage transient protection wherever feasible. However, a direct lightning strike can still do considerable damage, although it is now generally limited to the output transistor of the transmitters. We have had lightning puncture the ABS pipe of the buried unit (leading to water leakage and subsequent drowning) that have done little more than blow all the fuses and the transmitter transistor (the RF cable cannot be protected with very low voltage semiconductor "transorbs" because they rectify the RF). Lightning losses have been reduced to about 6 per year, from a previous level of over 15 per year. Further details are discussed later.

3. Rodents. Our battery vaults provide a tempting haven for field mice and other rodents and critters (like wasps), and the mice chew on everything available, even shorting main battery cables and frying themselves. Ordinary poison set out usually rots before it is found, so we have learned to make "cupcakes" by pouring paraffin over strychnine-laced peanuts in cupcake cups. These keep indefinitely, and the little rascals eventually chew into a fatal morsel. The new Hardigg enclosures are rodent proof, but provide a dry, safe haven for ants, who nest in the styrofoam insulation. Tight sealing of the cable holes remedies this, ... usually.

4. Radio failures. The Motorola radio links we are using are very old (early 1960's vintage) and subject to the inevitable breakdowns of material things. The most common transmitter failure has been deterioration of the deviation control. In both transmitters and receivers, cracking open of the small but critical capacitors has been an expensive problem to keep up with. (Only a professional shop can diagnose such failures.) The newer Monitron radios are generally more reliable, but cost considerably more. We have take to thermal shocking all the radio equipment to try to induce failures in the lab rather than in the field. Humidity proof enclosures for the radios have been particularly beneficial. See below.

5. Field fires. A number of stations are in agricultural areas where they harvest the winter wheat in June and torch the straw to make way for a second planting of beans. This has generally only caused singed cables, since the fires are rather quick. However, the sta-

tion ECD was totally destroyed (all but the buried unit, which is still functional) by a particularly intense fire that even burned up the air cells with their gallon of liquid caustic inside. We have negotiated with the farmer to keep the brush cleared away from the new station equipment (and not start the fire by throwing gas on the station) for a small annual consideration.

6. Other outage causes. You name it, and it's happened. We've had gravel pits excavate around a station site (NKT), vandalism only once (WCK), the usual phone line problems with the local companies who fail to understand the idea of <u>continuous</u> service, and meteorological problems. The latter range from thermal inversions in the embayment, which cause the VHF signal to refract out over the top of the receive sites, to glare ice covering the antennas in winter and disabling most of the network for several days. We even had one station go dead (POW) with either a bad connection or a stuck seismometer, and were able to get it fixed by having a local resident drop a large boulder on top of the sensor package.

III. A technical discussion of the performance of the seismic telemetry instrumentation in use, with recommendations for improvements and descriptions of new instrumental developments. This is a review, item by item, of every item in the signal path from the ground to the recording system specifically applied to the USGS-like equipment installed in New Madrid and at Adak, Alaska.

1. The seismometer. The Mark Products L4-C 1 hz seismometer is the standard sensor device. Its advantages are compact size and

moderate cost; its disadvantages are severe suspension resonances around 16 hz, period instability with aging, and inability to be repaired locally. Many of the units purchased in 1974 are suffering from suspensions sagging, resulting in an asymmetrical shorter period or a dead seismometer. In a pinch (at Adak) we have tilted the seismometer case as much as $10^{o}$ from vertical to allow the mass to rise up toward center and establish a normal 1.0 second period. There is currently a program underway in California to recycle the seismometers through Mark Products for readjustment and recalibration; we may try to get in on it. Even if this is not done, the S & T resistors should be redetermined (according to J. Eaton's method). These resistors set the damping to 0.8 of critical and standardize the output to 1 v/cm/sec. We have acquired battery-powered equipment so that we can now do this in the field once a program of general recalibration of the network gets underway.

For areas where 1 hz data is not required, we have found that 4.5 hz geophones (GSC11D, for example) work quite satisfactorily, and cost about 3% of what an L4-C does.

2. The seismic pre-amplifier. In the original USGS amplifier unit, both amplifiers operate at maximum gain (46 db) with an attenuator between them to set the seismic signal level. This has a drawback in that all of the input noise of the second amplifier is present in the output, and the thermally induced DC instabilities of operating at high gains cause the amplifiers to drift such that unnecessary clipping occurs as the signal approaches one of the power supply levels.

A remedy to this situation is to set the gains of each amplifier to the minimum required for proper modulation of the VCO by the seismic signal at a given site. Such a plan was implemented in the new Pre-Amp card designed and produced for the expansion of the New Madrid network. Figure 2 is the schematic of this system. Note that the gains of both stages can be set by DIP switches. A sufficiently low gain is available for proper shake table calibration in the 1-10 micron range, while the highest gain (90 db) is more than adequate for any application. The amplifiers are followed by a unity gain, four pole phase-linear low pass filter with a cut off at 25 hz. The hi-pass filters, to prevent DC drift from getting into the VCO, are comprised of the very large DC blocking capacitors between the first and second amplifiers and between the output and the VCO. These cut off at about 20 seconds. Thus the amplifier is linear between 15 seconds and 20 hz.

The amplifier operates from $\pm$ 4.05 VDC at 80 $\mu$-amperes. At 60 db gain the output noise level is less than 1 mv P-P, or 0.3 mv RMS. At the maximum gain of 90 db the output noise level is about 5 mv RMS, but 90 db is not required unless a magnification of $5 \times 10^6$ at 10 hz is feasible.

More commonly a gain of 72 db, or about 500 K at 10 hz (from an L4-C) is utilized, where the average amplifier shows a typical noise level of 3 mv P-P. Since the maximum output is 6 v P-P, this would represent a dynamic range of 66 db. We have found that this can be significantly improved by selecting the first amplifier prior to installation of the station. We have found that about one

out of ten LM4250N amplifiers exhibit an order of magnitude less noise than others, so these are used as the first amplifier. Some of our stations operate at a measured signal to noise ratio of 78 to 84 db where this first amplifier has been carefully selected and the audio carrier is not subject to contamination by intermodulation garbage in the process of telemetering it to SLU, and where the new SLU discriminator is in use.

3. The voltage controlled oscillator (VCO). The normal USGS design for the VCO provided a low cost, low power system, but the necessary compromises resulted in a unit with considerable thermal instability, non-linearity, and output distortion. Others have attempted to solve these problems with units of considerable complexity (such as the frequency correction scheme in the VCO of the J402 unit of the USGS). However, simpler solutions can be realized. Dynamic temperature compensation can be provided by summing the seismic data with the output of a micro-theromometer before the VCO IC (the 4046). To provide a low distortion sine wave output, the VCO is run at 8 times the desired output frequency, and the resulting square wave signal is then converted to an 8 step sine wave by a second IC. The first harmonic is the ninth, which is readily attenuated by a low pass output filter incorporated in the input to the output amplifier/line driver.

Figure 3 is the schematic of the new VCO being installed in the new New Madrid stations. The micro-thermometer sensor is the pair of biased diodes mounted on the board, and the compensation level is set by adjusting the current through the transistor. Two advan-

tages of operating the 4046 VCO at 8x the output frequency are that a small 2% tolerance low temperature co-efficient silver-mica capacitor can be used, and that the device operates in a more linear range of its specifications. The 4018 device is a counter, here used in a four-step ring that is clocked from the VCO frequency. The first three outputs define 3 steps of half the sine wave, the fourth inverts the output for the second half of the sine wave in the next three clock cycles. The schematic shows an optional bandpass filter that has proved unnecessary. The configuration of the output stage is such that a true 600 ohm source impedance is provided to the output transformer, optimizing the coupling to the load. The VCO operates on ± 4.05 volts at the following currents depending on the load:

| output | 600 Ω load | 10K Ω load |
|---|---|---|
| 0 dbm | 740 µA | 740 µA |
| -6 dbm | 680 µA | 394 µA |
| -12 dbm | 430 µA | 320 µA* |
| -18 dbm | 300 µA | 250 µA |

(Data from 1020 hz unit.)
*(typical transmitter drive)

4. The calibrator system. The old USGS calibrator has a number of weaknesses (still present, in fact, in the J402 unit), the greatest of which is the use of reed relays in the signal path. We have had considerable problems with the relays failing, thus permanently disabling the station. A number of times the calibrator would lock into its cycle and calibrate itself to death, which takes about 18

hours to kill the relay batteries. For these reasons all the calibrators were removed from the Adak network, since there is no way to repair failed stations. The old calibrators also only provided a DC step calibration, which has been difficult to utilize for determining the station response characteristics since all the high frequency information is contained in the pulse rise time. Sine wave calibration would be much more useful.

A further requirement, now that the data is being digitally acquired, is to have the computer catch the calibrations. Since the triggering algorithm is based on the sub-net configurations, a critical number of stations must calibrate simultaneously for the trigger to trip. Hence it is desirable to be able to exactly set the time of calibration within a given sub-net.

With this in mind, a multi-mode sine wave calibrator has been designed and produced. Figure 4 is the schematic of the unit. The trigger for the calibrator is an inexpensive LCD alarm wristwatch. Since the watch can be set to exact time, and they are generally quite accurate, the alarm function can be used to set the time for the calibration cycle. The common "Omni" brand watches use an IC circuit very similar to National device MM5890. The crystal can be tuned to better than 2 ppm, or 1 minute/year by setting the LCD backplane frequency to exactly 32.000 hz (31.250 msec). The "beep" output to the piezoelectric transducer in the back of the watch is used as input to trigger the calibrator. The trigger resets the sequencer device U5 and starts the clocking oscillator. After a 20 second delay, a DC pulse is turned on for 10 seconds. After

another 20 second delay, two 10 second sine wave sequences are produced. Any two frequencies can be selected at 10 hz, 4 hz, 3 hz, 1 hz, 2 seconds, 10 seconds, and 20 seconds. The 20 step sine wave is digitally generated by devices U7 and U8, and filtered by U9. U10 inverts the signal for application to a bridge circuit for calibrating seismometers without calibration coils; the two phase signal is required because one side of the bridge is grounded at the amplifier input. Figure 5 is a section of a test record with the alarm watch hourly "chime" feature on, triggering the calibrator hourly. The unit operates from ± 4.05 volts, drawing +120 μA and -80 μA in standby mode, and 1.2 ma during the 70 second calibration cycle. The LCD alarm watch operates from -1.6 VDC at 3 microamperes; its battery power is supplemented by the voltage divider, diode limiter circuit providing output to the pin marked "watch battery."

5. Power supply. The original Amp/VCO cannisters are powered by four TR233R batteries, producing ± 4.05 volts at 4.4 ampere hours, or 500 micro-ampere years. Since the package usually draws about 250 μ-amperes, two year operation is typical. Lately these batteries have been difficult to obtain since Mallory is more interested in the consumer market (but the Eveready E133N is identical). For applications drawing more than 250 μ-amperes, such as the new Amp/VCO package, 6 of the RM42RT2 batteries are used, providing 14 ampere-hours or 1600 μ-ampere years, again providing 2 years of operation for the new packages. However, we have been finding that about 1 out of 10 of these batteries fails after several months of operation. The use of batteries still requires digging up the

Amp/VCO unit every two years or so.

Others have experimented with or are using "Lithium" type batteries. A problem with these is that the output voltage is a function of load and temperature, varying about 100 mV from -20 to +20°C, which, if unregulated, would cause problems for a VCO. However, the high energy density of the lithium cells could allow for the inefficiency of a regulator system. A D size battery has a rating of 10 AH, requiring a four cell series/parallel combination to power the new Amp/VCO package and allow for 20% loss in a regulator.

An alternative is to power the Amp/VCO system from the air cell batteries that operate the radio. These are rated at 1100 AH at 80% capacity, or 150 ma/years at full capacity. Since the radio transmitter draws only 60 ma, reserve power is available from a two year budget to provide about 10 ma to a power unit for the Amp/VCO. A problem then is providing a voltage reference as stable as a mercury cell. Such a device, the LM136AH, is available from National. It is rated at a stability of 0.1% over a temperature range of -25°C to 85°C, and a long term stability of 20 ppm.

A realization of the application of the device is shown in Figure 6. Power from the transmitter batteries is provided through a choke (to provide a high impedance to the audio output of the VCO, since the same line to the transmitter is used for both the DC supply and the audio output) to a DC-DC power converter isolator unit. The diodes, LED, etc. in series are to drop the voltage to only that which is necessary, thus considerably reducing the current

consumption of the system. The LM136 is configured according to specifications for best stability, and its 2.490 VDC output is simply amplified to provide +4.05 VDC, which in turn is inverted to provide -4.05 VDC. LM741 op-amps proved most efficient in this application, and can provide up to 10 ma of current if necessary. Quiescent current for the system at 13.3 VDC is 9 ma. Under load it is about 11 ma. R5 can be changed to provide other voltages.

This system is being used to power the tiltmeter digital meteorological sub-systems at Adak, and also to power a package of 6 amps and VCOs for telemetering the ADK main (WWSSN) seismic data. Where a seismic station is to drive a phone line drop directly (without the radio link), a pair of air cells housed in a buried, vented case at the telephone pedestal will operate the system for 4-5 years. The DC-DC converter only needs to be changed to a 5v to $\pm$12 v unit. We had considered using the Intersel device ICL7660, which is a DC power inverter (a synchronous switch), but decided against it because it is a C-MOS device, and thus electrically too fragile to place in the lightning path between the radio and the VCO. The DTD12-12.2.35 converter provides 300 volts of isolation, which, along with the VCO output transformer, significantly protects the Amp/VCO/calibrator system from moderate lightning damage.

6. Housing of Seis/Amp/VCO. Following the USGS fashion, we have had very satisfactory results using 4" ABS pipe for a "vault" for the seismometer and the AMP/VCO cannister. We use a longer vault than usual because our seismometers have a long cap (for the calibration coil connection), and because we include 10 units of desiccant in

the package. We seal the pipe with a bead of RTV sealer over the cap joint, wrapped with 3M 88 tape for mechanical strength. Even after 2 1/2 years of burial, most units show less than 20% humidity on the enclosed indicator card. Careful sealing of the cables is of course necessary. The only failures have been lightning puncturing holes in the 1/4" wall of the pipe, which generally only get detected when the poor thing floods and drowns.

With regard to the new Amp/VCO/calibrator/power converter system, we have provided a physical configuration that fits inside the old standard USGS aluminum cannister (2 5/8" ID x 12" l), thus making retro-fitting stations quite feasible. (Running the DC power input and the audio output over the same wires to the transmitter enclosure also obviates the need to run new cables.) The physical arrangement is depicted in Figure 7. Placing all the connectors in the center of a flat panel, with a ribbon cable to the bulkhead terminal strip, facilitates assembly. With this arrangement, any unit of the system can readily be replaced. We have installed the seismometer S & T resistors (damping and output level setting) inside the connector of each seismometer to assure that they stay with the seismometer. In the USGS units, they are mounted on the calibrator board, and have to be changed every time the unit is changed.

7. Air cells and surface vault. The functions and capability of the air cell batteries (Edison Carbonaire units) has been discussed above. Originally they were enclosed in oil drums, either simply fitted over them, or half buried with a chained-on lid. In the

original New Madrid stations, a section of 30" culvert was fitted with a wooden lid and half buried. Cables were run through holes in the culvert. Where there was a problem with the ground flooding, the culvert was elevated on cedar posts about 1 meter above the ground. This arrangement had a number of drawbacks, chiefly that the lid was loose fitting, and wind driven rain could wet the air filters of the batteries, choking them off and temporarily killing the cell. The other problem, mentioned above, was the invasion of rodents, wasps, and other critters.

A constructive solution has been to use linear polyethylene aircraft shipping containers manufactured by Hardigg Industries. The model we use, the AL3018-1505, is 18" wide, 20" high, and 30" long, adequate to house 6 air cells and an enclosed radio. At Adak, they are white with aircraft orange tops so we can find them. At New Madrid, they are a dull grey so that others won't find them. They should be equipped with stainless steel hardware (hinges and clasps), since the galvanized hardware rusts out in a few years. We generally bolt them to cedar posts, either at ground level or elevated as the flooding hazard might dictate. They are provided with a 2" diameter screened louvered vent for air for the batteries. The cable entries are sealed with RTV to keep ants, snakes, and wasps out. An identification sign is fastened to the box giving the station code and address of the observatory.

Perhaps we should mention here an evaluation we entertained of utilizing solar power for the stations (in New Madrid; at Adak, sun is a wonder of nature). A set of five air cells costs about $185-

$200, and will operate a station for 2 years with no problems. An adequate solar panel costs about $300, and needs about $200 in additional storage batteries and regulators. With the attractiveness of the panel to vandalism, failures of the gel-cells (deep discharge cycles, etc.), the solar system might last an average of five years, which makes it just break even with 2 1/2 sets of air cell batteries.

8. The radio transmitter. These are either the more-or-less standard 100 mw VHF narrowband FM transmitter by Motorola, as modified by the USGS, or the similar unit from the Monitron Corporation. The Motorola units have been re-mounted from walkie-talkie type units. We have added a DC power fuse and a neon surge suppressor to the RF output of each unit; these seem to minimize damage due to lightning. We have also had some random failures in the transmitters, mainly failures of the IDC (deviation) control potentiometer. Most of the failures seemed related to moisture or humidity, so we have been enclosing the radios in 2 quart plastic freezer boxes with 5-10 units of desiccant. The cables pass through notched holes in the side that are sealed with RTV, as is the lid before it is taped into place. We have had no radio failures since we began enclosing them in this manner. The humidity indicators read less than 10% for several years.

In the New Madrid network, we are pushing 100 km or so transmission distances over relatively unrelieved terrain, so optimum performance of the transmitters is required to minimize fading. Often a transmitter's tuning is peaked up at the site. Unfortunately with

VHF, adding or removing a 16 inch length of cable and an RF meter can change the tuning significantly, particularly if the random length of cable to the antenna just happens to come out an integral number of half wave lengths long. Our solution to this is to use cheap ($30.00) RF meters that read both power and SWR and install them permanently at the site in the (larger) freezer box with the transmitter. Thus what you see is what you have. The cheap meters are calibrated in the lab against a standard Bird VHF wattmeter. For a few very long paths with obstructions, we are using a 1 watt power booster made from a modified Heathkit model HA-201A VHF amplifer. This draws 300 ma at 5 volts, provided by four extra air cells at the site. For driving it at this level, only four air cells are needed for the Motorola transmitter. With these power amplifiers, the permanent installation of the VHF power/SWR meter is a must.

Another complication arose with the new network, in that only Monitron radios could be obtained. They are not directly compatible with the Motorola units, either electrically or performance wise. Electrically, the Motorolas are positive ground, the Monitrons are negative ground. The Motorola units have an output transformer (a very successful device for blocking moderate level lightning), whereas the Monitrons only have an op-amp for output. Our solution to these problems was to build an adapter in a 1" x 1" x 2" box that reversed the grounds (i.e. provided one; Monitron was able to provide our radios with a floating ground) and provided the transformer and fuse. The input to the adapter is the standard 5 pin USGS radio connector; thus Monitron units and Motorola units

could be used interchangeably as necessary to keep stations alive.

Except for one major detail: the Motorola response curve is that of a standard EIA pre-emphasis for FM transmission (De-emphasis of the high frequencies in the receiver reduces noise by about 20 db, so the high frequencies must be pre-emphasized in the transmitter). The Monitron transmitters utilized a "true-FM" response, so were incompatible with Motorola receivers and the receivers were 10 times noisier receiving from a Motorola transmitter. Only recently has Monitron been able to provide for pre- and de-emphasis performance in their radios, (actually, what is termed "phase modulation" in the transmitter). Thus their radio links will not only be compatible with the Motorola links, but will be about 20 db quieter. The only drawback is that the extreme ends of the audio response curve are not as flat as true FM would provide, but none-the-less quite acceptable. One additional note is that we have stayed with UHF type RF connectors, per the USGS style, mainly because they cost a lot less and are easy to assemble in the field. (Type N connectors are used by some.)

9. The antenna. The antenna of choice is the Scala CA5-150 5 element Yagi antenna. It is very rugged yet has good forward gain (9 db) and front-to-back ratio. The balun design is also quite reliable. The USGS provided a "Sigma" type antenna (the low bid) some years ago, but it was nearly worthless. Some prefer to use the multi-element Cush-Craft antennas; they have greater forward gain (but not much, because the elements--rigid wires--have low Q), and are easily damaged by wind and ice.

In New Madrid, height is of the essence in getting the signal through. So generally a sturdy oak, hickory, walnut or cypress tree is selected as the mast for the station. The antenna is fastened to a 21' long 1 7/8" galvanized heavywall tube (lighter pipe snaps off in the wind) (it is chain-link fence line post material) that is fastened to the tree with heavy duty Ω brackets and 3" lag bolts (not bands around the limbs). A bolt is put through the mast base itself to prevent rotation. The tree is usually lightly topped out so that the antenna is about 10' above the tree top; this has to be repeated about every other year; vines also have to be removed. An aluminum wire (#6) is run down the tree to a 6' copper weld ground rod.

In the original 1974 installations, we stapled the RF cable to the tree. With time the tree grows (of course) and the cable is pinched off under the staple. We have been replacing all the cables of the old net, and installing the new ones with galvanized insulated cable stand-offs that mount the RG8-AU cable about 2" from the tree. In some locations of the expanded network, where the transmission distance is not great and no trees are available, the 21' mast is mounted by itself (usually clamped to a leg of the Hardigg box) and guyed to deeply driven stakes with 1/8" stainless steel cable. At a few sites, fire look-out towers are used for the mast, and the antenna clamp U-bolts are replaced with 3/8" J-bolts that clamp a length of 1/4" chain around the tower leg. This latter method is used at all the receive sites, where the antennas are mounted either to the water tower railing (at SIK) or to the legs of the cable TV towers (PGA, NMMO, CRMO).

A few other important points we've learned the hard way. It is very important to tape over the connection of the UHF cable connector to the antenna. If not, water will eventually corrode the connection, or even seep down the cable braid into the radio itself. At Adak, there was a problem in anchoring guy wires in areas of hard surface rock. For the first several years, stakes were laid sideways and covered with boulders, but these would work loose in the wind. Since 1978, the cables have been anchored to stakes driven into holes drilled into the rock by a portable gasoline operated drill/jackhammer unit made in Germany, called the Atlas-Copco "Cobra." Again, stainless steel cable was used with crimped-sleeve connections. We've had no guy or antenna wire failures since then.

10. Receive site considerations. In New Madrid, height is the essence of a good receive site. With the growing proliferation of cable TV towers, these are abundant choices for the site. We usually arrange for the use or lease of 10' of tower space at about the 300' level of the tower. Access is also arranged to the "head-end" building at the tower base to house the power supply/multiplexer cabinet. The receivers are mounted in a NEMA enclosure up on the tower near the antennas, since long coaxial cables would be bulky and lose much of the signal (about 70% would be lost in 300'). The Scala antennas are provided with a 3' boom extension of 1" tubing to get them away from the tower legs so people can climb past them. The Scala clamp is used with J-bolts and chains to fasten the antennas to the tower legs. A 9-pair Belden individually shielded cable is run up to the receiver enclosure to provide DC power and

return the outputs of the 8 receivers to the multiplexer at the base.

This arrangement has been rather successful. The major drawback is that the receivers are 300' up on the tower, so on-site repairs or tests require climbing the tower with tools, test equipment (including the oscilloscope), and spare parts. The receivers can really only be properly fine tuned by using the incoming signal. We do not have enough spare receivers to allow pre-tuning one for each channel with the crystal frequency meter. We are investigating the feasibility of providing only a VHF pre-amp (40 db gain) in place of the receivers, and multiplexing all the outputs to a single VHF cable down the tower to provide input to all the receivers mounted in the head-in building. The plan is practical but costs money that is not available.

11. Receiver considerations. For the new stations, the compatability problem described above between Motorola and Monitron also applies to the receivers. Also, the Monitron units draw twice the current of the Motorola, mainly because of their internal voltage regulator, so several pairs of wires up the tower are allocated for DC power. Failures in the Motorola receivers have generally been in the audio output sections: the volume control opens up (humidity again) or the output transistors start oscillating (a bias problem with old germanium transistors). The squelch level is set by resistors soldered to the board, but we have increased its sensitivity on a number of the longer links. Of course, lightning striking the tower wrecks havoc where it wants, but it is now gen-

erally limited to blowing fuses (one still has to climb the tower to solder in a new fuse. Note that fuses are soldered in; fuse clips corrode and open up.) Other receiver failures have been in the very small capacitors used in the IF sections. We have even had two incidences of the crystal failing.

12. Multiplexer system. The receiver outputs are multiplexed together into a single phone line for transmission to St. Louis. We are currently redesigning the multiplexer for better phase linearity and more proper impedance matching to the phone line. The phone lines are usually driven at a level of -6 dbm (400 mv RMS), and come out at St. Louis at -20 dbm. Because of the phone line frequency response (unconditioned lines), we have found that pre-emphasizing the higher frequencies at the multiplexer by 1 db per IRIG channel either side of 1020 hz will usually result in relatively even output levels at the St. Louis end. This is particularly suitable to a network involving only single channels coming into a receive site. If signals are remotely multiplexed and the above pre-emphasis used, they generally come out OK at the discriminator end.

One problem with multiplexing signals from 8 receivers is that you get 8 receivers worth of noise on poor propagation or severe VHF refraction days. Or one receiver will go bad and fill the whole line with noise. We have found a solution to this by employing passive band-pass filters between the receivers and the multiplexer. These are L-C devices from TTE Electronics, models Q142 through Q149 which were specifically designed for our IRIG channels

and 600 Ω input/output impedance. They cost $88.00. With such a filter installed, a given seismic station/telemetry link can only put noise in its own part of the audio spectrum, and not muddy the water for the other channels. These filters have greatly reduced the noise glitches in the data where they are employed. This is particularly helpful in reducing the mis-triggers in the acquisition computer. The removal of various stray harmonics from the main carrier of each channel reduces intermodulation noise and helps lower the noise level coming out of each discriminator.

13. Phone links. The long lines from the major multiplex sites have been very reliable, and repairs have generally been expeditious. The local lines, however, are another story altogether. Local installers are not familiar with the idea of continuous use of data lines. We have spent two years trying to get a large loss (30 db) removed from a line from CRMO to NMMO, without success. The CRMO signal gets to St. Louis about 20 db down from the other carriers, but the discriminator manages to find and demodulate it anyhow.

    A recent problem encountered with phone lines has been their use of a type 829A data terminal on the lines. These units require AC line power to operate, and thus would not pass the data in an emergency. We have had them replaced with the type 150A unit which is passive, an updated equivalent of the old coil unit.

14. The discriminators. The results of several years of design improvements have resulted in a new discriminator with considerable sophistication in managing the data carrier and the data output, but that is still quite reliable and inexpensive to produce. All

the inevitable compromises have been made favoring the recovery of seismic telemetry data only, rather than trying to make a general purpose unit. The system has been described in detail in technical reports from SLU and CIRES. About 100 units currently exist, and more have been ordered. The unit is physically identical to the original USGS discriminator in size and power requirements. Figure 8 is a list of the specifications of the discriminator.

Within the last year the 11/34 computer began digitizing the data from the discriminators. Since its input range is $\pm$ 5 volts, the discriminator output spans were doubled to $\pm$ 4 volts to better use the range of the computer. These discriminators have proved quite reliable, even in the 4x configuration at CIRES, used for recovering FM tape data reproduced 4 times faster than it was recorded. An example of the low noise of the discriminator output is in Figure 9. The AD3Z channel is intact, yet has a stuck seismometer (or bottomed out), so the trace noise is only system noise. The trace reveals that the noise is generally $\pm$ 1 LSB, or 5 millivolts out of $\pm$ 5 volts (a 12 bit system) for the whole telemetry system, including the FM carrier tapes. The small event shown is near the threshold for the Adak system, about $m_b$ 2 or so.

Note the amplitude of the tape speed compensation error that has been removed from the data channels. This is the first discriminator of this type of the author's acquaintance in that tape speed compensation reduces this noise by over 40 db. This is a result of finding that tape speed compensation must be done before the phase changes introduced by the data output filters, and the compensation

signal must be similarly derived.

15. Develocorder operations. For the additional New Madrid stations, a second develocorder was provided with all the modifications that had accumulated in the first one. These have been reviewed elsewhere, and include such items as replacing the time fiducial mirror with a 1 mil glass plate, so that the galvos can be recorded over the full width of the screen.

Assiduous care on the part of the Data Technician has preserved them quite nicely. The major weakness, aside from the pump tubing replacement requirement, is the film transport control microswitch, which has to be replaced annually. Since installing the units on a table with an edge and drains in it, they have been rather intimidated about causing floods. A growing problem has been deterioration of the galvanometer contacts in the galvo magnet block. The only solution is to remove the whole thing and clean them.

16. Seismic data center. A major addition to the seismic data center has been a large uninterruptable AC power system to operate the develocorders and monitor drums, among other things. It is similar to the system installed at Adak two years ago, and provides 800 watts for four hours, which is judged sufficient time to get a generator going. One would think that AC power in a large city would be reliable, but we have had to count on the back-up system almost once a month or so. The inverter is a 1 kw Topaz unit, operating from a 12 volt (nominal) 660 AH battery pack. A crystal oscillator from an old Sprengnether TS-100 clock provides 0.01% frequency stability. A 12 v, 250 ampere power supply obtained surplus provides

the DC power and charges the batteries. Since the data systems operate from the inverter continuously, there are no change-over transients. But if the inverter fails, the control system automatically switches the load to the AC mains.

Other efforts include a new monitor drum interface system to provide attenuation, filters (including notch filters for 3 hz embayment microseisms), time marks, etc., for the 15 channels of data that are monitored with pen and ink recorders. Our previous systems relied on mercury cells and relays for the time mark offset, but the new circuit utilizes an opto-isolator and diode reference, thus eliminating the maintenance problem of the cells and relays. The schematic is available on request.

## IV. Conclusions

The above discussions have elaborated on a way to get the job done, but of course are not the only way. Others have different problems and the necessary compromises can lead to rather different solutions, which, it must be observed, do not conflict with our solutions. We have succeeded in establishing a rather reliable and consistent technology and methodology for getting seismic data from remote sites to the researcher's computer at a minimum of cost and manpower overhead, while preserving or conveying as undistorted a representation of the true data as is reasonably possible. Naturally, new insights crop up every day, and we may have to scrap yesterday's best idea and go with the better one, even if it means redesigning the hardware.

The net result of these improvements over the last three years has

been a general increase in the average signal to noise ratio of the incoming data of about 20 db. Thus a 60 db dynamic range is typical of most stations, while some approach 80 db.

20 March 1981

Report Figures

1. Network Performance Over The Last Three Years
2. Seismic Pre-Amp Schematic
3. VCO Schematic (With Square-Sine Converter)
4. Calibrator System Schematic (Muli-Mode Sine Wave)*
5. Sample Record of Calibration Sequences
6. Power Supply System Schematic
7. Amp/VCO/Calibrator/Power Card Cannister Drawing
8. Discriminator Specifications
9. Noise Sample from Adak Data

* Not currently available in a small page format. Write for the schematic.

Figure 1

USGS Telemetry Network Operation Summary

| Date | Quarter | Stations | % Operational | Outage Days | Stations Affected | by Lightning | Radio Failures | Batteries Out | Other* |
|---|---|---|---|---|---|---|---|---|---|
| 1977 | | | | | | | | | |
| OCT-DEC | 14 | 16 | 83 | 256 | 8 | 4 | 2 | 2 | 0 |
| 1978 | | | | | | | | | |
| JAN-MAR | 15 | 16 | 78 | 338 | 11 | 0 | 4 | 2 | 5 |
| APR-JUN | 16 | 16 | 94 | 91 | 11 | 0 | 3 | 5 | 3 |
| JUL-SEP | 17 | 17 | 86 | 212 | 10 | 3 | 3 | 0 | 4 |
| OCT-DEC | 18 | 17 | 90 | 158 | 4 | 2 | 1 | 0 | 1 |
| 1979 | | | | | | | | | |
| JAN-MAR | 19 | 17 | 88 | 178 | 6 | 1 | 2 | 1 | 2 |
| APR-JUN | 20 | 18 | 87 | 206 | 6 | 2 | 0 | 2 | 2 |
| JUL-SEP | 21 | 18 | 83 | 284 | 11 | 4 | 0 | 5 | 2 |
| OCT-DEC | 22 | 18 | 88 | 197 | 6 | 0 | 0 | 4 | 2 |
| 1980 | | | | | | | | | |
| JAN-MAR | 23 | 18 | 83 | 274 | 5 | 0 | 0 | 4 | 1 |
| APR-JUN | 24 | 20 | 93 | 121 | 10 | 1 | 1 | 6 | 2 |
| JUL-SEP | 25 | 21 | 86 | 225 | 12 | 3 | 5 | 2 | 2 |
| OCT-DEC | 26 | 24 | 96 | 83 | 14 | 2 | 5 | 3 | 1 |
| Summary | Totals | 24 | 87% av. | -- | 114 | 22<br>19% | 26<br>23% | 36<br>32% | 30<br>26% |

"Other" includes vandalism, rodents, fire, etc.

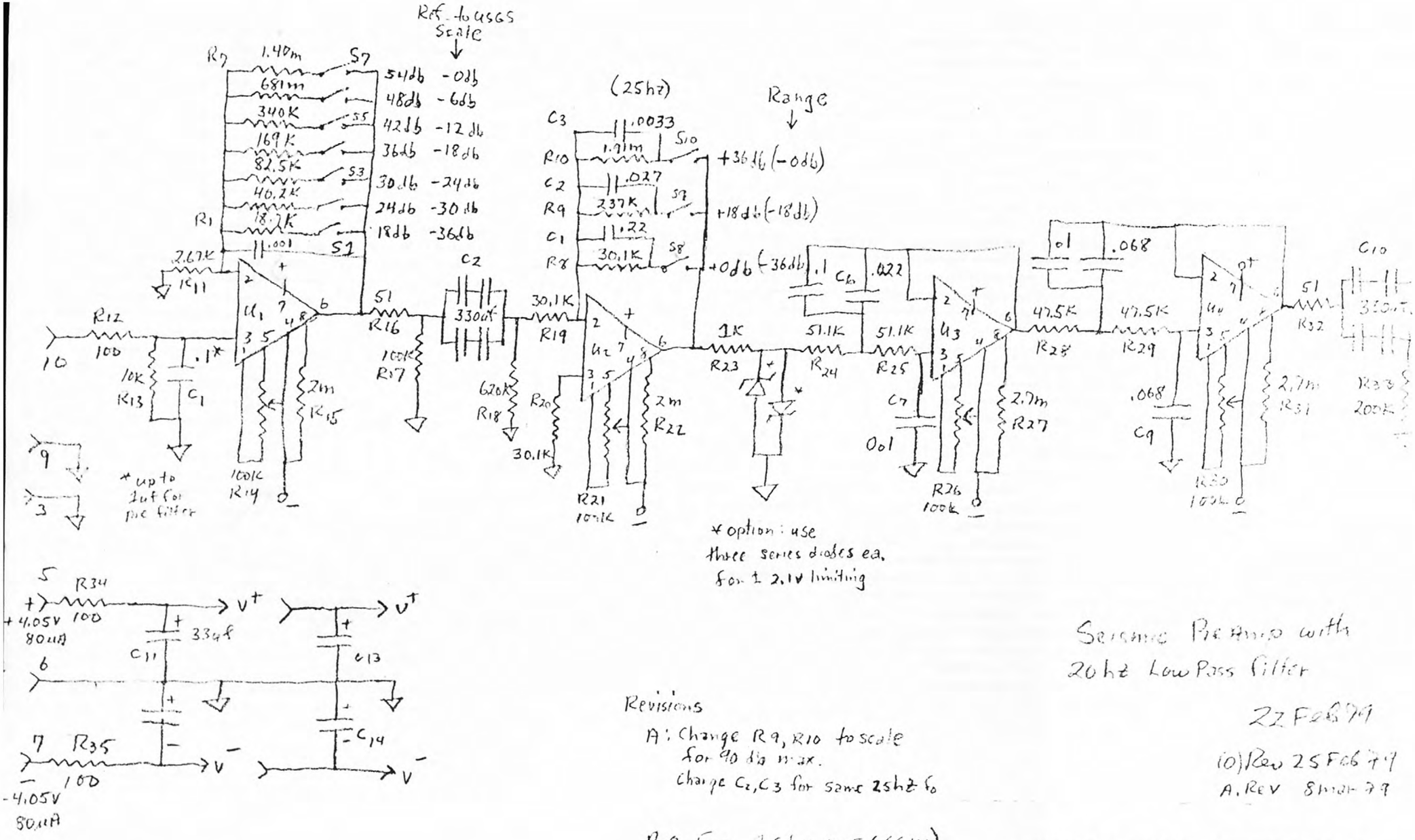


FIGURE 2

Seismic Pre Amp with 20 hz Low Pass Filter

22 Feb 79

10) Rev 25 Feb 79

A. Rev 8 Mar 79

Revisions

A: Change R9, R10 to scale for 90 db max.
Change $C_2$, $C_3$ for same 25hz fc

B: For 2.5 hz LPF (C6 in)
Change R24 R25 to 511K
R28, R29 to 475K


SAINT LOUIS UNIVERSITY
DEPARTMENT OF EARTH AND ATMOSPHERIC SCIENCES
P. O. BOX 8099 - LACLEDE STATION
SAINT LOUIS, MISSOURI 63156

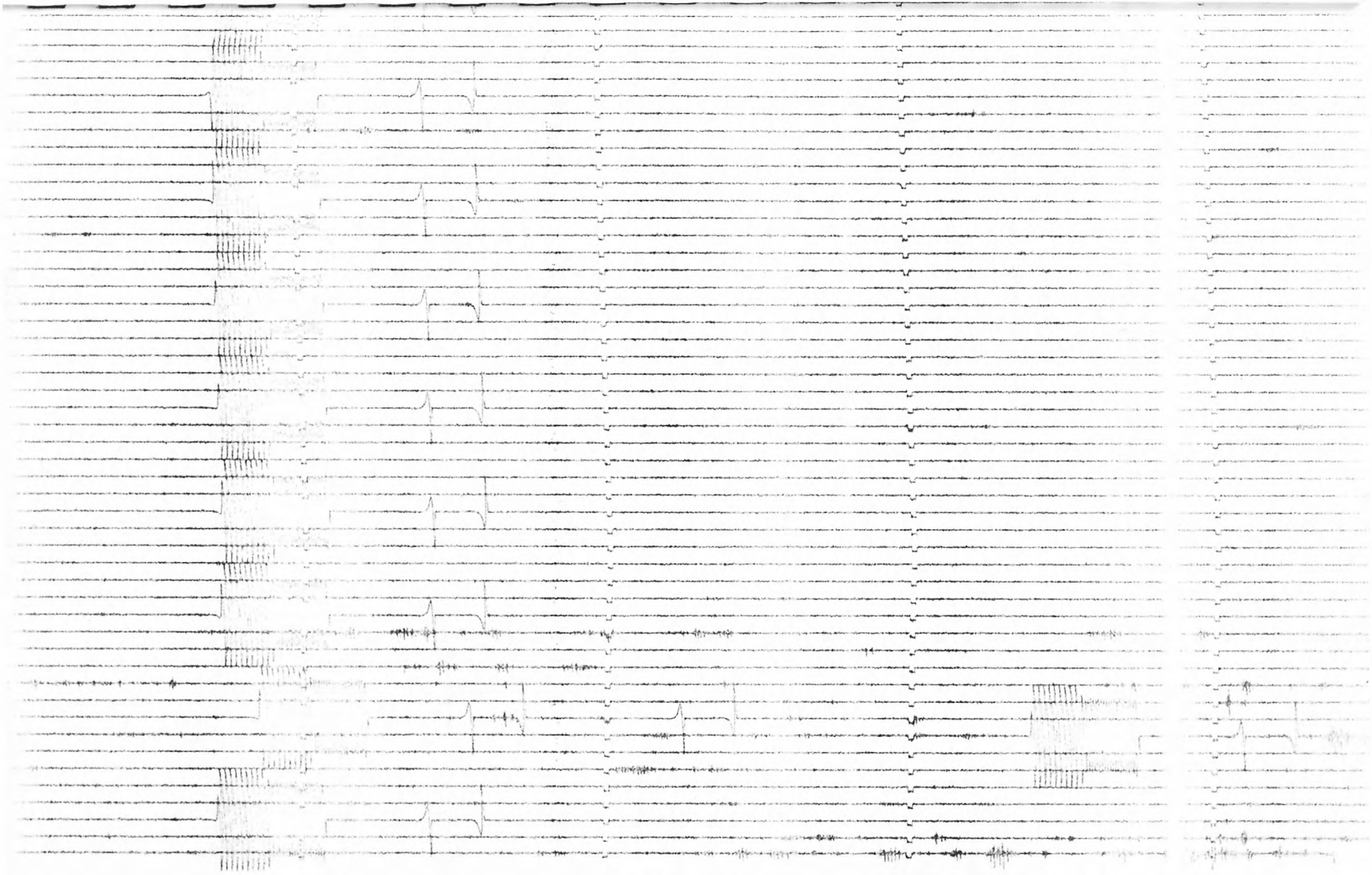

FIGURE 5

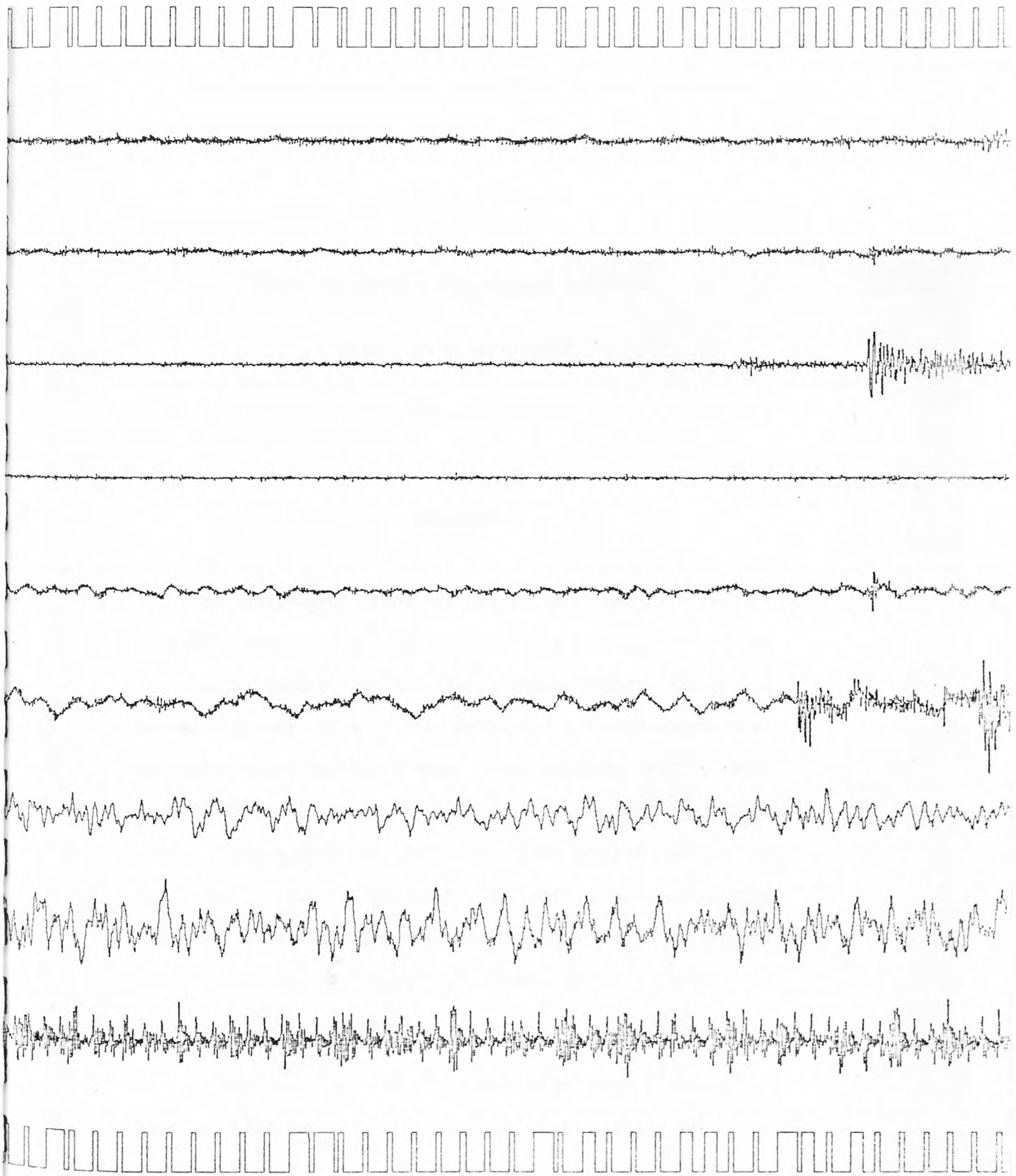

FIGURE 9

# The Sharpsburg, Kentucky Earthquake of July 27, 1980

by Robert B. Herrmann

Dept. of Earth & Atmospheric Sciences

Saint Louis University

St. Louis, MO 63156

## ABSTRACT

The Sharpsburg, Kentucky earthquake was the second largest earthquake to have occurred in the U.S., east of the Continental Divide in the past twenty years, having a seismic moment of 4.0E + 23 dyne-cm. A surface-wave focal mechanism study defines a nodal plane striking N30°E, dipping 50°SE and a nearly vertical nodal plane striking N60°W. P-wave first motion data indicates right-lateral motion on the nodal plane striking N30°E, with the pressure axes oriented east-west. The surface-wave solution is reinforced by a modeling of long-period seismograms at regional distances.

Extensive aftershock monitoring disclosed a distribution of aftershocks striking N30°E and dipping 50°SE. A

stress drop of 7 bars is obtained for the main event.

## MAIN SHOCK SOURCE STUDIES

The $m_b$ = 5.1 earthquake occurred at $18^h52^m20.0^s$ with coordinates $38.2^\circ$N and $83.9^\circ$W. Due to the size of the earthquake, it was well recorded by seismograph stations throughout the United States and Canada. A number of different types of analysis were used to study this event.

### Surface Wave Studies.

The focal mechanism, focal depth and seismic moment were estimated using the techniques described by Herrmann (1979). The Central United States earth model of Table 1 and the surface-wave anelastic attenuation coefficients of Herrmann and Mitchell (1975) were used for the inversion of the surface-wave data. Rayleigh wave spectral amplitude data in the period range of 6 to 45 seconds were obtained from the fourteen seismograph stations OTT, STJ, WES, BLA, SHA, EPT, LUB, ALQ, FVM, SLM, DUG, COR, PNT and YKC to yield a total of 184 spectral amplitude-period pairs for analysis. Love-wave data in the period range 6 to 50 seconds yielded 156 spectral amplitude-period pairs from the eleven seismograph stations OTT, STJ, WES, BLA, SHA, EPT, LUB, ALQ, DUG, COR and YKC.

After systematically searching through all possible focal mechanisms, the surface-wave amplitude spectra and P-wave first motion data were best fit by the focal mechanism given in Figure 1. The pressure axis trends at $247^\circ$ and plunges at $17^\circ$ while the tension axis trends at $353^\circ$ and plunges at $17^\circ$. Proceeding clockwise from north, the seismograph stations and their P-wave polarities are AAM(+), AM3(+), BV1(-), HWV(-), BLA(-), NAV(-), TKL(+), PWLA(-), WCK(-), DWM(-), RMB(-), BLC(-),

DON(-), FVM(-), TYS(-), SLM(-), BLO(-), CHI(+), FCC(+), AN11(+), AN10(+), AN8(+) and AN1(+). For regional P-phases, the P-wave take-off angles of $47^{\circ}$ and $49^{\circ}$ were used for stations at distances greater than and less than 400 km, respectively. The surface-wave data were quite sensitive to the dip and strike of the nodal planes, so that these parameters are known to within $\pm 10^{\circ}$. Perhaps due to the nature of the focal mechanism, as well as the small number of spectral-amplitude pairs, the surface-wave data were not very sensitive to focal depth such that any focal depth between 12 and 22 km would fit the spectral amplitude data equally well. An acceptable value would be a focal depth of 15 km, for which the seismic moment is estimated to be 4.0E + 23 dyne-cm. Following Herrmann (1979), the correlation coefficient between the observed and predicted Rayleigh-wave vertical component spectral amplitudes is $r_R = 0.767$, while for the Love-wave data it is $r_L = 0.744$. The anelastic attenuation corrected observed Rayleigh and Love wave data are compared to theoretical radiation patterns in Figures 2 and 3, respectively. The fits are excellent, as indicated by the large values of the correlation coefficients.

Regional Waveform Studies.

Because of the distribution of excellent first motion data, there is no problem in defining the compressional and dilatational quadrants of the focal mechanism. An independent test of the correctness of the solution could be obtained by computing observed and predicted surface-wave phases at selected stations for a range of periods. In order to do this, the seismograph stations must be at relatively short epicentral distances so that errors in phase velocity do not affect the comparison

in phases. Another way to perform this test is to compare actual and predicted waveforms rather than spectral phases.

Using the approach used by Herrmann et al. (1980), a point source dislocation source with focal mechanism given by Figure 1 and a seismic moment of 4.0E + 23 dyne-cm was placed at a depth of 15 km in the Central U.S. earth model of Table 1. A source time function with duration of 1.0 second was used for the synthesis. The numerical seismograms were obtained by performing a double Fourier, Fourer-Bessel transform over the frequency range 0-2 Hz and over the phase slowness range 0-2.0 sec/km. The resultant time histories were passed through a numerical realization of a 15-100 WWSSN long period seismograph with a peak magnification of 3000.

Figure 4 shows the observed SLM vertical component seismogram and Figure 5 shows the predicted vertical, north-south and east-west seismograms at SLM, a distance of 555.5 km at an azimuth of 277°. Except for the rippling motion after the first part of the surface wave, the waveforms and amplitudes agree well, especially the first ten seconds of the surface wave arrival. In making this comparison, the predicted vertical trace was time shifted 2 seconds later. Figure 6 presents the observed 3 component seismograms at BLA, a distance of 325.9 km along an azimuth of 109° from the earthquake. A non-linear spring resonance effect is seen in the vertical component record. The sense of motion and amplitudes of the observed and predicted traces are in good agreement. The SH motion on the horizontal components matches the observed traces well if the predicted trace is shifted two seconds later. However, this time shift will not yield a good match of the Rayleigh wave

motion on the vertical and east-west traces.

In order to provide a better fit to the BLA traces, synthetic time histories were generated for the same source as above but at depths of 11 and 20 km. The fine character of the SH arrivals changes, but the time separation between the SH and Rayleigh wave was not affected. The propagation path between the epicenter and Blacksburg, VA is perpendicular to the Appalachian Mountain front, with the depth to the Precambrian changing from about 1 km at Sharpsburg to 5+ km in eastern Kentucky. This indicated that the Central U.S. earth model is certainly not applicable for that path.

Multiple-filter analysis was used to study the Rayleigh and Love wave dispersion to BLA. In order to match the group velocity, the upper layer of the Central U.S. earth model was increased in thickness. The resulting Appalachian Basin model is given in Table 1. A suite of seismograms were generated for a depth of 14 km in that model. The discrepancy between the observed and predicted Rayleigh and SH phases was not completely resolved, but one focal mechanism solution, dip = $50^{\circ}$, strike = $30^{\circ}$ and slip = $190^{\circ}$, did provide a better fit. The corresponding traces are shown in Figure 8. However, changing the focal mechanism parameters by just $10^{\circ}$ eliminates the good fit of both phases.

The use of synthetic seismograms reinforced the surface wave P-wave first motion conclusions concerning the focal parameters. The observed seismograms were fit in their major characteristics, but as seen from the discussion of the BLA records, the problem of crustal structure is important, but the quality of data was not sufficient to start a study of crustal structure.

## AFTERSHOCK STUDIES

Because of the size and location of this earthquake, portable instruments for aftershock studies were emplaced within 24 hours of the mainshock by the U.S. Geological Survey, the University of Michigan, Virginia Polytechnic Institute and State University, the University of Kentucky and the Tennessee Earthquake Information Center. Aftershock data from a total of 38 station sites are available for 51 aftershocks for the time period July 28 - August 25, 1980. (Data were collected and interpreted by Mr. J. Zollweg, TEIC, who made the following results available.)

The aftershocks were relocated using a joint hypocenter determination algorithm described by Herrmann et al. (1981). The results of the relocation are shown in Figures 9-12. Figures 9-10 show the relationship of the epicenters to the network of seismograph stations, while Figures 11-12 are projections of the relocated hypocenters onto vertical planes striking N30°E and N120°E. The aftershocks were projected onto planes striking 0° to 180°. The tightest spatial pattern occurred for a strike of 120°. Presumably, then this represents a view down strike and a strike of N30°E with a dip of 50°SE is indicated for the fault plane. Thus the northeast striking fault plane of Figure 1 is the preferred fault plane.

Figures 13 and 14 show the data of Figures 11 and 12, respectively, but without the error bars. From Figure 13, the aftershock area is about 27km$^2$. Using the seismic moment of $M_o$ = 4.0E+23dyne-cm, an average fault radius of r = 2.9km and a stress drop

$$\Delta\sigma = \frac{7 M_o}{16 r^3} = 7 \text{bars}$$

is obtained (Brune, 1970, Eq. 31). This value of stress drop is similar to that estimated for other central and eastern U.S. earthquakes of similar magnitude (Street et al., 1975; Street and Turcotte, 1977).

## DISCUSSION

For the first time, a large number of aftershocks of an eastern U.S. earthquake have been recorded. Thus independent constraints on source parameters are available. The strike and dip of the aftershock distribution are in agreement with the surface-wave focal mechanism, but the aftershock depths provide a better resolution on the depth of the mainshock than was possible from surface waves. The aftershocks cluster around a depth of 12 km, while the surface wave solution found the depth range of 11-20 km quite acceptable. Assuming the equivalence of the aftershock area and the fault plane of the main event, an estimate of stress drop was made, which yielded a 7 bar result, typical of eastern U.S. earthquakes of the same size.

Table 1

Earth Models

| | Thickness (km) | $V_p$ (km/sec) | $V_s$ (km/sec) | $\rho$ (gm/cm$^3$) | $Q_\alpha$ | $Q_\beta$ |
|---|---|---|---|---|---|---|
| Central U.S. | | | | | | |
| | 1 | 5.0 | 2.89 | 2.5 | 4000 | 2000 |
| | 9 | 6.10 | 3.52 | 2.7 | 4000 | 2000 |
| | 10 | 6.40 | 3.70 | 2.9 | 4000 | 2000 |
| | 20 | 6.70 | 3.87 | 3.0 | 4000 | 2000 |
| | -- | 8.15 | 4.70 | 3.4 | 4000 | 2000 |
| Appalachian Basin | | | | | | |
| | 3 | 5.00 | 2.89 | 2.5 | 4000 | 2000 |
| | 9 | 6.10 | 3.52 | 2.7 | 4000 | 2000 |
| | 10 | 6.40 | 3.70 | 2.9 | 4000 | 2000 |
| | 20 | 6.70 | 3.87 | 3.0 | 4000 | 2000 |
| | -- | 8.15 | 4.70 | 3.4 | 4000 | 2000 |

## REFERENCES

Brune, J.N. (1970). Tectonic stress and the spectra of seismic shear waves from earthquakes, J. Geophys. Res. 75, 4997-5009.

Herrmann, R.B. and NB.J. Mitchell (1975). Statistical analysis and interpretation of surface-wave anelastic attenuation data for the stable interior of North America, Bull. Seism. Soc. Am. 67, 209-218.

Herrmann, R.B. (1979). Surface wave focal mechanisms for eastern North American earthquakes with tectonic implications, J. Geophys. Res. 84, 3543-3552.

Herrmann, R.B., J.W. Dewey and S.K. Park (1980). The Dulce, New Mexico, Earthquake of 23 January 1966, Bull. Seism. Soc. Am. 70, 2171-2184.

Herrmann, R.B., S.K. Park and C.Y. Wang (1981). The Denver Earthquakes of 1967-1968, Bull. Seism. Soc. Am. 71, (in press).

Street, R.L., R.B. Herrmann and O.W. Nuttli (1975). Spectral characteristics of the Lg wave generated by central United States earthquakes, Geophys. J. 41, 51-63.

Street, R.L. and F.T. Turcotte (1977). A study of northeastern North American spectral moments, magnitudes and intensities, Bull. Seism. Soc. Am. 67, 599-614.

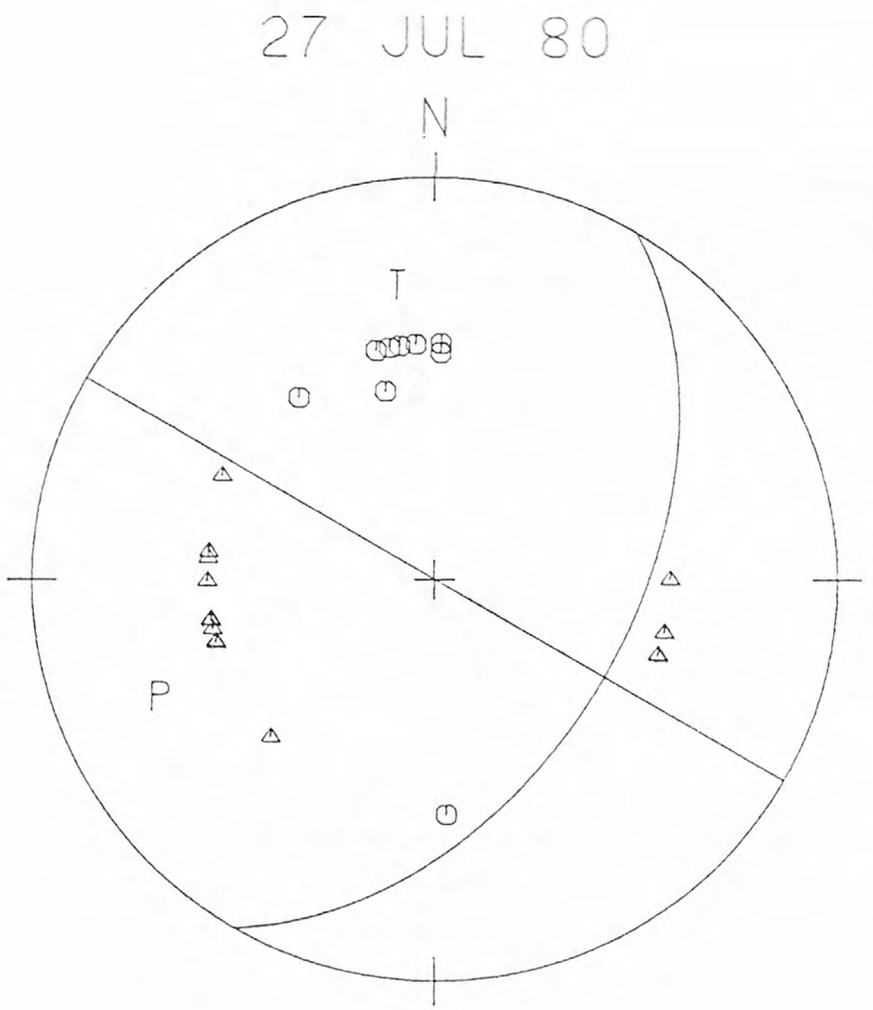


Figure 1. The nodal planes satisfy surface-wave spectral amplitude data as well as P-wave first motion data. Circles and triangles indicate compressional and dilatational first motion, respectively. The symbols T and P are intersections of the tension and pressure axes, respectively, with the lower hemisphere. An equal area lower hemisphere projection is used. Only sharp, impulsive first motion data are used. The northeast nodal plane strikes $30^{\circ}$, dips $55^{\circ}$, and has a slip angle of $180^{\circ}$.

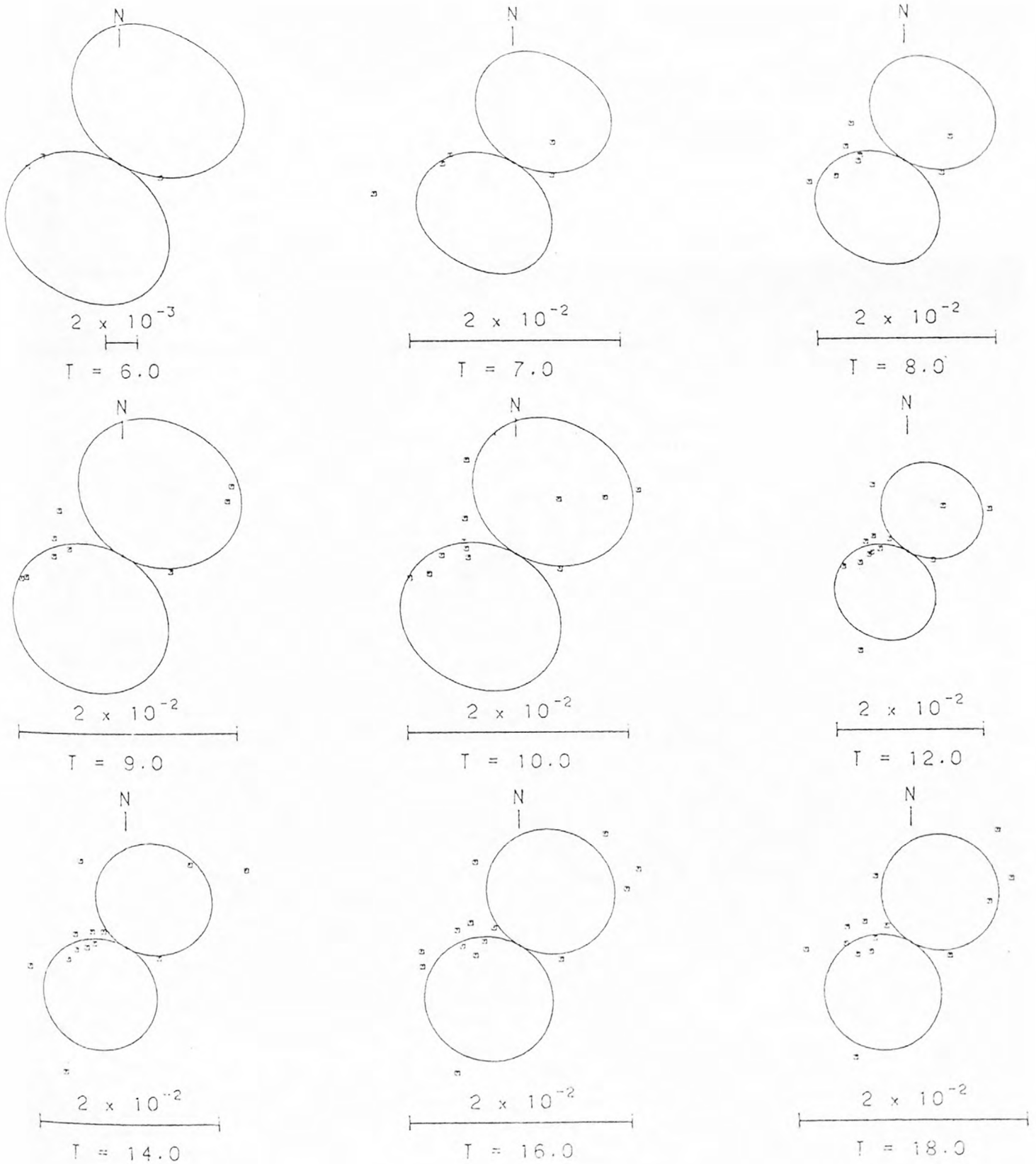


Figure 2. Comparison between an elastic attenuation corrected observed and predicted Rayleigh-wave radiation patterns at selected periods T. The scaling bars are spectral amplitudes in units of cm-sec at a reference distance of $9^{\circ}$ from the source.

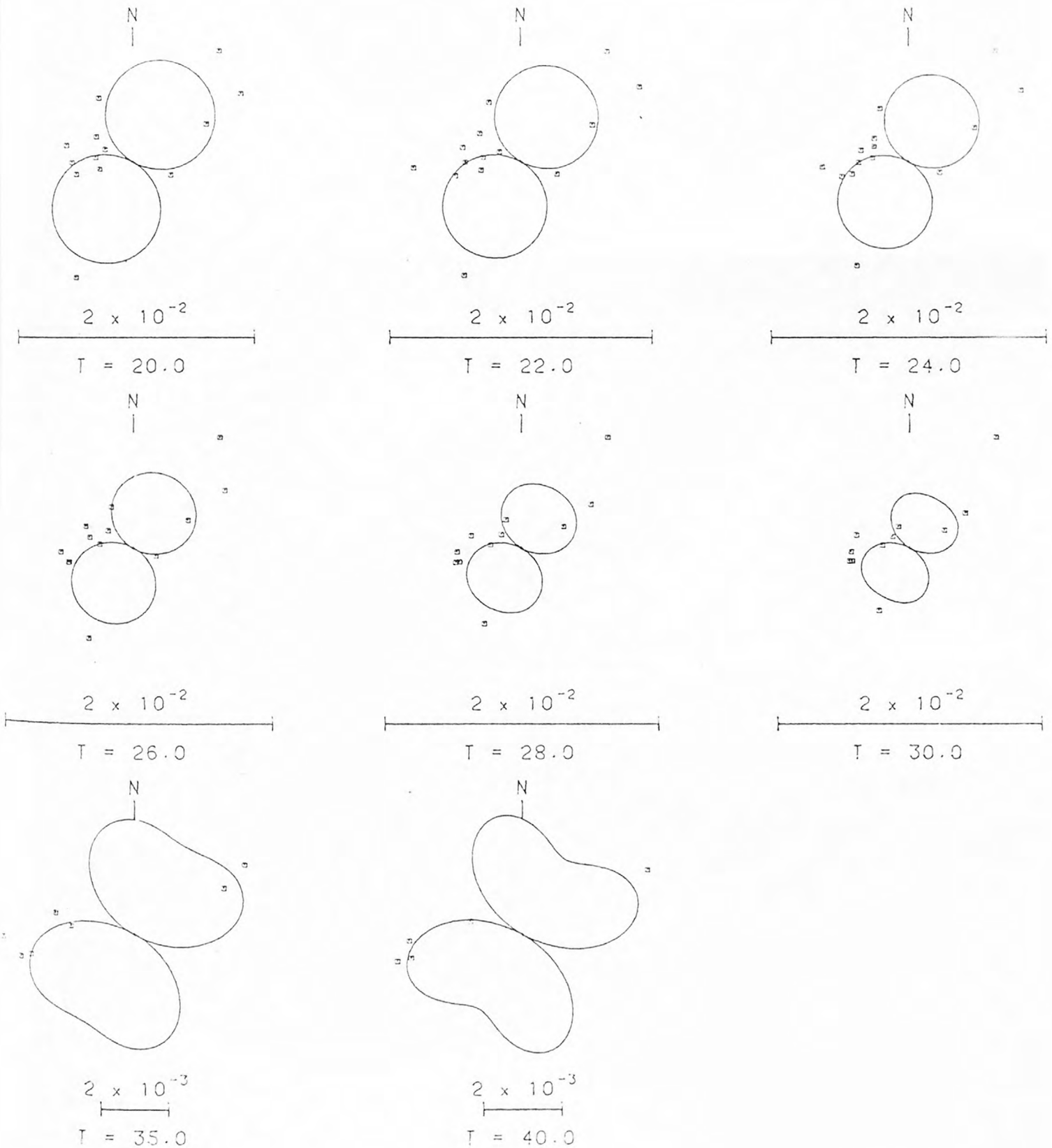


Figure 2 continued

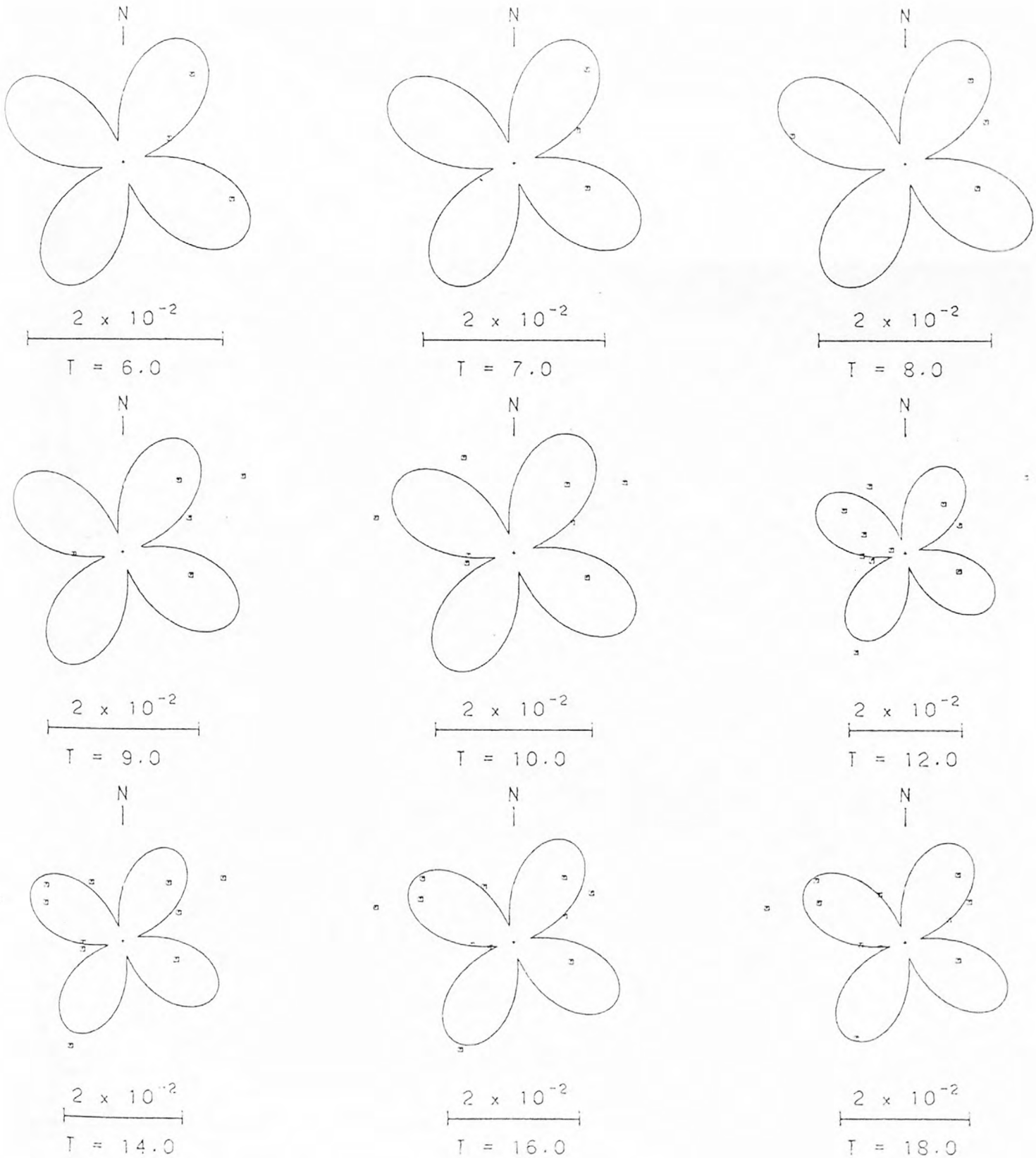


Figure 3. Comparison between anelastic attenuation corrected observed and predicted Love-wave radiation patterns at selected periods T. The scaling bars are spectral amplitudes in units of cm-sec at a reference distance of $9^{\circ}$ from the source.

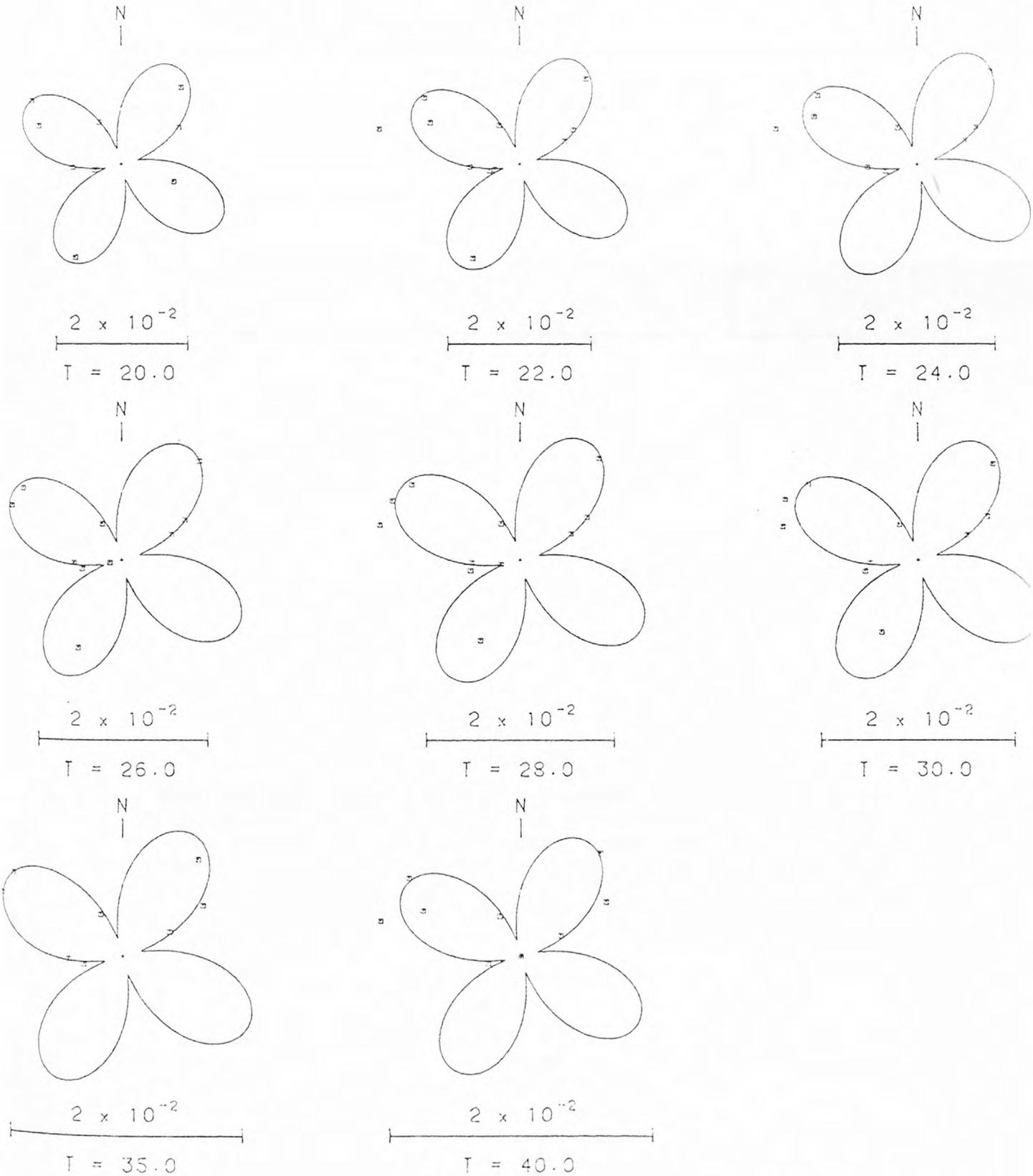


Figure 3 continued

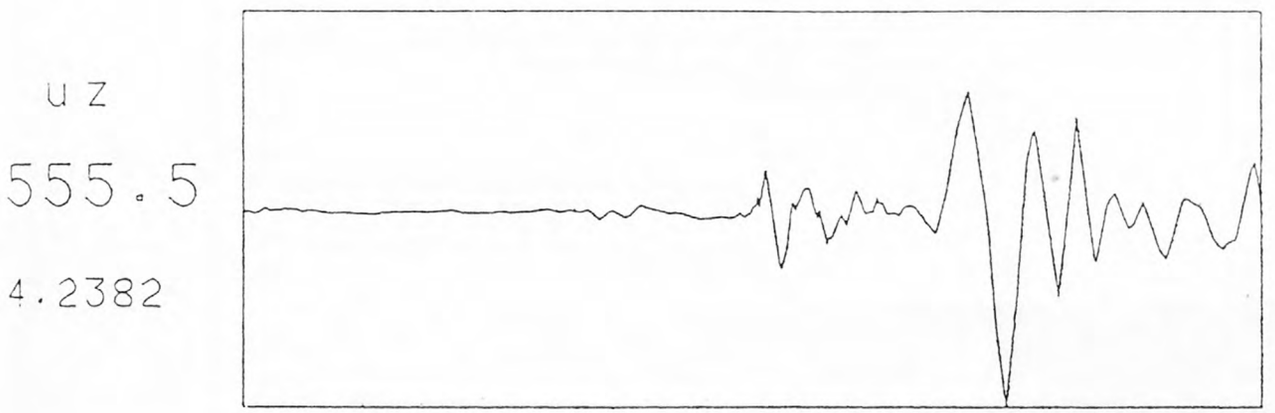


Figure 4. Observed long period vertical seismogram at SLM, a distance of 555.5 km from the earthquake. The plot represents 128 seconds of the time history, starting 90 seconds after the origin time. The maximum trace excursion is 4.2 cm on an instrument with 3000 magnification.

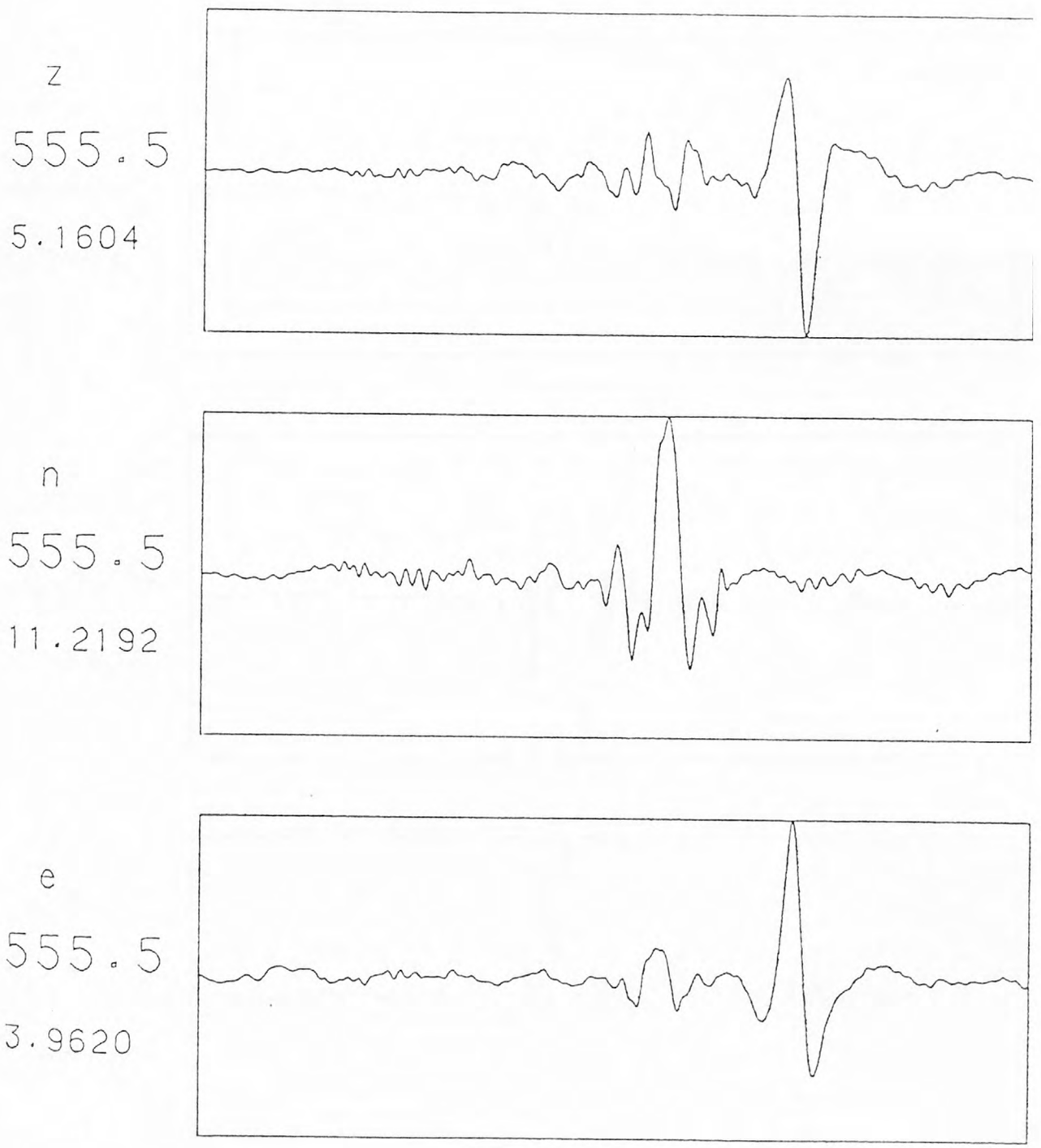


Figure 5. Predicted seismograms at SLM. The smaller numbers give the maximum trace excursion in cm. 128 seconds of time history are plotted, with the traces starting 90 seconds after the origin time.

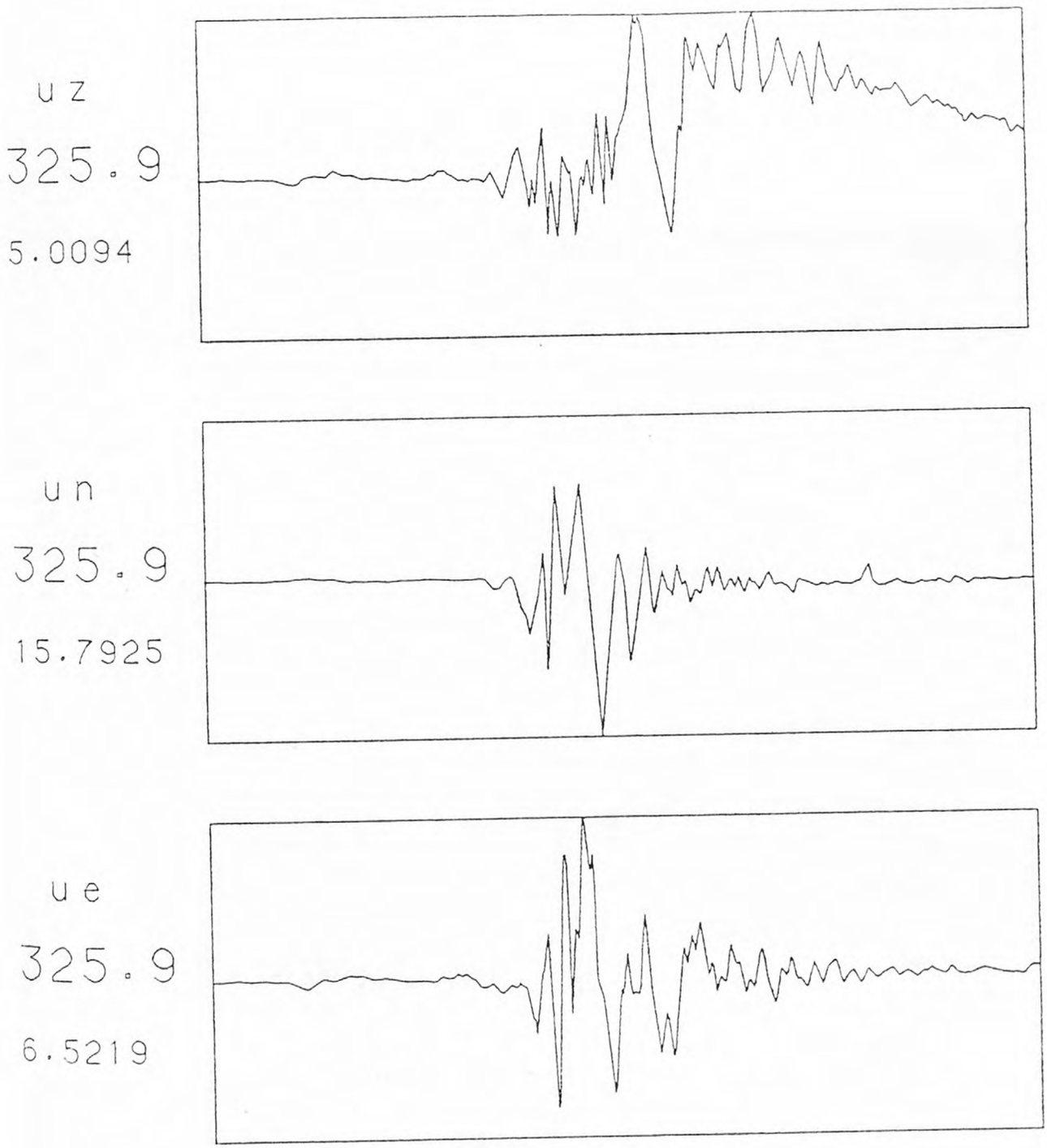


Figure 6. Observed seismograms at BLA, a distance of 325.9 km and an azimuth of 109° from the earthquake. 128 seconds of time history are plotted, starting 325.9/8.1 seconds after the origin time. The smaller numbers give the maximum trace excursion on a 3000 magnification 15-100 seismogram.

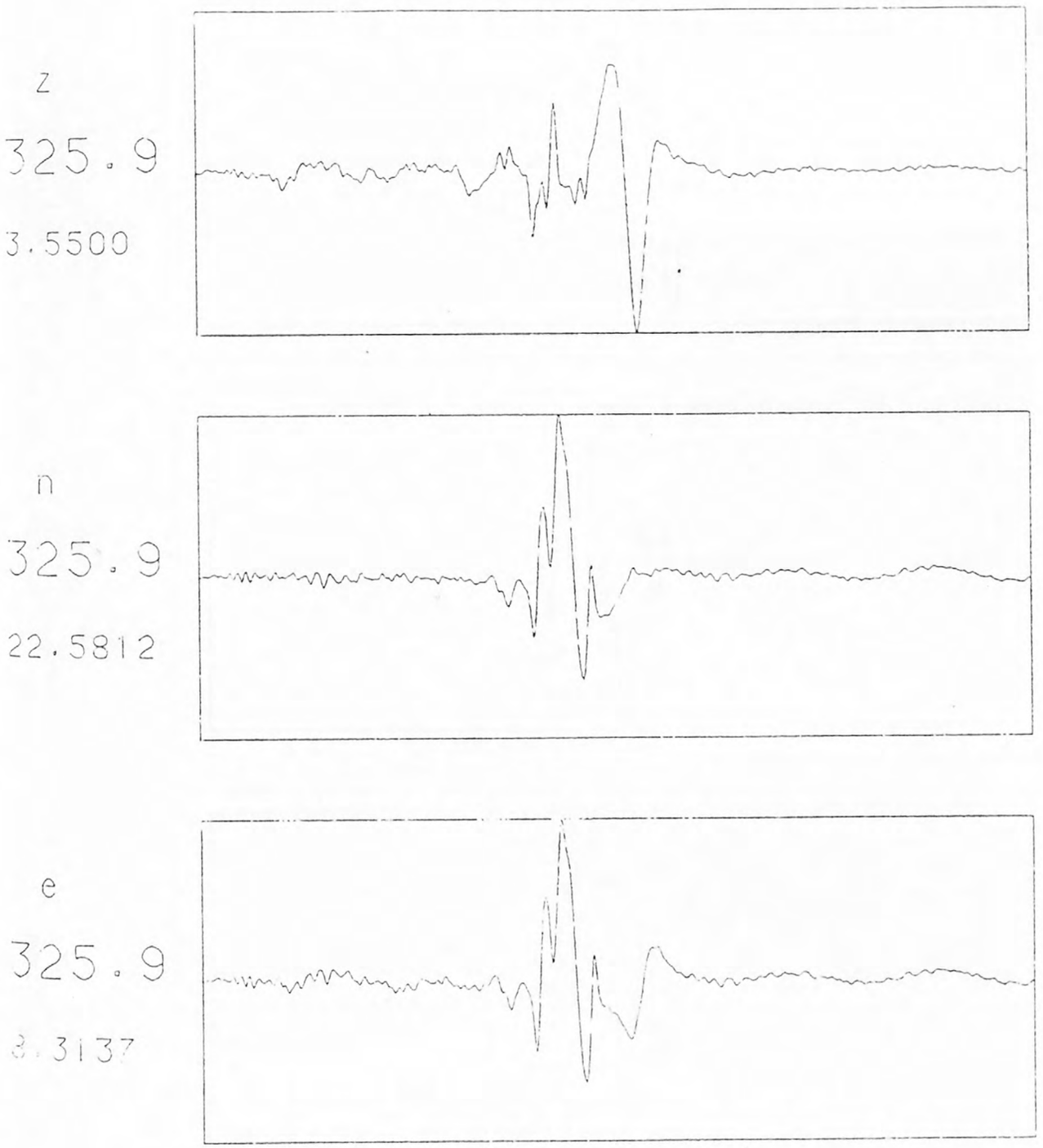


Figure 7. Predicted long-period seismograms at BLA. The maximum trace amplitude in cm is indicated by the smaller set of numbers.

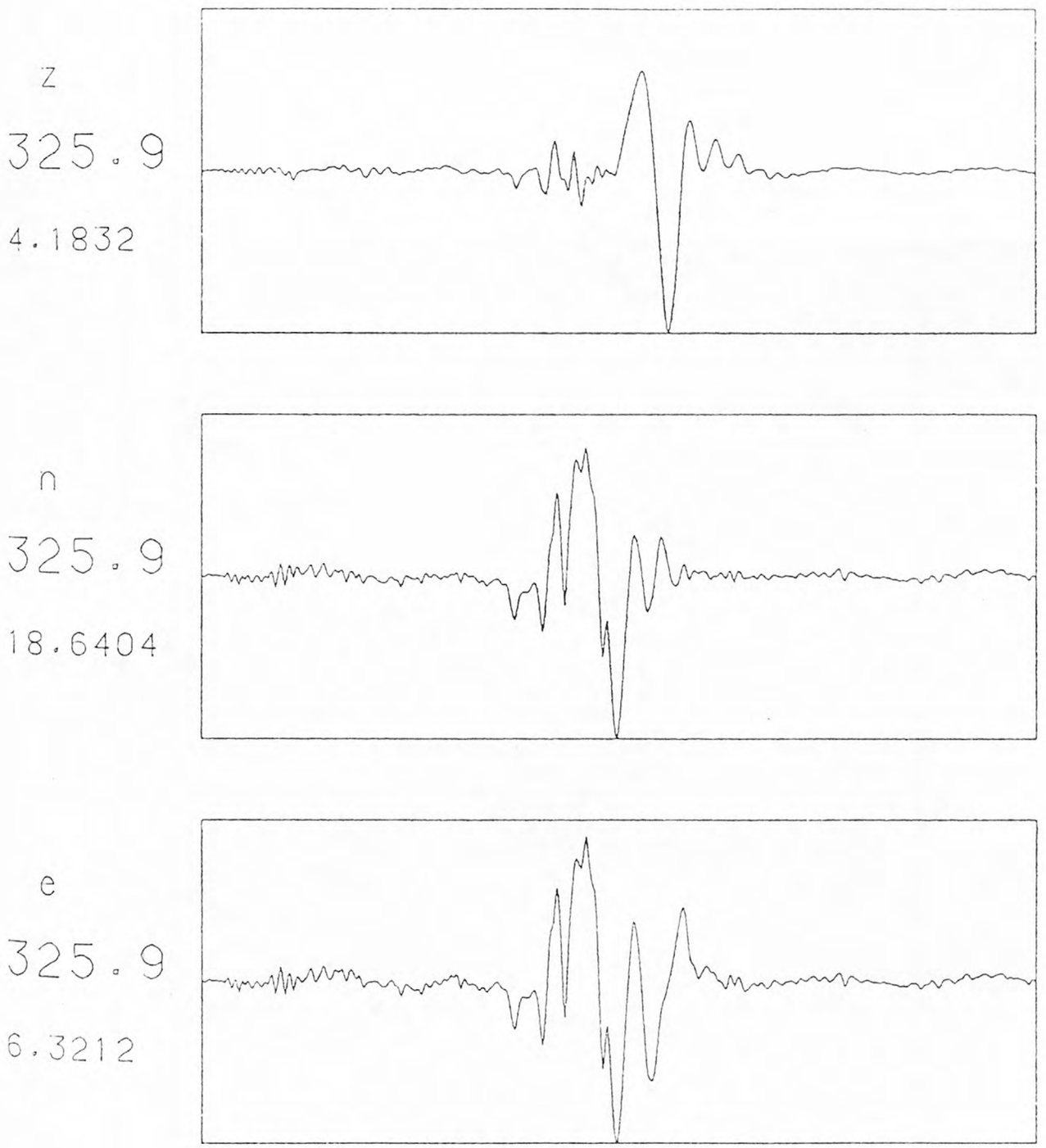


Figure 8. Predicted long-period seismograms at BLA using the Appalachian Basin model. For these, a strike of 30°, dip of 50° and a slip of 150° was used.

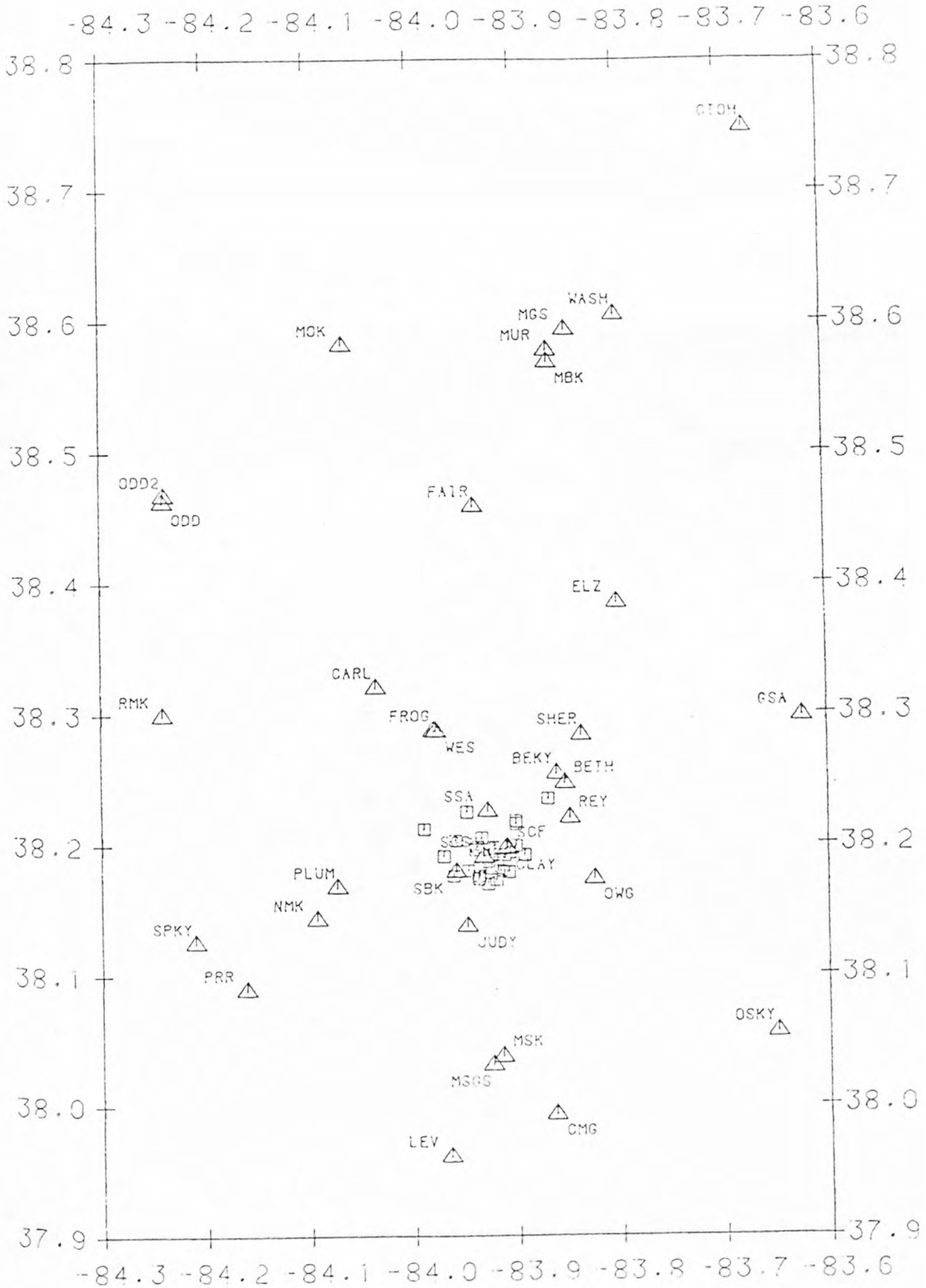


Figure 9. Location of seismograph stations, triangles, and relocated aftershocks, squares. A total of 52 aftershocks are plotted.

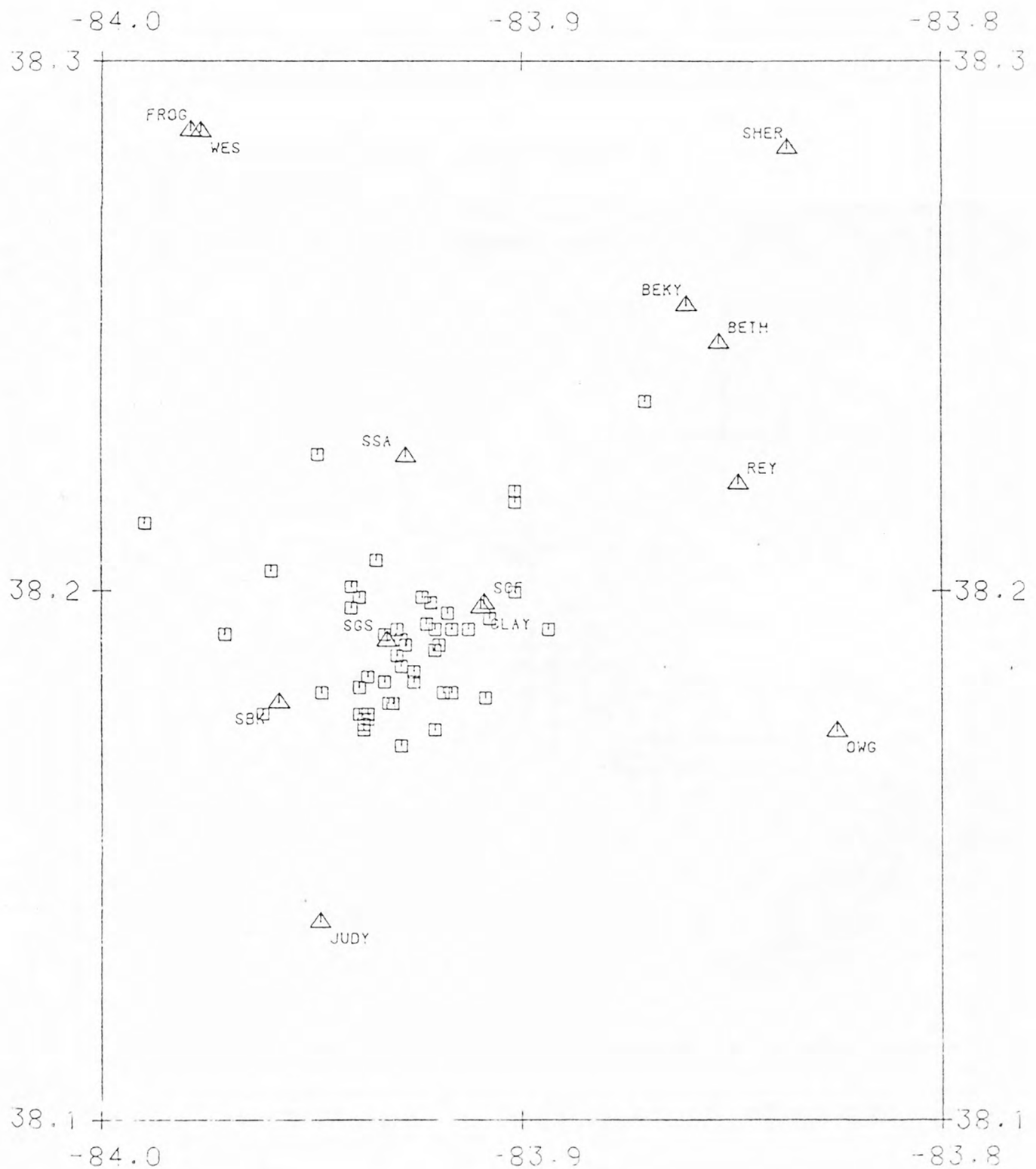


Figure 10. Enhanced plot showing more detail on the spatial distribution of aftershocks.

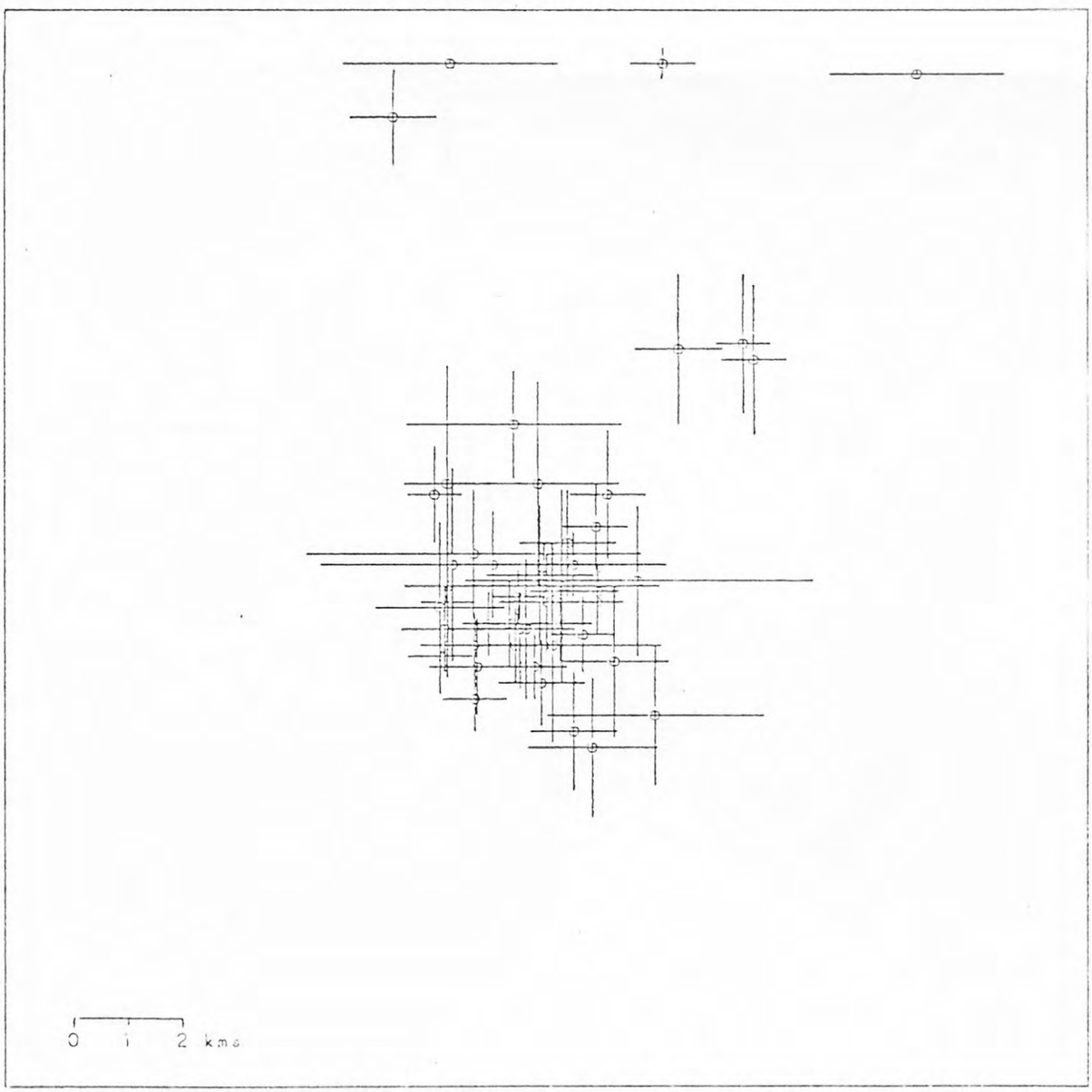


Figure 11. Projection of relocated aftershocks onto a plane striking N30°E. One standard error confidence bars are indicated. There is no vertical exaggeration.

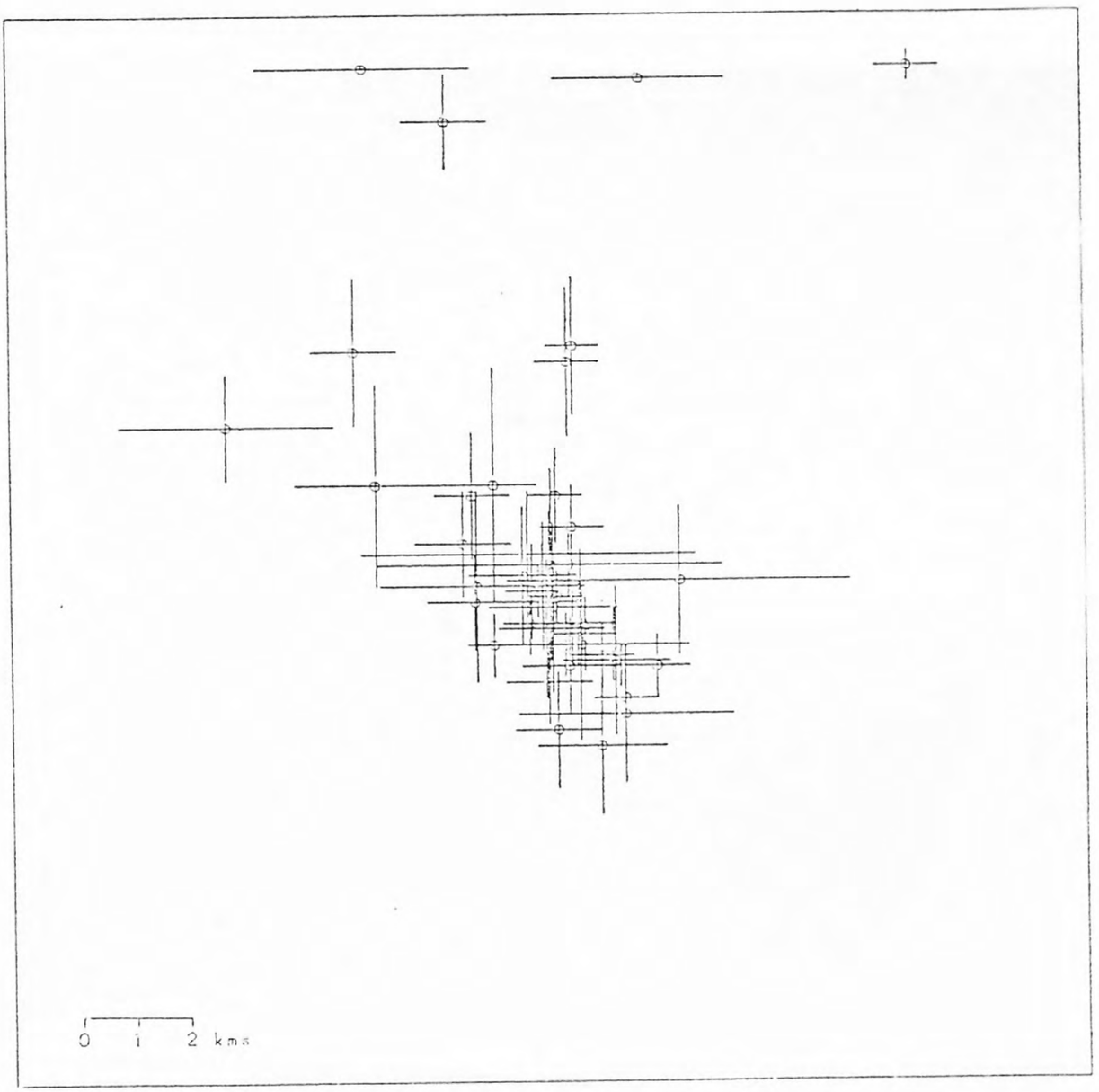


Figure 12. Projection of relocated aftershocks onto a plane striking N120°E.


Figure 13. Same data as Figure 11 but without error bars.


Figure 14. Same data as Figure 12 but without error bars.

# The Ridgely Well Air Gun Experiment

A Special Technical Report

by

B.J. Mitchell, S.-T. Morrissey, M.T. Dablain, and Billy H. Kingsley

Contents

# I. Introduction

During September, 1980, a seismic reflection experiment was conducted at Ridgely, Tennessee utilizing an air gun source in a deep abandoned water well. One purpose of the experiment was to attempt to detect reflections from the basement surface and from reflectors within the basement rock. A second purpose was to attempt to observe temporal variations of travel times of the reflections from basement interfaces. Such variations have been observed previously in California, using a vibroseis source (Clymer, 1980). Some of those results suggest that the variations correlate in phase with the solid Earth tides.

The present study benefits from the availability of deep wells previously located in the area of the New Madrid seismic zone. By placing a source in a deep well it is possible to partially avoid the adverse effects of highly attenuating alluvium near the surface in that region.

A seismic reflection survey was conducted near Ridgely by the USGS (Zoback, 1979). Record sections obtained from that survey extend to times of 1.5 seconds. They therefore provided information with which to compare possible relection times determined in our experiment.

## II. Experimental Set-up

The Ridgely well penetrates to a depth of 201 meters. It was abandoned as a city water supply several years ago and its levels are currently being monitored in an attempt to observe correlations between water well levels and earthquake activity (Mitchell et al., 1977).

The technical requirements for the experiment were as follows:

a) a headframe and winching system capable of lowering the air gun (~ 100 kg) and cables into the well and retrieving it as necessary;

b) a source of compressed air for the air gun;

c) the air gun itself, with an internal time break transducer for shot time;

d) a precision delayed-time trigger for the recording system, such that the recording system would be capable of resolving time to less than a millisecond for events (wave packets) arriving up to 99 seconds after the gun was fired;

e) a means of digitally recording and subsequent digital stacking of the arrival waveforms. This was realized by the use of a Nicolet digital storage oscilloscope as described below;

f) a sensor for the received signal was required. We sought first to obtain direct vertical reflections from beneath the well with a local seismometer. We also attempted to record refracted or reflected arrivals from a nearby seismic telemetry station (GRT, about 6.5 km east of the well).

The complete system is schematically illustrated in Figure 1. Each of the above will be described in some detail below. For more detailed information, consult the authors.

### IIa. The Hoist Frame and Winching System

Commercially available winches are generally capable of handling cable lengths of 30 to 50 meters at most. Beyond these small units, the next available size is equipment designed for well drilling and logging operations, capable of operating to great depths and costing

Figure 1

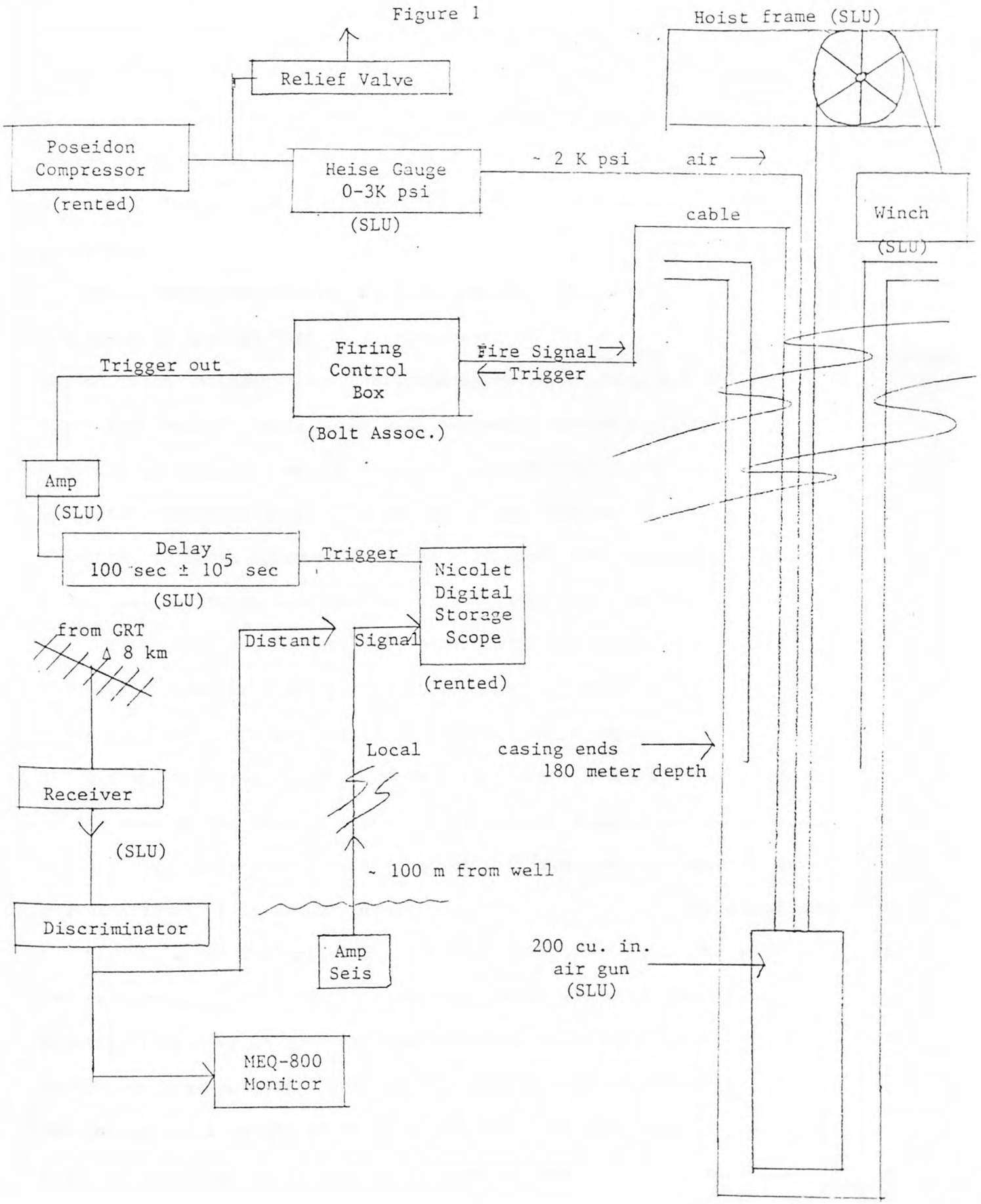
Hoist frame (SLU)
Relief Valve
Poseidon Compressor
(rented)
Heise Gauge 0-3K psi
(SLU)
~ 2 K psi
air
cable
Winch
(SLU)
Firing Control Box
(Bolt Assoc.)
Fire Signal
Trigger
Trigger out
Amp
(SLU)
Delay 100 sec ± 10^5 sec
(SLU)
Trigger
Nicolet Digital Storage Scope
(rented)
from GRT
Δ 8 km
Distant
Signal
Local
casing ends
180 meter depth
Receiver
(SLU)
~ 100 m from well
Discriminator
Amp Seis
200 cu. in. air gun
(SLU)
MEQ-800 Monitor

thousands of dollars. Our needs were for a unit capable of handling up to 160 kgm and working to depths of 800 meters (the depth of the USGS test well at Linda, MO). A further requirement was that the system be postable, easily transported and quickly assembled at the site, and operate from less than 3 kw of 110 AC power from our portable generator.

These requirements were met using readily available hardware, with a minimum of special shop work. The heart of the winch system is a Dayton (from Grainger, Inc.) variable speed reversible, 3/4 hp, (permanent magnet field) motor with automatic torque limiting. This was coupled through a mating electric magnetic disc brake unit to a 40:1 gear reduction unit. The output of the gear was fitted with a 1" pitch, 12 tooth sprocket to drive a 36 tooth chain sprocket on the winch reel shaft itself. The winch reel is an empty "spiral-4" cable reel fitted with a 1" square drive shaft with end adaptors machined to fit the 2" diameter shaft of the pillow bearing blocks and the chain drive sprocket. The net result of all this has a capability of lifting 175 kgm at an average rate of 20 meters/minute (depending on the depth of the wind on the reel). Figure 2a is a block diagram of the winch. All the components were bolted to a welded frame that was mounted to the headframe. Figures 2b, c, and d are details of the major components.

For cable for the hoist, 1/4" (~ 6mm) galvanized aircraft cable was selected for its flexibility and reliability. This cable has a working tension up to 2300 kg; smaller cable would have sufficed, but would have been much more difficult to handle. The cable length of 300 meters had a weight of 58 kgm (105 lbs). As the cable was wound from the shipping reel to the winch reel, it was carefully marked

Figure 2a: Block Diagram of Winch

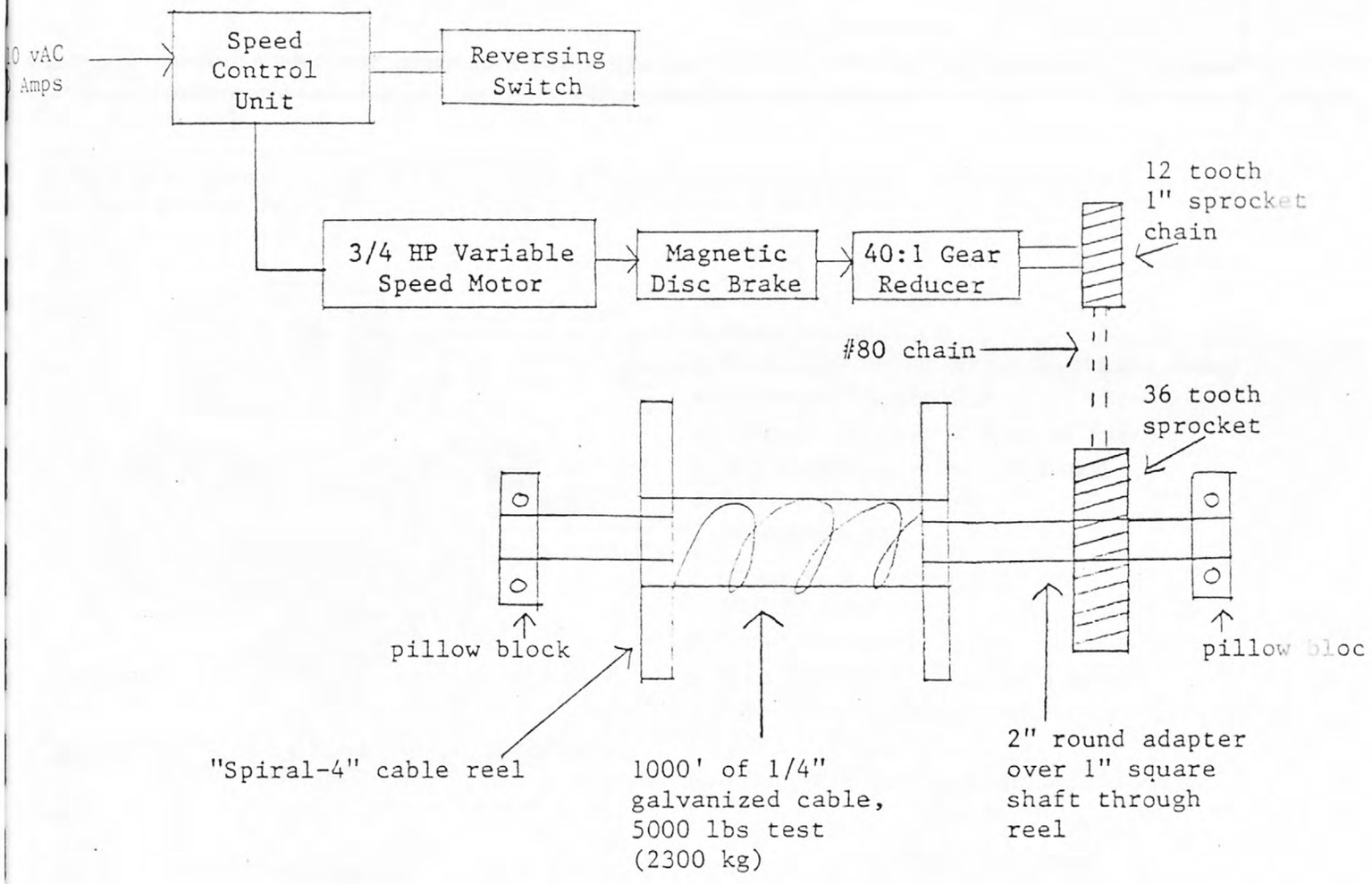

INSTALLATION INSTRUCTIONS & PARTS LIST

# ADJUSTABLE SPEED MOTOR

## MODEL 2Z846

FORM
5S1983
3520

THE DAYTON ELECTRIC MANUFACTURING CO. CHICAGO 60648

0180/014/15
2C

**ATTENTION: READ CAREFULLY BEFORE ATTEMPTING TO INSTALL, OPERATE OR SERVICE THE DAYTON ADJUSTABLE SPEED MOTOR. RETAIN FOR FUTURE REFERENCE!**

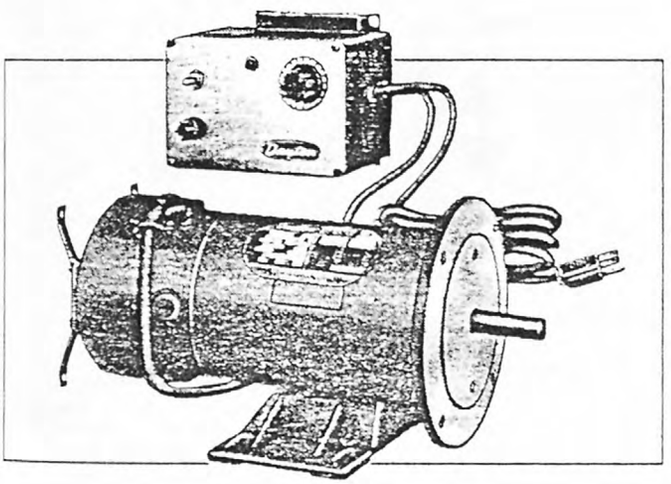

Figure 1 — Adjustable Speed Motor; Controller Mounted Separately

MOTOR CONTROLLER FEATURES

- Speed Range: 20 to 1 constant torque
- Speed Regulation: Within 5% of base speed
- Full-Wave Rectification
- Current/Torque Limit: Built-in (fixed)
- IR Compensation: Built-in (fixed)
- Soft Start Acceleration
- Transient and Surge Protection
- Line Voltage Compensation
- All Control Circuitry on One Printed Board
- Control and Motor Protection: Fused
- Forward On/Off/Reverse On Switch
- Power On Indicator Light
- NEMA 1 Enclosure

See Specifications for additional information.

## *Description*

The Dayton adjustable speed permanent magnet DC motor, equipped with motor controller, is designed for use on constant (or diminishing) torque applications such as conveyors, fans, blowers, etc.

**WARNING: Not intended for use with saws, drill presses or other constant HP applications. Do not use in explosive atmosphere.**

## *Specifications*

MOTOR CONTROLLER: 115 VAC +10% −5%, single phase, 60/50 Hz Input, 9.3 Full Load Amps, 10 Amp Type 3AB Fuse, 0-100 Speed Control Incrementation, Reversible Rotation (CCW or CW) Switch, NEMA 1 Enclosure.

PERMANENT MAGNET DC MOTOR: ¾ HP, 2500 RPM, 102 VDC Armature, Totally Enclosed, Fan-Cooled, Continuous Duty, 8 Hour Day, 1.0 Service Factor, 40° C. Maximum Ambient, Class F Insulation, NEMA 56C/56 Frame, All-Position Mount.

Figure 2 — Adjustable Speed Motor Dimensions; Controller Mounted on Motor

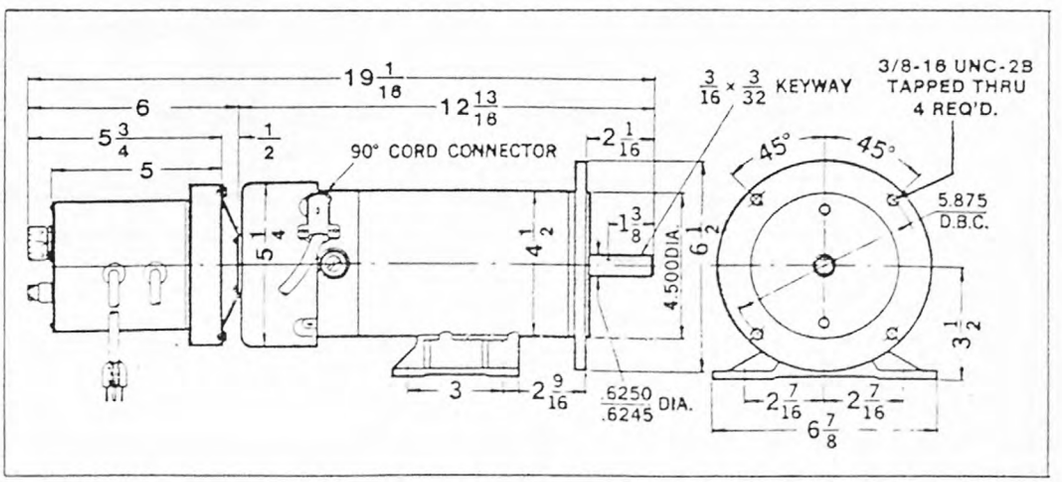


Figure 2b: Description of Motor Unit

# MAGNETIC DISC BRAKES

## MODELS 6K233B & 3M366A-DOUBLE "C" FACE

FORM 5S1782 4018

DAYTON ELECTRIC MANUFACTURING CO. CHICAGO, 60648

0479/0683 2BC

**ATTENTION: READ CAREFULLY BEFORE ATTEMPTING TO INSTALL, OPERATE OR SERVICE THE DAYTON MAGNETIC DISC BRAKE. RETAIN FOR FUTURE REFERENCE!**

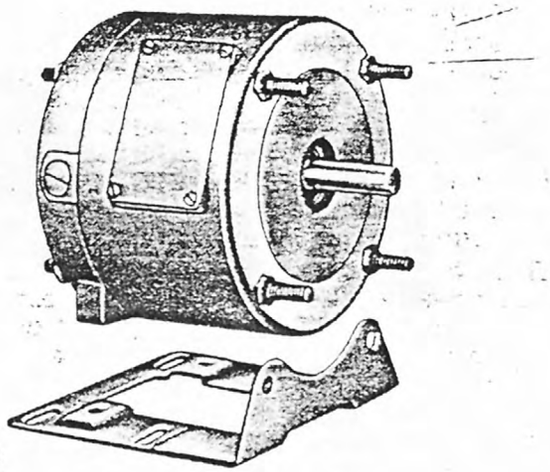

Figure 1

### *Description*

Dayton magnetic disc brake Model 6K233A is used on 56C face motors and speed reducers. Model 3M366 is used on 56C, 143TC and 145TC face motors and speed reducers. Both models are intended for service factor 1 operation. **These brakes are not rated for more than three stops per minute.** They can be mounted in either of two ways: 1) between a motor and a speed reducer, coupling them; 2) on the end of a motor, with the bearing equipped brake output shaft serving as the motor output shaft.

NOTE: These brakes are not intended for accurate positioning applications. They are designed for applications that require rapid stopping and holding power such as conveyors, door openers, etc.

**WARNING: DO NOT INSTALL OR USE THESE BRAKES IN AN EXPLOSIVE ATMOSPHERE.**

| Model | Brake-Hub Bore "X" | NEMA Motor Frame Size |
|---|---|---|
| 6K233B | 5/8" | 56C |
| 3M366A | 7/8"* | 143TC<br>145TC<br>56C |

* With 7/8" OD x 5/8" ID bushing.

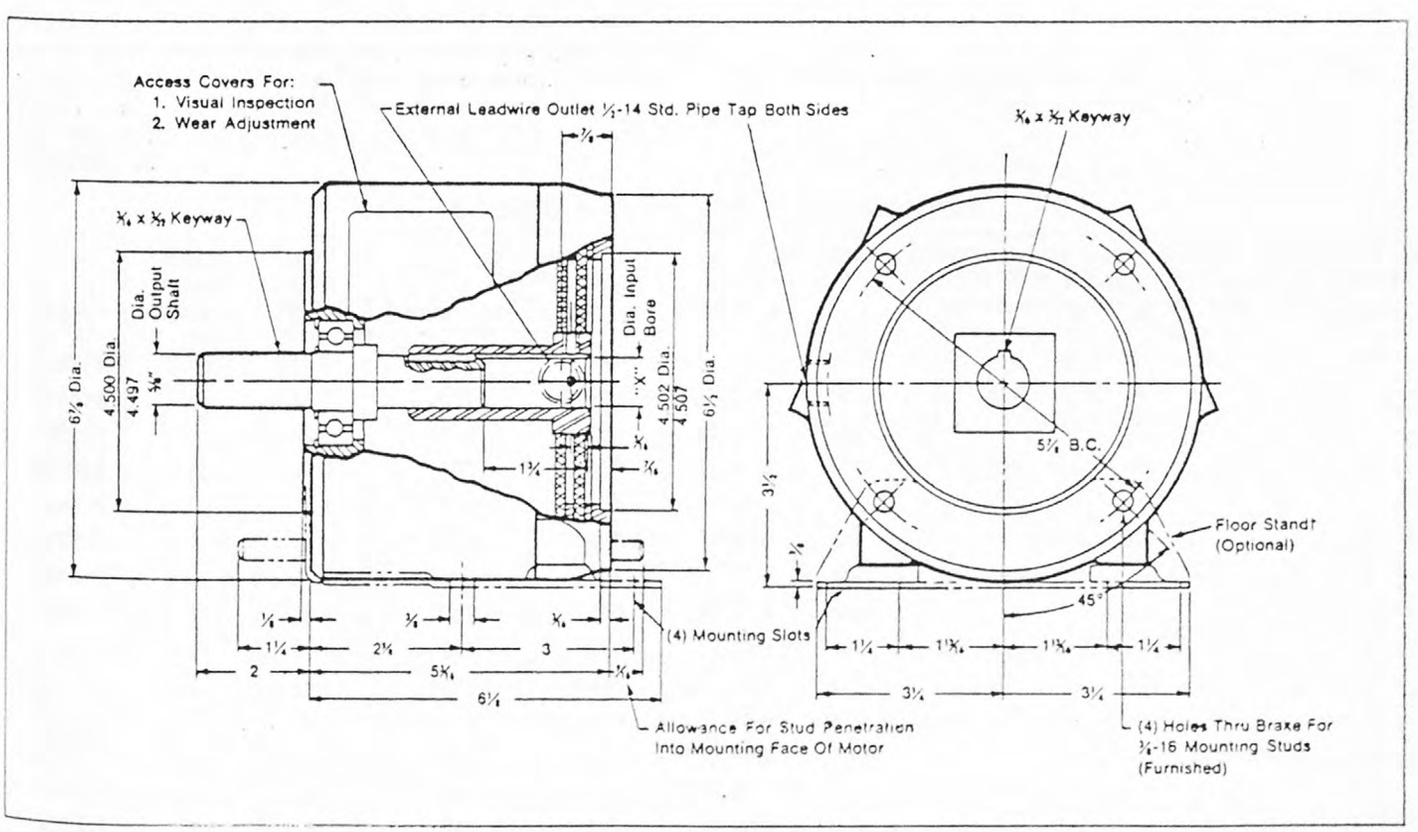


Figure 2c: Description of Brake Unit

INSTALLATION INSTRUCTIONS & PARTS LIST

# RIGHT ANGLE SPEED REDUCER

## MODELS 4Z001B THRU 4Z014B

FORM
5S1283
3520

DAYTON ELECTRIC MANUFACTURING CO. CHICAGO 60648

0280/069/55C

**ATTENTION: READ CAREFULLY BEFORE ATTEMPTING TO INSTALL, OPERATE OR SERVICE THE DAYTON RIGHT ANGLE SPEED REDUCER. RETAIN FOR FUTURE REFERENCE!**

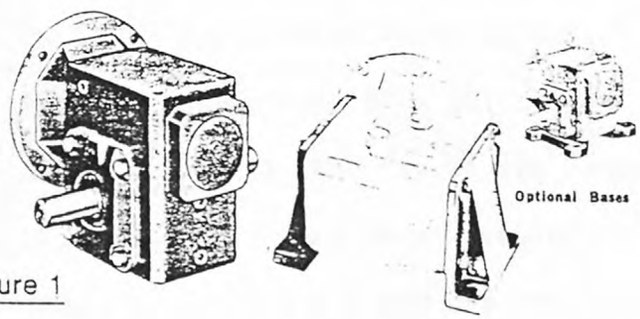


Figure 1

## Description

These Dayton right angle speed reducers are suitable for continuous, low speed, high torque applications in areas where space is limited. They will accommodate NEMA C-face motors (not included). Each reducer is an assembly consisting of a cast iron housing, steel output shaft with key and plastic cover, tapered roller bearing, steel worm mating gear, and manganese bronze worm gear.

Drilled and tapped holes in the top and bottom of the reducer enable mounting it to flat surfaces. Optional mounting bases 6X499, 6X500, 6X502, and 6X503 provide additional mounting positions. (See Figure 1.) The reducer operates correctly when floor, wall, or ceiling mounted in any position **except** with the input flange down (motor shaft pointing up).

### *LIMITED WARRANTY*

*Dayton right angle speed reducers, Models 4Z001B thru 4Z014B, are warranted by Dayton Electric Mfg. Co. (Dayton) to the original user against defects in workmanship or materials under normal use (rental use excluded), for one year after date of purchase. Any part which is determined to be defective in material or workmanship and returned to an authorized service location, as Dayton designates, shipping costs prepaid, will be repaired or replaced at Dayton's option. For warranty claim procedures, see "Prompt Disposition" below. This warranty gives purchasers specific legal rights, and purchasers may also have other rights which vary from state to state.*

*WARRANTY DISCLAIMER. Dayton has made a diligent effort to illustrate and describe the products in this literature accurately; however, such illustrations and descriptions are for the sole purpose of identification, and do not express or imply a warranty that the products are merchantable, or fit for a particular purpose, or that the products will necessarily conform to the illustrations or descriptions.*

*Except as provided below, no warranty or affirmation of fact, express or implied, other than as stated in "LIMITED WARRANTY" above is made or authorized by Dayton, and Dayton's liability in all events is limited to the purchase price paid.*

*Certain aspects of disclaimers are not applicable to consumer products; e.g., (a) some states do not allow the exclusion or limitation of incidental or consequential damages, so the above limitation or exclusion may not apply to you; (b) also, some states do not allow limitations on how long an implied warranty lasts, consequently the above limitation may not apply to you; and (c) by law, during the period of this Limited Warranty, any implied warranties of merchantability or fitness for a particular purpose applicable to consumer products purchased by consumers, may not be excluded or otherwise disclaimed.*

*PROMPT DISPOSITION. Dayton will make a good faith effort for prompt correction or other adjustment with respect to any product which proves to be defective within warranty. For any product believed to be defective within warranty, first write or call dealer from whom product was purchased. Dealer will give additional directions. If unable to resolve satisfactorily, write to Dayton at address below, giving dealer's name, address, date and number of dealer's invoice, and describing the nature of the defect. If product was damaged in transit to you, file claim with carrier.*

**DAYTON ELECTRIC MFG. CO., 5959 W. HOWARD STREET**
**CHICAGO, ILLINOIS 60648**

## *Specifications and Performance*

| Model | Worm Center Distance | Nom. Gear Ratio | Output Shaft End Thrust (Lbs) | Output Shaft Overhung Load (Lbs) | Nom. Output @ 1725 RPM Input | NEMA Frame Size | Continuous Duty Output Torque (In-Lbs) @ Input of 1725 RPM & Given HP (1.0 Service Factor) ¼ HP | 1/3 HP | ½ HP | ¾ HP | 1 HP | 1½ HP | 2 HP |
|---|---|---|---|---|---|---|---|---|---|---|---|---|---|
| 4Z001B | 1.33 | 60:1 | 1270 | 554 | 29 RPM | 56C | 272 | — | — | — | — | — | — |
| 4Z008B | 2.06 | 60:1 | 2071 | 1420 | 29 RPM | 56C | — | 427 | 641 | — | — | — | — |
| 4Z002B | 1.33 | 40:1 | 1104 | 554 | 43 RPM | 56C | 225 | — | — | — | — | — | — |
| 4Z009B | 2.06 | 40:1 | 1783 | 1420 | 43 RPM | 56C | — | 333 | 500 | — | — | — | — |
| 4Z003B | 1.33 | 30:1 | 990 | 554 | 58 RPM | 56C | 182 | 242 | — | — | — | — | — |
| 4Z010B | 2.06 | 30:1 | 1584 | 1420 | 58 RPM | 56C | — | — | 414 | 621 | — | — | — |
| 4Z004B | 1.33 | 20:1 | 652 | 554 | 86 RPM | 56C | 137 | 183 | 275 | — | — | — | — |
| 4Z011B | 2.06 | 20:1 | 1329 | 1420 | 86 RPM | 56C | — | — | — | 447 | 597 | — | — |
| 4Z005B | 1.33 | 15:1 | 759 | 554 | 115 RPM | 56C | 108 | 144 | 216 | — | — | — | — |
| 4Z012B | 2.06 | 15:1 | 1187 | 1420 | 115 RPM | 56C | — | — | — | 344 | 459 | 689 | — |
| 4Z006B | 1.33 | 10:1 | 625 | 554 | 173 RPM | 56C | 76 | 102 | 153 | 230 | — | — | — |
| 4Z013B | 2.06 | 10:1 | 956 | 1373 | 173 RPM | 56C | — | — | — | — | 315 | 472 | 630 |
| 4Z007B | 1.33 | 5:1 | 502 | 554 | 345 RPM | 56C | 40 | 53 | 80 | 120 | 160 | — | — |
| 4Z014B | 2.06 | 5:1 | 761 | 1093 | 345 RPM | 56C | — | — | — | — | — | 249 | 332 |

Figure 2d: Description of Gear Unit

with color coded stripes every 10 feet so that the exact depth of the air-gun in the well would always be known. A linear measuring device will be used for the deep well, where a Vector marine signal cable will be used to lower a seismometer package to the bottom.

The headframe for the hoist was constructed of treated wood and designed to be easily assembled in the field. It consists essentially of five major pieces that are bolted together with 1/2" carriage bolts. Most of the wood is 2" x 10" beams, double beams, or T beams formed with lag bolts. The top of the headframe supports the hoisting pulley, a 12" diameter cast wheel running on a 2" diameter shaft to pillow bearing blocks. Two men can assemble the frame in about 2 hours.

The winch system performed as expected during the experiment. Raising or lowering the air gun would take about 1 hour, mostly involving taping the cables together or coiling them up coming out.

## IIb. The Compressor for the Air Gun

The operating pressure for the air gun was 2000 psi (135 atmospheres or 140 $kgm/cm^2$). A reliable portable source of high pressure is a compressor used for re-filling scuba diving tanks. Such a unit was rented locally. The compressor, a "Poseidon" brand (German made) unit with an integral 2-stroke gas motor (model P91/R) had an output of 5.4 $m^3/hr$ at 1 atmosphere. Since the volume of the gun was $3.3 \times 10^{-3}$ $m^3$ (3.3 liters), and the operating pressure was 135 atmospheres, it would take 26 minutes to fully charge the gun. In practice, the gun did not fully discharge itself, the line (which alone had a volume of 40 cu. inches (643 $cm^3$)) and the reservoir of the compressor, so the gun could be fired about every 12 minutes. Usually the pressure would drop to about half with a single firing.

Since the compressor could produce 320 atmospheres, more than twice the rating of the air gun, a high pressure relief valve was purchased, pre-set at 170 atmospheres. It was installed in the line between the compressor and the monitor/control panel. The panel included a 10" diameter, 3 K psi Heise gauge with three high pressure valves (all obtained from surplus) to allow charging, venting, or closing off the gun. It was necessary to maintain pressure on the gun at all times to prevent water entry. At 185 meters (600 feet) depth the minimum pressure required is 20 atmospheres (300 psi). The Heise gauge was very useful for determining the leakage rate of the gun or lines, especially for determining if the system would hold sufficient air overnight.

## IIc. The Air Gun Itself

This was a Bolt Associates PAR air gun model DHS-1900B, with a time break solenoid valve and a 200 cubic inch chamber. It is designed for down hole use, and has a maximum diameter of only 15 cm (6"). Further details of the gun can be obtained from the Bolt Associates literature.

An integral feature of this gun was a time break solenoid and pressure transducer that was to provide an electrical indication of the actual firing of the gun by sensing the re-pressurization of the operating chamber by the upward movement of the shuttle assembly de-pressurizing the firing chamber. Since the firing solenoid only triggers the release of the shuttle, this pressure transducer would provide a much more accurate time-break than the pulse on the firing line.

Power for the firing circuit and time break signal was obtained from a separate control unit powered from the AC line.

## IId. The Trigger Time Delay

As described below, the horizontal scale of the storage oscilloscope could accomodate 4028 points using the full memory. In order to have less than millisecond resolution, then, only one second of data could appropriately be stored. So for seeking arrivals later than that, a precise time delay between the firing of the air gun and the triggering of the scope was needed. Further requirements were that it be battery operated and easily set to the precise delay desired.

Figure 3 is the schematic of the unit constructed utilizing the Motorola device MC14522B programmable BCD 4-bit counter. The unit includes a 1 mhz crystal oscillator divided to 10 Khz or $10^{-4}$ sec/cycle. Thus the least resolution of the unit is $10^{-4}$ second. The six cascaded counters are programmed by 6 thumb wheel switches to provide delays up to 99.9999 seconds. The unit was housed in a 5 x 15 x 25 cm aluminum box.

## IIe. The Digital Storage Oscilloscope

One of the requirements of the experiment was to attempt to increase the signal-to-noise ratio of the signal by repeatedly firing the air gun and storing the data from a number of shots. Then the data would be simply added or stacked with the expectation that the noise would randomly cancel and the signal would be enhanced. All available digital storage oscilloscopes were examined, and the Nicolet Explorer III system was selected as meeting our needs. It not only has a large 4098 x 12 bit capacity, but an integral mini-floppy disc recording system for storage and retrieval of data. Figures 4a-d provide general details and specifications of the unit. Further understanding of its operation will be discussed under III below.

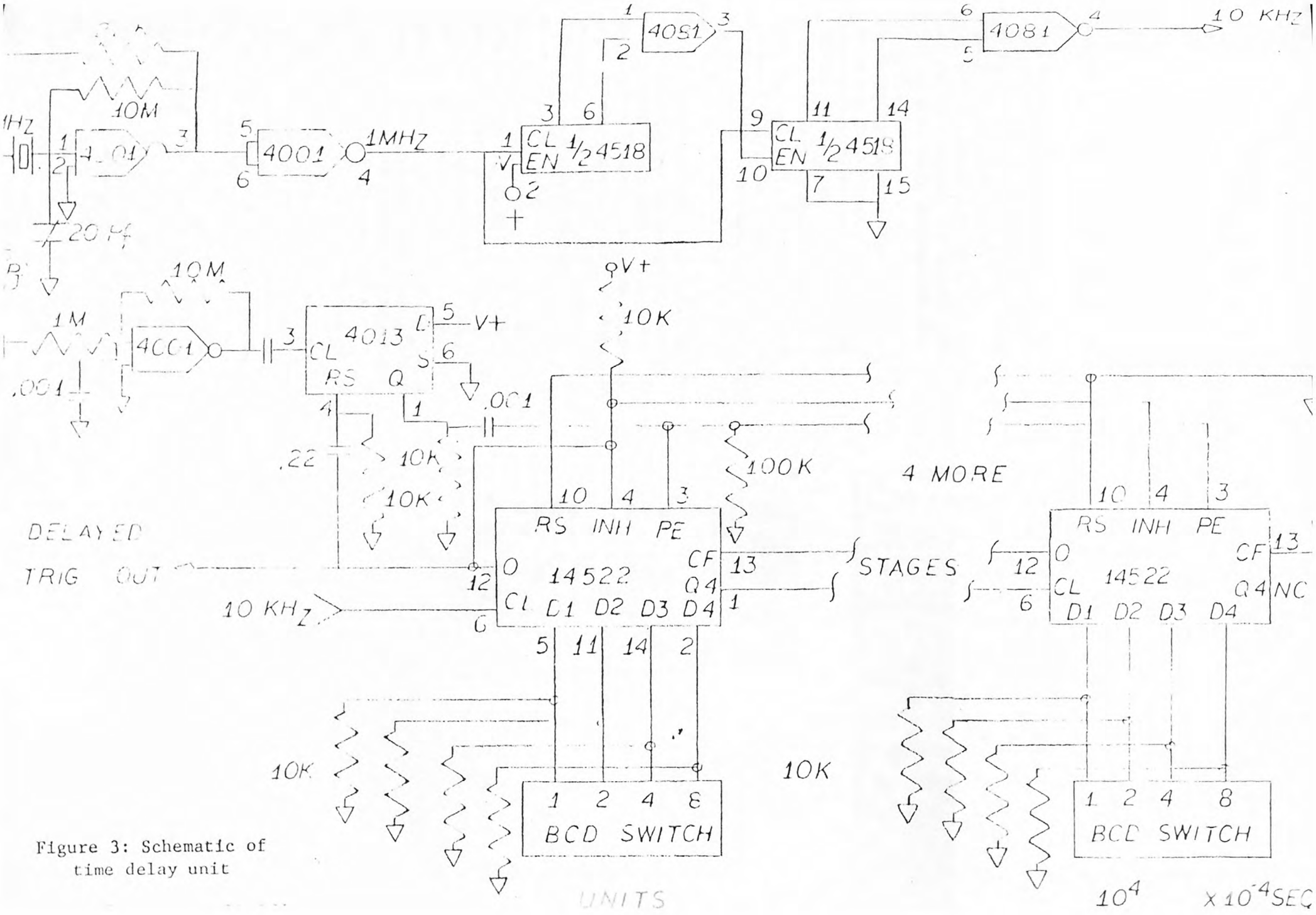


Figure 3: Schematic of time delay unit

Figure 4a

EXPLORER III

This is identical to the Explorer II, but is constructed to include a third mainframe bay which includes whatever digital interface option has been ordered, or the magnetic disk recorder, or both.

Explorer III is truly a remarkable instrument, whether used as a "pure oscilloscope" with the disk option, or as a component in highly sophisticated data analysis systems.

In the "pure oscilloscope" role, where signals are observed without computer aids, the disk gives the instrument the extraordinary capability of storing literally as many signal waveforms as you wish, for as long as you wish, for quick and easy recall.

Waveforms may be stored automatically, as each signal occurs. This is helpful if signals occur in rapid succession, and even more helpful if they occur rarely over a long period, since your presence is not required.

In systems including computers, the Explorer III with IEEE-488 (GPIB) interface can be controlled by the computer to initiate a measurement, furnish the information to the computer, then initiate successive measurements and readouts. Detailed information on this interface and on the RS-232 and parallel 12-bit binary interface is available on request.

SELECTING A PLUG-IN UNIT

Always select the lowest bandwidth plug-in unit which will satisfy your expected needs. The lower the bandwidth, for a given cost, the better the precision, sensitivity, and noise characteristics that can be attained. This effect is not noticed much in analog oscilloscopes, because the cathode-ray tube limits or disguises the effects, so fundamental amplifier effects are not noticed. Thus, the tendency is to obtain as much bandwidth as possible, and this tendency should be avoided in the case of digital oscilloscopes. This is because digital display expansion, and numerical voltage and time values eliminate CRT limitations and expose fundamental limits. Long sweep times expose drift and ultra-low-frequency noise effects that most of us never experienced before.

THE MODEL 201 PLUG-IN

This is a low frequency plug-in (15-35 kHz, depending upon sensitivity setting). It utilizes very high input impedance, low bias current instrumentation amplifiers in each of the two signal channels. The low noise, low drift, high common mode rejection characteristics of the amplifier make high sensitivity possible. With an ADC resolution of 12 bits, and a sensitivity of ±10 millivolts full scale, signal details as low as 5 μv are observable. Hours-long sweeps may be used. For most measurements involving transducers, this plug-in unit is excellent.

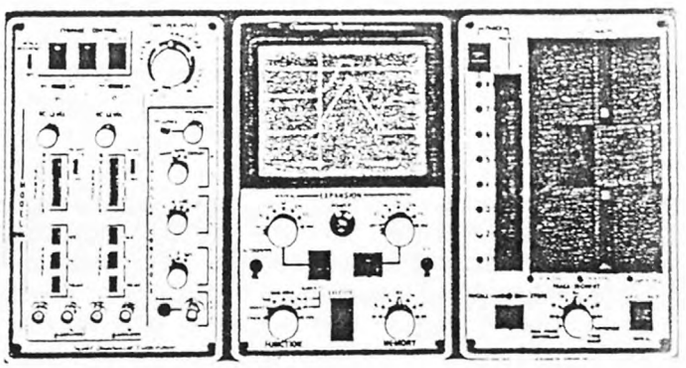

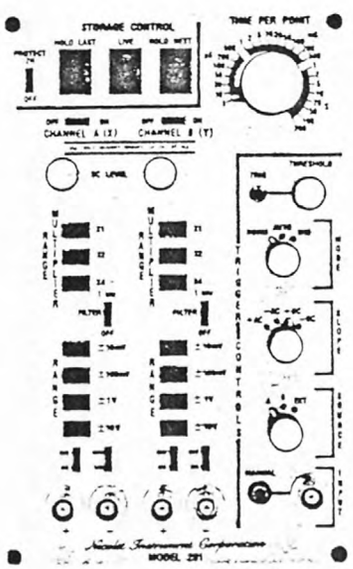

Figure 4b

THE MODEL 206 PLUG-IN

The most popular plug-in is the two channel model 206, because of its combination of high speed (500 ns rise time) and high resolution (12 bits). It is useful in almost all transducer measurements, except fast photoelectric transducers, and for a great variety of direct electrical signal measurements. As is the case for all Explorer plug-in units, it provides the mid-signal trigger feature. In the case of the model 206, you can select what percentage of the sweep will correspond to pre-trigger information.

THE MODEL 204-A PLUG-IN UNIT

For medium resolution measurements, the two channel model 204-A plug-in provides 50 ns rise times with 8 bit resolution. Its most frequent application is for capture of single transients, but this unit is exceedingly valuable in design and troubleshooting of medium speed digital electronic circuits. In such applications the mid-signal triggering characteristic is invaluable, since it allows observation of conditions preceding sporadic events.

THE DISK RECORDER

The disk recorder can store 32K data points, along with information indicating the voltage and time settings used in each of the measurements. It can store 32, 16 or 8 waveforms of 1024, 2048 or 4096 points, or a single waveform of 32,768 points (under certain conditions). Storage may be by manual command whenever interesting signals have been stored in the mainframe memory. This requires 2 seconds for 4096 points. Storage also may be in automatic sequence as each signal occurs, until the disk is full, at a maximum rate of ½ second per 1024 points plus about 1 second for disk motor start. The disk motor automatically stops after 5 seconds if no new signal has occurred, and restarts automatically when the next signal occurs.

For low frequency information, involving sweep speeds of 500 μsec per point or longer, the disk can record one continuous "sweep" of 32K data points. If two signal channels are in use, sweep speeds must be 1 millisecond per point or slower. In the case of very slow sweep speeds, the disk motor does not run continuously, but waits until 1024 data points have been received by the mainframe, and restarts to record these on the disk. It again waits for the next 1024 points. The process ends after 32K points have been recorded.

The disks can be removed or inserted in two or three seconds. The recording format is not "standard", but disks recorded in one Explorer can be read by another. Disks may be reused many times, or filed as long as desired.

Since voltage and time scales are recorded with each waveform, when information is recalled to the mainframe, the displayed numerical voltage and time values will be proper for each waveform, even if different for each.

Information on disks is accessible via IEEE-488 (GPIB) bus; external computers can control the disk recorder to cause any recorded waveform to be transferred to the computer, and modified data may be received from the computer for recording and display. The computer may initiate the measurement and the recordings on disk.

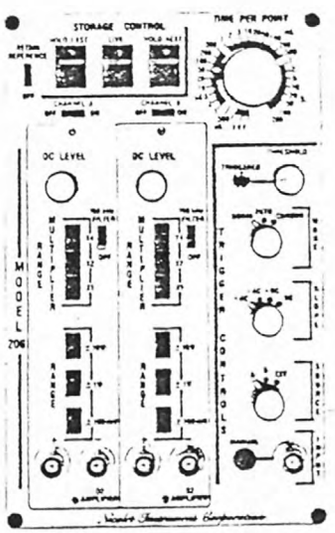


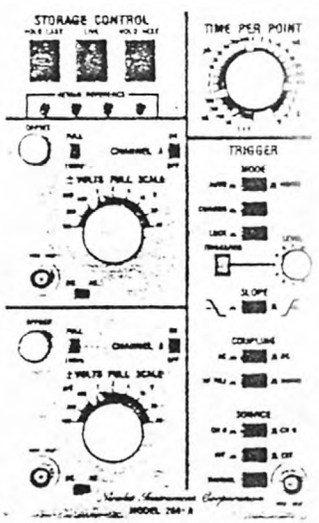


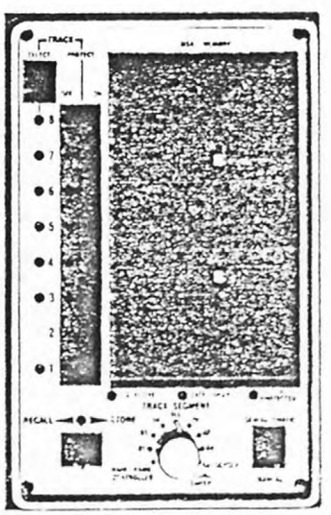

Figure 4c

# EXPLORER SPECIFICATIONS

| EXPLORER I: | |
|---|---|
| Memory: | 4,096 words by 12 bits. Data can be stored in all or half of memory. |
| Power Requirements: | 101, 115, 202 or 230 volts ac (±10%) 50-60 Hz (±5%), 225 volt-amperes. |
| Display Expansion: | Digital expansions of x2, x4, x8, x16, x32 or x64, horizontal and/or vertical. Display may be automatically centered around intersection of horizontal and vertical cursors. |
| Display Mode: | Choice of X/Y or Y/T. |
| Data Functions: | Data may be inverted, moved, added, subtracted, outputted to a pen recorder or manually erased. |
| Pen Recording: | Control signals to operate an external XY pen recorder are provided. Information is read out at a variable rate, many data points per second in featureless regions of the plot, and more slowly in regions where the pen movement is substantial. The linear velocity of the pen is maintained essentially constant, adjustable to match the speed capabilities of the recorder. Output voltages are nominally 0-5 volts. |
| Physical Size: | |
| Length: | 18⅝" (47.3 cm) |
| Width: | 11¼" (28.6 cm) |
| Height: | 9⅝" (24.5 cm) |
| Weight: | 30 lbs. (13.5 kg) |

| EXPLORER II: | |
|---|---|
| Memory: | 4,096 words by 12 bits. Data may be stored in all of memory, either half or any quarter. |
| Power Requirements: | 101, 115, 202, 230 volts ac (±10%) 50-60 Hz (±5%), 225 volt-amperes. |
| Display Expansion: | Digital expansions of x2, x4, x8, x16, x32 or x64, horizontal and/or vertical. Display may be automatically centered around intersection of horizontal and vertical cursors. |
| Display Mode: | Choice of X/Y or Y/T. |
| Data Functions: | Data may be inverted, moved, added, subtracted, outputted to a pen recorder or manually erased. |
| Pen Recording: | Control signals to operate an external XY pen recorder are provided. Information is read out at a variable rate, many data points per second in featureless regions of the plot, and more slowly in regions where the pen movement is substantial. The linear velocity of the pen is maintained essentially constant, adjustable to match the speed capabilities of the recorder. Output voltages are nominally 0-5 volts. |
| Plug-Ins: | Accepts Models 201-2, 204-A, 206-1 and 206-2. |
| Physical Size: | |
| Length: | 18⅝" (47.3 cm) |
| Width: | 11¼" (28.6 cm) |
| Height: | 9⅝" (24.5 cm) |
| Weight: | 30 lbs. (13.5 kg) |

Figure 4d

# MEASUREMENT SPECIFICATIONS

| PARAMETER | EXPLORER I | 201 | 204 | 206 |
|---|---|---|---|---|
| Maximum digitizing rate, MHz | 1 | 0.2 | 20 | 2 |
| Resolution, percent | 0.025 | 0.025 | 0.4 | 0.025 |
| Accuracy, % of full scale | 0.2 | 0.1 | 0.5 | 0.2 |
| Linearity, % of full scale | 0.1 | 0.1 | 0.5 | 0.1 |
| Maximum sensitivity, full scale range, millivolts | ±100 | ±10 | ±100 | ±100 |
| Maximum voltage range, volts | ±40 | ±40 | ±40 | ±40 |
| Safe overload, at maximum sensitivity, volts | 100 | 100 | 100 | 100 |
| Safe overload, at minimum sensitivity, volts | 200 | 200 | 200 | 200 |
| Amplifier bandwidth, at maximum sensitivity, MHz | 0.2 | 0.015 | 7 | 1 |
| Amplifier bandwidth, at minimum sensitivity, MHz | 0.5 | 0.035 | 7 | 1 |
| Sample time uncertainty, ns | 25 | 25 | 3 | 10 |
| Noise, >100 Hz, % of full scale, rms | 0.02 | 0.02 | 0.4 | 0.02 |
| Noise, 0.01 Hz to 100 Hz, $\mu$v rms | 25 | 2 | 100 | 25 |
| Drift/°C, % of full scale | 0.02 | 0.02 | 0.2 | 0.02 |
| Input impedance, most sensitive amplifier settings, megohms | 1000 | 10,000 | 1 | 1 |
| Input impedance, least sensitive amplifier settings, megohms | 1 | 1 | 1 | 1 |
| Input bias current, 25°C ambient, pa | 20 | 10 | — | — |
| Common mode rejection ratio at maximum amplifier sensitivity setting | $10^4$ | $10^5$ | (Note 2) | $10^4$ |
| Common mode voltage range, percent of full scale range setting | 150 | 150 | (Note 2) | 150 |
| DC offset range, % of full scale range setting | 100 | 100 | 150 | 100 |
| Sweep Speed ranges for all plug-in units are in steps of 1, 2, 5, 10, . . . times maximum speed setting in microseconds per point. | | | | |
| Maximum speed, time per point, $\mu$sec | 1 | 5 | 0.05 | 0.5 |
| Minimum speed, time per point, seconds | 20 | 200 | 20 | 200 |
| Trigger sensitivity, % of full scale range, internal triggering | 10 | 10 | 10 | 10 |
| Trigger sensitivity, volts, external triggering | 0.5 | 0.5 | 0.5 | 0.5 |
| Trigger range, volts, external triggering | 5 | 5 | 5 | 5 |
| Trigger range, % of full scale, internal triggering | 10 | 10 | 10 | 10 |
| Mid-signal trigger point, percent of one sweep | 25 | 25 | 0-100 | 0-100 |
| Number of data points per waveform when using a single channel | 2K, 4K | 2K, 4K | 1K, 2K, 4K | 1K, 2K, 4K |
| Number of data points per waveform when using two channels | 2K | 1K, 2K | 512, 1K, 2K | 512, 1K, 2K |

NOTES:
1. The Model 206 plug-in is available in one or two-channel versions, 206-1, and 206-2.
2. Model 204 plug-in utilizes single-ended amplifiers; common-mode rejection data do not apply.
3. All plug-in units provide the "retain reference" capability, in which alternate data points are protected against change during observation of live waveforms. This permits easy comparison of live and stored signals.

## IIf. Signal Sources

Two types of arrivals were sought: deep arrivals from below the well, and long-path refracted arrivals from some nearby seismic station. For arrivals from beneath the well, a single vertical component seismometer/amplifier package was installed about 50 meters from the well. It was operated at moderate gain because of the relative high industrial noise around the well site (a couple of cotton gins were operating nearby). The frequency response of the unit was flat to velocity from 1 to 20 hz.

For an attempt to record a refracted arrival over some distance, the permanent station GRT was received by telemetry and discriminated using SLU telemetry equipment. Again, response was flat to velocity from 1 to 20 hz. The received signal from GRT was recorded on an MEQ-800 as a monitor so as to avoid firing during high local noise at GRT. GRT is 6.5 km to the east, so a refracted arrival would be expected to take about 1.7 seconds for a head wave in the upper layer.

Later in the experiment at Ridgely, an attempt was made to use a string of geophones connected in series to enhance the signal. However, we were unfamiliar with such procedures, and the hasty attempt produced only 60 hz noise because the string was placed under power wires alongside a railroad track. If future studies of this kind are attempted, a geophone array will be deployed at a greater distance from the source in a noise-free region.

# III. Data Acquisition

## IIIa. Experimental Procedure

The general course of each data-acquisition session followed the same basic routine. The gun was charged to the operating pressure and manually fired as desired. The pressure-relief valve on the air line proved to be quite useful in the event of distractions with the equipment; its noisy blat reminded us that the compressor was running and charging the gun. We found that the output of the gun's time break pressure transducer needed to be amplified by a modified sono-buoy hydrophone amplifier to provide a very sharp pulse to the trigger delay unit

The trigger delay and oscilloscope time base were adjusted to suitably display the event in the time domain of interest. Upon being triggered, the oscilloscope would acquire and display the data immediately. We used half of the available storage, or 2014 points, for each event. This seemed sufficient for our resolution, and allowed 16 events to be stored on each disc. It also facilitated summing the data, since both events to be summed could be stored in the memory of the scope.

Because of the slow recharge time of the gun, and other problems discussed below, the gun was only able to be fired about every 20 minutes. This would have provided at best marginal resolution of stacked data if velocity anomalies due to tidal stress were to be observed. It also meant that it would take about 4-5 hours to record 15 arrivals. Generally the work was done at night when cultural noise was at a minimum.

## IIIb. Preliminary Test at CCMO

In order to evaluate the whole system's performance, arrangements were made to test the entire system at the CCMO test site 25 km west of St. Louis. A shallow pond was available about 100 meters west of the farmhouse, and the seismic station was about 200 meters west of the pond. So it was convenient to receive the seismic telemetry signal at the house, discriminate it, and use the resultant signal. A hydrophone had also been installed in the pond and was used for some of the tests.

Initially the air gun was strapped to a wooden pallet submerged about 1.5 meters. A nice water spout resulted, but coupling to the ground was poor, until the wood was blown apart and the gun settled into the mud at the bottom of the pond. The frogs in the pond all seemed to survive.

The first experiments were done on 13 September 1980, after a 3 hour delay to repair the seismic telemetry station after a lightning strike. Initially the gun was fired at only 400 psi, but eventually worked up to 2000 psi. Generally, the pressure dropped only to 1500 psi. In all, 24 events were recorded, with and without the trigger delay. The events could be stacked rather reliably. The travel time to the station was exactly 117.0 msec as long as the gun pressure was greater than 1300 psi. It was less at lower pressures (110 msec at 400 psi; 115 msec at 1000 psi) for some unknown reason. The tests were continued on September 14.

## IIIc. Data Acquisition at Ridgely Well

The hoist and headframe were erected over the well on 17 September 1980. The air gun was lowered down the well the next day. The logistics of keeping 245 meters (800 feet) of firing line and air hose from tangling up made the process take about 2 hours. Periodically the gun was hoisted to make sure it had not lodged in the well. There was particular concern after the first few firings that something in the well might come loose and wedge the gun in, but no such event occurred. As a precaution at the surface, a slatted plywood cover was provided to keep foreign objects from falling in.

Initial firings began on 18 September using a geophone near the well for the signal receiver. Unfortunately, it picked up considerable noise from the compressor, so the next day it was relocated to a field 50 meters from the other side of the well. At night it became necessary to shut off the compressor before firing the fun if data from the local unit was being used.

An initial surprise and problem was the length of time it took for the air bubble to clear the well. It actually took about 12 minutes for the bubble to reach the top of the water 10 m down in the well. If the gun was fired twice in succession, not only was the data terrible (because of the complex water column), but two bubbles rising would actually pump the well and cause it to overflow. A rough calculation of the bubble volume, assuming that half the air in the chamber was released, shows that the bubble would occupy only 34 cm of the 20 cm diameter water column at the 180 meter depth but 6.9 meters of the column at the surface.

At first we were uncertain of what we were seeing in the data, and

most of the data from September 18 and September 19 were of a trial and error nature. Considerable time was spent attempting to acquire data from the GRT station. Most of the shots were fired at night in order to minimize noise from cultural activity. A summation of the data suggested several possible pulses with travel-times as great as 8 seconds. However, repeated firings failed to yield consistent arrival times, so those pulses were inferred to be caused by noise or disturbances near the station.

Later experiments attempted to find reflectors directly below the well. The results of this effort are discussed below. Unfortunately, this work was compromised when apparent errors in the delay timer or shot time break started to show up, compromising most of the later data.

On September 24 the batteries in the delay time and time break amplifer were replaced, but evidence of instability in the time break from the gun persisted. Also the amplitude of the arrival was much smaller, indicating that the gun was partially filled with water (dicussed below with repect to the gun leak rate and maintaining a minimum pressure between work periods). The gun was hoisted out and emptied of water on September 25 and seemed to seal properly.

Further efforts on subsequent days were fruitless because of the time break instability problem and a rather serious leak rate from the gun that was not remedied when the gun was dismantled and the seals were replaced. The experiment was terminated when the power supply transformer in the air gun firing control box burned out altogether.

## IIId. Discussion of Problems Encountered

1) The length of time that was required for the air bubble to clear the well was discussed above. It would certainly preclude any rapid firing of the gun even if a larger air compressor were available.

2) The air compressor performed reasonably well, although the engine needed some carburetor adjustments and the drive belt wore out in just five days. A more conservatively designed unit would be preferred. The need to bleed water condensate from the traps every 15 minutes or so was a nuisance; an automatic drain device would be preferred.

3) The problem of maintaining a minimum air pressure in the gun while the experiment was inactive was aggravated by the increasing leakage rate from the gun. Nonetheless, a storage cylinder on the air line to the gun would certainly have helped. Normal leak rates averaged 150 psi/hour, which allowed about 12 hours of time before the minimum 500 psi level was reached if the gun were left charged at 2000 psi. Accelerated leakage rates required frequent visits to the site to recharge the system. (Note: At the CCMO tests, the leakage rate was only about 200 lbs/day at 1500 psi.)

The attempt to replace the seals in the gun was unsuccessful, either because of the fact that one or more spare seals were not supplied, or because of errors in re-assembly, although the manual was followed very carefully. Our unfamiliarity with the air gun device most likely contributed to the problem.

4) The time break instability problem was never fully resolved, but may have been a result of a shorted winding in the control box transformer. When this occurred, the load for the shorted secondary

winding was connected to the other good winding. The transformer still overheated, so was only turned on to fire the gun, until it failed altogether. In the mean time, the power to operate the firing circuit and and time break pressure transducer were obtained from the same marginal power source. This may have allowed firing noise into the time break circuit. Or there may have been a malfunction in the gun itself, or water in the operating chamber. The problem was never resolved.

5) The signal to noise ratio of the seismic signals was acceptable but not the best available. The deployment of geophone arrays at GRT and for the local unit would certainly have been of advantage. Perhaps a station about 1 km from the well would also have been quite useful, since the arrivals from the water column would probably be attenuated enough.

# IV. Results

The only possibility that deep reflections were observed occurred when the detector was located near the well. Figure 5 depicts seismograms from one of the shots as recorded by a geophone 30 m from the well. Similar wave forms occurred for all shots that did not exhibit malfunctions. The first wave packet in each case commences at about 0.3 s and continues to beyond 0.5 s. The earlier of these times corresponds approximately to that predicted by a wave travelling up the water column. The velocities (474 m/s) are only slightly faster than the velocity of sound in water (435 m/s), presumably because a small portion of the path near the surface is through sediments, rather than water. The later part of the packet arises from waves reflected at the bottom of the well before travelling upwards.

The second wave packet, between 0.8 s and 1.0 s, corresponds to waves which travel up the well, are reflected at the surface, travel down the well, and are reflected at the bottom of the well before travelling to the surface. These waves thus make three traverses through the well. Again, the latter part of the wave packet corresponds to energy reflected off the bottom of the well just after leaving the gun. The average velocity obtained for the early part of the wave packet is about 473 m/s, a value very close to that obtained for the wave travelling through the well only once.

Using a value of 473 m/s, arrival times for later multiple reflections of waves travelling in the water column can be predicted. The next packet of energy for the waves restricted to the bore hole should arrive at 1.70 s. Note that a small arrival does occur at about

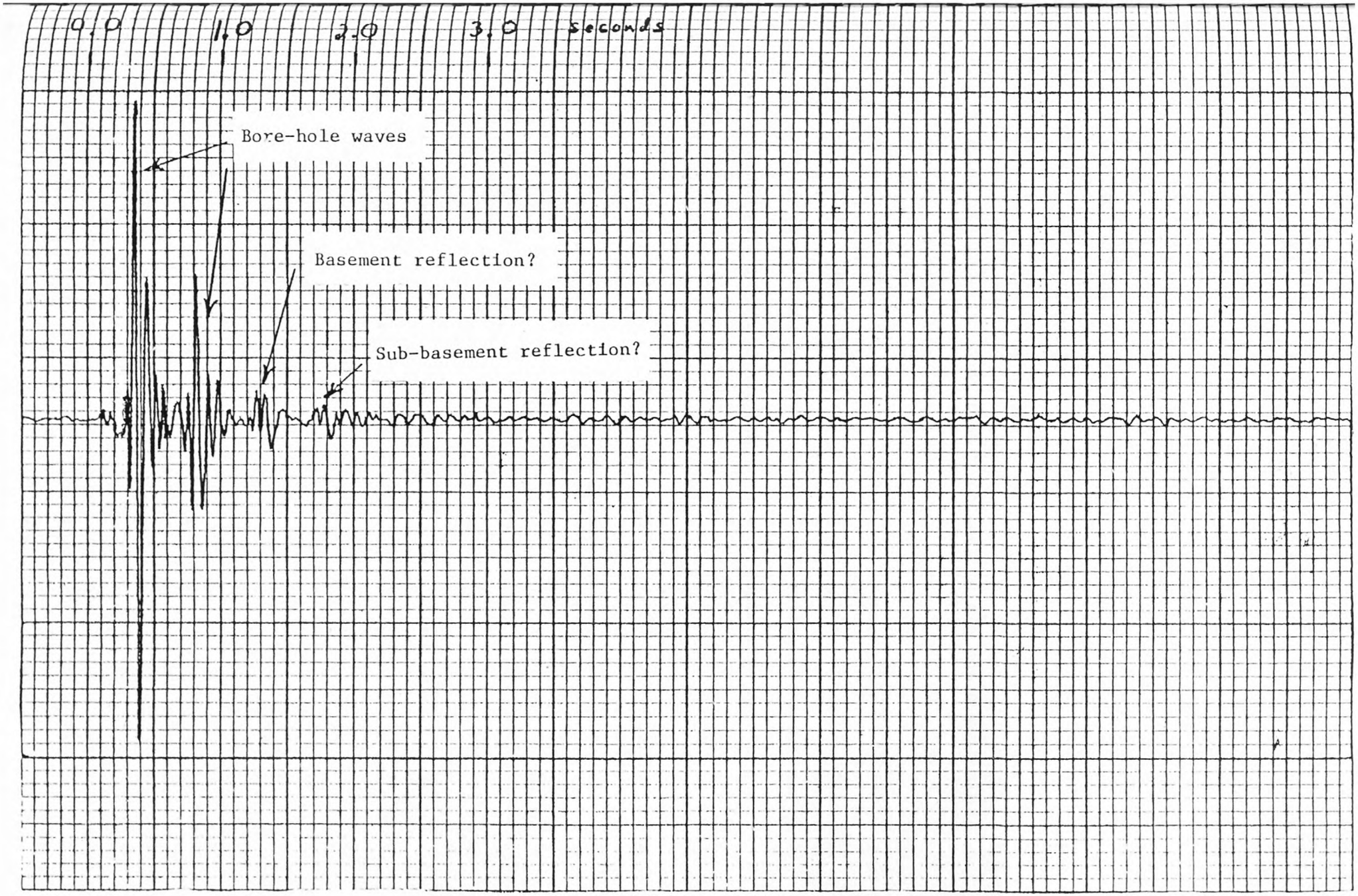


Figure 5. Example seismogram recorded 30 meters from the Ridgely well.

1.7 s; however, the wave shape differs substantially from that of the earlier arriving waves.

One more wave arrives at a time of 1.3 s. This time cannot be explained by waves confined to the well, and we interpret is as either a reflection from the basement surface or a multiple reflection from the Paleozoic surface. That time corresponds approximately to times of scattered reflections in the record sections of Zoback (1979). The relatively large amplitude of the phase we recorded perhaps favors the possibility that it is a primary reflection and not a multiple.

There is a possibility that the latest arrival (~ 1.8 s) is a reflection from deeper in the basement. Assuming a basement velocity of 6 km/s, that time would imply that the reflector lies at a depth of about 1.5 km beneath the basement surface. However, the possibility that the phase is a multiple reflection cannot be ruled out.

## V. Conclusions

It appears that we may have been successful in recording a reflection from the basement surface (if the possibility of a multiple reflection can be ruled out) and possibly from an interface within the basement. We therefore achieved one of the goals of the project. The second goal, that of observing temporal variations in travel time was not achieved, primarily because of difficulty in achieving stable triggering times.

It is important to note, however, that arrival times could be resolved to 1 or 2 ms. That resolution is good enough to permit detection of temporal variations in arrival times produced by Earth tides, as inferred from earlier studies. If problems of triggering stability and seepage into the gun can be overcome, it will be worthwhile to repeat the experiment.

# VI. Appendix

## Hardware and Equipment Costs

Hoist and headframe costs:

| | | |
|---|---|---|
| Motor, variable speed | $255.00 | |
| Magnetic brake | 83.00 | |
| Gear reducer and mounts | 228.00 | |
| Reversing switch | 22.00 | |
| | | $ 558.00 |
| Sprocket gears and chain | 200.00 | |
| Pillow blocks | 170.00 | |
| Shaft material and machinery | 220.00 | |
| | | $ 590.00 |
| Headframe pulley (surplus) | 40.00 | |
| Wood for headframe | 240.00 | |
| Hoist cable, 1000', 1/4" | 470.00 | |
| | | $ 750.00 |
| Hoist & headframe subtotal: | | $1898.00 |

Other costs:

| | | |
|---|---|---|
| Air gun rental | 3600.00 | |
| Nicolet scope and x-y recorder rental | 1128.00 | |
| Compressor rental | 250.00 | |
| Relief valve for compressor | 200.00 | |
| Other costs subtotal: | | $5178.00 |
| Grand total: | | $7076.00 |

## VII. References

Clymer, R.W., High-precision travel-time monitoring with seismic reflection techniques, Ph.D. Thesis, University of California, Berkeley, 188 pp., 1980.

Mitchell, B.J., W. Stauder, and C.C. Cheng, The New Madrid seismic zone as a laboratory for earthquake prediction research, J. Phys. Earth, 25, Suppl., 543-549, 1977.

Zoback, N.D., Recurrent faulting in the vicinity of Reelfoot Lake, northwestern Tennessee, Geol. Soc. Am. Bull., Part I., 90, 1019-1024, 1979.

# Earthquake Location and Apparent Velocity using Curved Wave Fronts across a Regional Array

by

Brian J. Mitchell

The previous semi-annual technical report described a method for determining apparent velocity (or $dT/d\Delta$), azimuth of approach, and epicentral distance to seismic events using wavefront curvature and non-linear least-squares. The computer program which applies this method has recently been improved to permit the assignment of quality factors to each reading. It has been implemented in time sharing on the PDP 11/70 at Saint Louis University and on the IBM 4331 at NORSAR (Norwegian Seismic Array).

A write-up on the applications and use of the program appears on the following pages. Examples, utilizing hypothetical arrival times at Saint Louis University's Southeastern Missouri network and Svalbard network, are also provided.

The program has been used successfully to locate earthquakes in Svalbard which occurred about 200 km north of the Svalbard network (Bungum, Mitchell, and Kristoffersen, 1981). Since those earthquakes were well outside the network, HYPO71 did not provide useful locations. Further, when plane waves, rather than spherical waves, were assumed, large errors were associated with the locations. Consequently, this first application of BEAM4 was highly successful.

## Reference

Bungum, H., B.J. Mitchell, and Y. Kristoffersen, Concentrated earthquake zones in Svalbard, Tectonophysics, submitted, 1981.

# Program BEAM4

by

**B.J. Mitchell**

## Description

BEAM4 is a program which can be used to determine (1) apparent velocity and (2) direction of approach of any seismic phase across a network of 4 or more stations. When using the program it is not necessary to make the usual assumption that the wave fronts are plane. If spherical waves are assumed, the epicentral distance can be assumed to be known or can be solved for as a third unknown. After the direction of approach and epicentral distance have been determined, the epicentral coordinates can be calculated. A third mode of operation assumes that the epicentral coordinates are known and only the apparent velocity is solved for.

To date, the program has been implemented (in time sharing) on the PDP 11/70 at Saint Louis University and on the IBM 4331 at NORSAR (Norwegian Seismic Array). It currently can be used for arrival times from an array of up to 25 stations (300 differential travel times). All of the necessary directions for use of the program are displayed on the terminal screen as they are needed. The necessary equations employ spherical trigonometry and are fairly lengthy so they will not be given here. A brief summary of the theory employed in the program is given in the April 1980 semiannual report to the USGS from the Department of Earth and Atmospheric Sciences, Saint Louis University. It is expected that a fuller description will appear in a forthcoming publication.

## Applications

BEAM4 has several potential uses, among which are those given below:

1. Approximate locations for teleseismic events. The best way to perform these locations will be to solve for direction of approach and apparent velocity assuming plane wave fronts. Knowing the direction of approach, the epicentral distance (obtained from an S-P distance relation) can be entered to compute the epicentral coordinates.

2. Location of regional events outside the network. Two possibilities exist for this computation, in both of which curved wave fronts must be assumed.
   a. Compute apparent velocity and direction of approach, assuming the distance to the nearest station is known through an S-P distance relationship, or
   b. Compute apparent velocity, direction of approach and distance (R) simultaneously. If the distance to the event is greater than a few array dimensions, R will not be very well determined.
3. $dT/d\Delta$ measurements using teleseismic events. Assume plane waves if the events are more than several hundred km distant and assume curved wave fronts at shorter distances.
4. Phase velocity determinations of surface waves from nearby sources. If the epicentral location is known, solve for only apparent velocity and direction of approach assuming curved wave fronts. If it is not known, solve for apparent velocity, direction of approach and distance simultaneously.

Options Available with BEAM4

In order to use BEAM4 you must assume that the projection of the travelling wave front on the earth's surface is either plane or circular. A first guess is then made for the following paramters:

$V_a$ - apparent velocity (km/sec) of the wave front across the array

BAZ - back-azimuth (degrees) to the seismic event from the nearest station

R - distance (km) between the event and the nearest station (for plane waves the value of R is immaterial).

The following flowchart indicates the options which are then available. These options are implemented by making BAZ and R either positive or negative in the first guess.

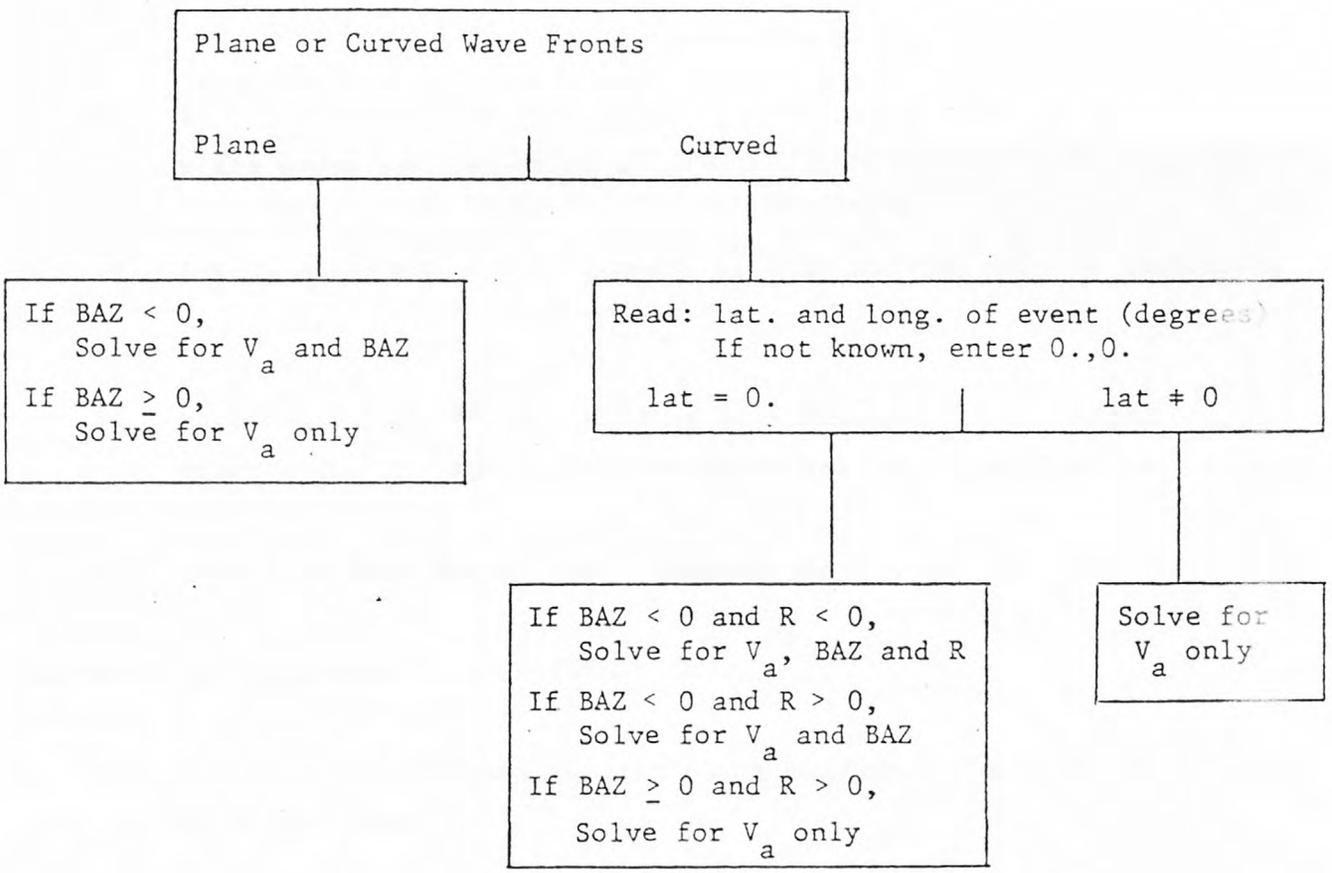


Using BEAM4

It is assumed that a library file of network stations has been created which includes station name, station latitude and station longitude (N and E positive) in the format (1X, A4, 5X, 2F10.4). For example, the stations of the Central Mississippi Valley network are on a file named NETWORK on the PDP 11/70 at Saint Louis University.

After going into execution, the following message will appear on the screen.

1. Enter: date of event (max 80 characters)

After the date is entered, you will get the message

2. Enter: event information (max 80 characters)

Entries for 1 and 2 above are in 20A4 format. Entries for later statements, except 5 and 7 below, are in free format, the numbers being separated by commas.

3. if curvature of the wave front is considered enter 1, if plane waves assumed enter 0

If 1 is entered, statement 4 will appear; if 0 is entered skip to statement 5.

4. enter: lat, lon (to thousandths of a degree). If not known enter 0.,0. if lat and lon are known only $V_a$ is solved for

5. enter: seismic phase (max 4 characters)

The entry for statement 5 is in format A4

6. enter: no of stations (NS) at which readings taken for the selected phase

7. enter: station name (4 characters rt adjusted), phase quality, arrival time of phase (ihour, imin, sec). There will be ns entries using format (A4, 1X, I1, 2X, I2, 1X, I2, 1X, F6.2)

Phase quality in the above statement ranges between 0 (best) and 4 (worst) according to HYPO71 procedure. Since BEAM4 works with differential times between stations, the phase quality values for each station pair are summed and the sum is used as a weight in the least-squares procedure to locate the event. If the observed time difference for a station pair is less than 0.5 seconds, the program will not allow the phase quality to be less than 3. If the time difference is less than 0.2 seconds, the phase quality can be no less than 5, and if the time difference is less than 0.1 seconds, the phase quality is set at 8. These values override those resulting from the sum of the quality values entered for each phase.

8. enter: (1) max number of iterations, (2) first guess app vel, (3) 1st guess direction of approach (BAZ), (4) 1st guess distance to nearest station (R). If BAZ and R are positive, they are fixed at the indicated values. If they are negative they are solved for. For plane waves, R=0.

At this point a nonlinear, least-squares procedure is used to solve for the parameters designated earlier. After each iteration of the process, statements 9 and 10 will appear.

9. if epicentral location desired, enter distance form network to event either computed above or obtained independently. if not desired, enter 0.

10. if arrival time and distance information at each station are desired for this iteration, enter 1, if not enter 0. if 1 is entered, the information is written on a file which can be retrieved on the line printer.

Example outputs for five stations of the Svalbard network (eastern hemisphere) and Central Mississippi Valley network (western hemisphere) are attached.

After the correct number of iterations (entered earlier), the following statement appears

11. to go to another event, enter 0, to use the same set of times, enter 1, to stop, enter 2.

If 0 is entered the sequence of statements beginning with statement 1 will be repeated. If 1 is entered the sequence of statements beginning with statement 3 will be repeated.

Example using BEAM4 with 5 stations of the Svalbard network (in the eastern hemisphere). A curved wave front is assumed for a source which is 221.5 km from the nearest station (NGF). In this example, only apparent velocity and direction of approach at the nearest station have been solved for.

APP VEL = 8.058+- 0.0275 BAZ = 11.677+- 0.5985 R = 221.50+- 0.0
SUM OF SQUARES OF RESIDUALS = 0.54918-01

| STATION PR | G | DIS STA1 | DIS STA2 | BAZ STA1 | BAZ STA2 | T-S DIS | T-S AZ | CPS TIME DIF | TH TIME DIF | OBS-TH | AP VEL |
|---|---|---|---|---|---|---|---|---|---|---|---|
| NGF- SCF | 2 | 221.5 | 281.2 | 11.7 | 11.5 | 59.756 | 191.481 | 7.410 | 7.4[illegible] | 0.046 | [illegible] |
| NGF- KVF | 3 | 221.5 | 281.6 | 11.7 | 360.5 | 83.762 | 140.904 | 7.970 | 7.9[illegible] | 0.046 | [illegible] |
| NGF- BZT | 1 | 221.5 | 304.8 | 11.7 | 22.3 | 109.322 | 236.987 | 10.410 | 10.3[illegible] | 0.087 | [illegible] |
| NGF- BCF | 2 | 221.5 | 319.5 | 11.7 | 372.8 | 97.609 | 199.425 | 12.010 | 13.039 | -0.028 | [illegible] |
| SCF- KVF | 8 | 281.2 | 281.6 | 11.5 | 360.5 | 67.333 | 65.236 | 0.960 | 0.986 | -0.026 | [illegible] |
| SCF- BZT | 3 | 281.2 | 304.8 | 11.5 | 22.3 | 74.209 | 270.030 | 2.900 | 2.923 | -0.023 | [illegible] |
| SCF- BCF | 4 | 281.2 | 319.5 | 11.5 | 372.8 | 38.567 | 208.050 | 4.500 | 4.624 | -0.124 | [illegible] |
| KVF- BZT | 1 | 281.6 | 304.8 | 360.5 | 22.3 | 141.402 | 275.204 | 2.540 | 2.540 | 0.000 | [illegible] |
| KVF- BCF | 2 | 281.6 | 319.5 | 360.5 | 372.8 | 89.680 | 254.518 | 4.440 | 4.534 | -0.094 | [illegible] |
| BZT- BCF | 3 | 304.8 | 319.5 | 22.3 | 372.8 | 65.625 | 118.374 | 1.600 | 1.649 | -0.049 | [illegible] |

EPICENTER AT 79.994 DEGREES N 21.042 DEGREES E
79 DEG 59 MIN 36.8 SEC N 21 DEG 2 MIN 29.5 SEC E

Examples using BEAM with 5 stations of the Central Mississippi Valley network (in the western hemisphere). In the upper example a curved wave front is assumed for a source 91.6 km from the nearest station (DON) and in the lower example a plane wave is assumed. In both cases apparent velocity and direction of approach are solved for.

P WAVES FOR THE EVENT OF 20 AUG 78
NEW MADRID TEST
APP VEL = 5.997+- 0.0554 THETA = 355.521+- 1.3815 R = 91.60+- 0.0
SUM OF SQUARES OF RESIDUALS = 0.39596E+00

| STATION PR | C | OIS STA1 | OIS STA2 | AZ STA1 | AZ STA2 | T-S OIS | T-S AZ | OBS TIME DIF | TH TIME DIF | OBS-TH | AP VEL |
|---|---|---|---|---|---|---|---|---|---|---|---|
| DON- ELC | 1 | 91.6 | 105.9 | 355.6 | 318.9 | 63.906 | 78.879 | 2.010 | 1.682 | 0.328 | 6.502 |
| DON- CWM | 3 | 91.6 | 140.4 | 355.6 | 340.8 | 87.054 | 136.050 | 6.710 | 6.955 | -0.245 | 7.254 |
| DON- CRL | 2 | 91.6 | 179.0 | 355.6 | 330.9 | 103.903 | 129.084 | 12.610 | 12.499 | 0.111 | 6.931 |
| DON- ECC | 1 | 91.6 | 219.2 | 355.6 | 358.2 | 123.893 | 181.543 | 17.610 | 17.665 | -0.055 | 7.021 |
| ELC- CWM | 4 | 105.9 | 140.4 | 318.9 | 340.8 | 58.243 | 203.923 | 4.700 | 4.997 | -0.297 | 7.434 |
| ELC- CRL | 3 | 105.9 | 179.0 | 318.9 | 330.8 | 78.822 | 166.229 | 10.600 | 10.838 | 0.062 | 6.741 |
| ELC- ECC | 2 | 105.9 | 219.2 | 318.9 | 358.2 | 150.183 | 205.364 | 15.600 | 15.689 | -0.089 | 7.038 |
| CWM- CRL | 5 | 140.4 | 179.0 | 340.8 | 330.8 | 48.149 | 118.809 | 5.900 | 5.527 | 0.373 | 6.356 |
| CWM- ECC | 4 | 140.4 | 219.2 | 340.8 | 358.2 | 92.019 | 206.180 | 10.900 | 10.698 | 0.202 | 6.694 |
| CRL- ECC | 3 | 179.0 | 219.2 | 330.8 | 358.2 | 101.759 | 234.580 | 5.000 | 5.171 | -0.171 | 7.237 |

EPICENTER AT 37.696 DEGREES N 90.010 DEGREES W
= 37 DEG 59 MIN 55.3 SEC N 90 DEG 0 MIN 34.4 SEC W

P WAVES FOR THE EVENT OF 20 AUG 78
NEW MADRID TEST
APP VEL = 6.831+- 0.2810 THETA = 342.086+- 2.4542 PLANE WAVES ASSUMED
SUM OF SQUARES OF RESIDUALS = 0.77938E-01

| STATION PR | C | T-S OIS | T-S AZ | OBS TIME DIF | TH TIME DIF | OBS-TH | AP VEL |
|---|---|---|---|---|---|---|---|
| DON- ELC | 1 | 63.906 | 78.879 | 2.010 | 1.506 | 0.504 | 3.758 |
| DON- CWM | 3 | 87.054 | 136.050 | 6.710 | 7.506 | -0.796 | 7.641 |
| DON- CRL | 2 | 103.903 | 128.084 | 12.610 | 12.609 | 0.001 | 6.821 |
| DON- ECC | 1 | 123.893 | 181.543 | 17.610 | 17.101 | 0.509 | 6.634 |
| ELC- CWM | 4 | 58.243 | 203.923 | 4.700 | 6.352 | -1.652 | 9.233 |
| ELC- CRL | 3 | 78.822 | 166.229 | 10.600 | 11.509 | -0.909 | 7.417 |
| ELC- ECC | 2 | 150.183 | 205.364 | 15.600 | 16.006 | -0.406 | 7.005 |
| CWM- CRL | 5 | 48.149 | 118.809 | 5.900 | 5.131 | 0.769 | 5.941 |
| CWM- ECC | 4 | 92.019 | 206.180 | 10.900 | 9.675 | 1.225 | 6.063 |
| CRL- ECC | 3 | 101.759 | 234.580 | 5.000 | 4.481 | 0.519 | 6.122 |

# The Denver Earthquakes of 1967-1968

Robert B. Herrmann, Sam-Kuen Park and Chien-Ying Wang

## ABSTRACT

A detailed study of the earthquakes associated with the Rocky Mountain Arsenal disposal well is presented. Long period surface-wave studies are used together with P-wave first motions to show that the April 10, August 9 and November 27, 1967 earthquakes occurred at depths of 3-5 km and were characterized by normal faulting along a northwest striking fault plane. A joint hypocenter relocation of 103 microearthquakes out of a data set of 279 recorded between 1967 and 1968 shows a hypocenter pattern striking N $50^{\circ}$ W, with most of the events located about 5 km northwest of the disposal well at depths between 3 - 8 km. A fault plane dipping southwest is tenuously suggested by those earthquakes with depths less than 5 km. Modeling of near-field seismoscope observations lend support to the focal mechanisms derived.

# INTRODUCTION

The Denver earthquakes associated with the Rocky Mountain Arsenal disposal well during the 1960's are very important because they represent one of the first documented cases of the triggering of earthquakes due to high-pressure injection of fluids into host rock. The 3671.3 meter well into the top of the Precambrian was completed in 1961 and fluid injection commenced in early 1962 (Evans, 1966). Almost immediately, the relatively aseismic Denver area became seismically active. Following the suggestion of Evans (1966) of the possible causal relationship between the earthquakes and fluid injection, a number of geological and geophysical studies were initiated.

A detailed study of the seismicity and geology near the disposal well is contained in a report edited by Hollister and Weimer (1968). A study by Healy et al. (1968) reported on the results of a local seismograph array set up near the well together with the relationship of pumping activity to earthquake activity. The distribution of seismicity in 1966 indicated a narrow, shallow zone of seismicity striking northwest with the well near the center of epicenters. On the basis of a nodal plane of P-wave first motions crossing one of their L-shaped seismograph arrays, they inferred right lateral strike-slip faulting on a fault plane striking northwest. Hoover and Dietrich (1969) tabulated hypocenter locations recorded by a USGS microearthquake array at the Arsenal during 1967-1968. These studies suggest that the seismicity migrated away from the well since the fluid injection began in 1962. Van Poollen and Hoover (1970) reviewed the history of the episode and discussed various causative mechanisms for the earthquakes as well as

the results of a fluid removal experiment.

The best earthquake data was that collected by Hoover and Dietrich (1969). Using their local velocity model (Arsenal Model of Table 1), we have relocated the earthquakes they recorded using HYPO71 (Lee and Lahr, 1972). Figure 1 shows the locations of the arsenal well and the USGS seismograph locations, the epicenters, and projection of the epicenters onto vertical planes striking $40^{\circ}$ and $130^{\circ}$ with respect to north. The vertical line in the depth profiles indicates the well. It is obvious that few of the 289 hypocenters plotted are located at the well itself.

In spite of the many earthquakes recorded, little else is known about the sequence, primarily because they occurred almost 10 to 20 years ago when the concept of portable microearthquake arrays was in its infancy. The focal depths and focal mechanisms of these earthquakes are poorly constrained. This paper seeks to examine other seismological data that can provide some information on these earthquakes.

## SURFACE WAVE STUDIES

The April 10, August 9 and November 27 earthquakes of 1967 were large enough to generate long period seismograms with a sufficiently large signal-to-noise ratio to warrant a detailed study. The focal mechanism, focal depth and seismic moment were obtained using the techniques described by Herrmann (1979). The Central United States earth model of Table 1 was used together with the eastern North American anelastic attenuation coefficients of Herrmann and Mitchell (1975) for the inversion of the surface wave-spectral amplitude data. This choice is acceptable since the spectral amplitude data are relatively insensitive to earth model changes and since the models apply to most of the paths

along which data were acquired.

Earthquake of April 10, 1967. This event was estimated to occur at 1900 UT at 39.9°N, 104.8°W (ISC). We estimate $m_{bLg}$ = 4.3±0.2 and $M_S$ = 4.2±0.2, for the event using the relations of Nuttli (1973) and 13 short and long period WWSSN records. A total of 306 spectral amplitude-period pairs in the 6 to 40 second period range from the twenty-one seismograph stations FFC, BLC, GWC, OTT, OGD, BLA, SLM, ATL, LUB, ALQ, TUC, DUG, LON, VIC, PHC, PNT, BOZ, FSJ, SES, YKC and CMC made up the vertical component Rayleigh-wave data set while 251 spectral amplitude-period pairs in the 6 to 40 second period range from the same seismograph stations made up the Love-wave data set.

The focal mechanism solution which best fits the P-wave first motion and surface-wave data is shown in Figure 2. An equal area, lower hemisphere projection is used. Proceeding clockwise from north, the seismograph stations and their P-wave polarities are RKON(-), FKCO(-), ALQ(X), TUC(X), DEN(+), KNUT(+), GOL(+), DUG(+), LON(-), BOZ(+), PGBC(X) ans SES(+). The P wave takeoff angles used were 90° for distances of 30 -100 km, 67° for distances of 160 - 185 km, 49° for 185-600 km, 47° for 600 - 1650 km. At distances greater than 15° the table of Nuttli (1969) was used. The tension axis trends at 244° and plunges at 7°, and the pressure axis trends at 127° and plunges at 76°. A focal depth of 4 km and a seismic moment of 7.1 x $10^{22}$ dyne-cm were obtained. The correlation coefficients between the observed and predicted Rayleigh- and Love-wave spectral amplitudes were $r_R$ =0.001 and $r_L$ =0.522. The poor correlation coefficient $r_R$ indicates first that the Rayleigh- wave data were of poor quality. Hence the focal mechanism is not well con-

strained. A comparison of the anelastic attenuation corrected and theoretical radiation patterns is shown in Figures 3 and 4 for selected periods of the Love- and Rayleigh- wave data sets, respectively.

Given the sparse P-wave first motion data set, another test of the choice of compression and dilatation quadrants is a comparison of observed and theoretical surface wave phases at selected stations. This is appropriate since the surface-wave amplitude spectra were used to specify the nodal planes while the P-wave first motion data were used to constrain the nodal planes somewhat, but more importantly the first motions were used to specify the compression and dilatation quadrants. ALQ at a distance of 572 km and DUG at a distance of 693 km were the closest seismograph stations that had on-scale long-period surface wave recordings. The observed data were corrected for instrumental phase response as well as for the linear phase shift due to the difference between the origin time and the start of digitizing. An examination of the group velocities of the Love and Rayleigh waves indicated that the Colorado Plateau earth model of Bucher and Smith (1971) would be a suitable regional model for the phase study. This earth model is given in Table 1.

Using that earth model, observed and theoretical phase spectra were compared at 17 periods between 16 and 32 seconds. The average phase differences for the vertical component Rayleigh waves at ALQ and DUG were $0.805 \pm 0.128$ and $0.798 \pm 0.122$ circles, respectively. For the Love waves, the differences at ALQ and DUG were $0.943 \pm 0.032$ and $0.831 \pm 0.120$ circles, respectively. Since the phase differences given are in circles, 0.0 or 1.0 circles indicates a correct choice of the compressional

and dilatational quadrants and 0.5 circles indicates an incorrect choice. Thus the choice of compression and dilatation quadrants is supported by the surface wave phase data.

Earthquake of August 9, 1967. This earthquake occurred at 1325 UT at 39.9°N and 104.7°W (ISC). Nuttli et al. (1979) assigned an $m_b$ = 4.9 and an $M_S$ = 4.4 to this event. A total of 279 spectral amplitude-period data pairs from the eighteen seismograph stations BLC, FBC, GWC, SFA, OTT, SCB, AAM, OGD, ATL, OXF, DAL, ALQ, DUG, LON, BOZ, FSJ, EDM and YKC in the 5 to 40 second period range made up the vertical- component Rayleigh-wave spectral amplitude data set. The Love-wave spectral-amplitude data set was composed of 217 spectral amplitude-period data points in the 6 to 40 second period range from the fifteen seismograph stations FBC, SFA, OTT, SCB, OGD, ATL, OXF, DAL, LUB, DUG, LON, BOZ, FSJ, EDM and YKC.

The focal mechanism which best fits the P-wave first motion and surface- wave data is shown in Figure 2. The tension axis trends at 40° and plunges at 10° while the pressure axis trends at 220° and plunges at 80°. A focal depth of 3 km and a seismic moment of 2.1 x $10^{23}$ dyne-cm were obtained. The seismograph stations and their P-wave first motions, clockwise from north, are RKON(+), OXF(-), LCNM(+), ALQ(-), DEN(+), KNUT(-), GOL(+), DUG(-), HLID(-), LON(+), PNT(-), SES(-). The correlation coefficients between the observed and predicted Rayleigh- and Love-wave spectral amplitudes are $r_R$ = 0.692 and $r_L$ = 0.697, respectively. A comparison of the observed and predicted radiation patterns for selected periods of the Love- and Rayleigh-wave data sets is made in Figures 3 and 4.

For the focal mechanism given Figure 2 for this earthquake, the average differences in circles between observed and theoretical phase spectra were 0.880±0.071 and 0.109±0.067 for the vertical component Rayleigh wave at ALQ and DUG, respectively, and 0.143±0.040 for the Love wave at DUG. These support the normal fault focal- mechanism solution.

Earthquake of November 27, 1967. This event occurred at 0509 UT at 40.0°N, 104.7°W (ISC). Nuttli et al. (1979) estimated an $m_b$ = 4.6 and an $M_S$ = 3.8 for this earthquake. The twenty-three seismograph stations FFC, BLC, RKON, WES, BLA, FLO, ATL, DAL, JCT, LUB, LCNM, ALQ, TUC, GSC, DUG, LON, PHWA, PNT, BOZ, PGBC, SES, HVMA and YKC yielded 436 Rayleigh-wave and 435 Love-wave spectral amplitude-period observations in the same period range.

The resultant focal mechanism is shown in Figure 2. The tension axis trends at 230° and plunges at 4° while the pressure axis trends at 131° and plunges at 69°. A focal depth of 5 km and a seismic moment of $7.2 \times 10^{22}$ dyne-cm were obtained. The P wave first motion data are, clockwise from north, WNSD(+), LCNM(+), ALQ(+), DEN(+), GOL(+), DUG(+), HLID(-), TLWY(-), PGBC(+), WHYK(+), HVMA(-) and NPNT(-). The Rayleigh- and Love-wave correlation coefficients between the observed and predicted data were $r_R$ = 0.566 and $r_L$ = 0.603. Radiation pattern plots at selected periods are shown in Figure 3. For the focal mechanism derived, the differences in circles between observed and theoretical phase spectra were 0.899±0.079 and 0.137±0.035 for the vertical component Rayleigh wave at ALQ and DUG, respectively, and 0.118±0.044 and 0.066±0.035 for the Love wave at ALQ and DUG, respectively. These results support the choice of the compressional and dilatational qua-

drants.

The focal mechanism solutions of the August 9 and November 27 are very good and would be Quality A solutions of Herrmann (1979). The April 10 solution is not very good. Because of background noise due to a large teleseism some hours before as well as low spectral amplitudes due to the focal mechanism and depth, the fit between the observed and predicted Rayleigh-wave spectral amplitude data was marginal. In fact the Rayleigh-wave data are more consistent with a normal fault striking northeast rather than northwest. The accepted northwest solution fits the Love wave data as well and is also in agreement with the focal mechanisms of the other two earthquakes studied. The April 10 earthquake would be rated Quality C.

## HYPOCENTER RELOCATION

Hoover and Dietrich (1969) reported on the operation of an array of seismographs located near the disposal well. The locations of the stations are shown in Figure 1. Through the efforts of Dr. Hoover, punched data cards for 289 earthquakes recorded in the time period 1967 to early 1969 were obtained. The array operation was not continuous. No data from the array were available for the large April 10, August 9 and November 27, 1967 earthquakes. Thus a detailed study of their aftershocks with the goal of understanding the rupture process was not possible. However, the spatial relationship of these individual events to the disposal well was of interest.

This large earthquake data set encouraged the use of a joint hypocenter relocation technique (Douglas, 1967). The object is to simultaneously relocate all earthquakes, determining their hypocenters and

origin times, and to obtain the station corrections and/or refined earth model. Normally this would not be feasible since a 1174 x 1174 matrix inverse ( 4 x 289 hypocenter parameters and 18 station corrections) would have to be calculated. However, a matrix partitioning technique outlined in the Appendix was used to solve the problem in such a way that the largest matrix inverted is only 18 x 18. Care must be taken in choosing the earthquakes used for relocation since poorly constrained earthquakes will contaminate the location of the other earthquakes which are all interrelated through the station corrections.

Since this study was the first experience with joint hypocenter relocation techniques by the authors, a number of decisions were made. First, a subset of 106 earthquakes, recorded by at least 8 stations including one northwest of the well, was used. This requirement was established by trial and error in order to reduce the standard errors of the resulting epicenters and station corrections. Because of the complexity of the joint hypocenter relocations equations (Appendix A-1), it is difficult to visualize the interrelation between hypocenter and station correction adjustments. In order to stabilize the problem either one hypocenter or one staion correction must be fixed. A completely unconstrained solution is not possible since a systematic change in station corrections would be accounted for by a similar change in origin times, e.g. increasing station corrections by 1.0 second would force all origin times to be 1.0 second earlier. Thus, a hypocenter or station correction constraint is required.

Since no one earthquake was better than any other, we decided to set the station correction at W3 equal to zero. As the reviewer, Dr.

James Dewey, pointed out, this constraint affects only origin times and station corrections, but this does not affect the hypocenters which are free to move. This inversion thus uses the minimal number of side constraints. The fact that the inversion was stable was due to a wide range of raypaths available. If the source zone had been very localized, an "a priori" assumption of the loction of one event would have been required. The simplicity of just fixing one station correction may not be valid unless the station corrections obtained actually reflect near-surface travel time anomalies.

The results of the relocation are shown in Figure 5. From top to bottom, this figure shows the epicenter locations and projections of the epicenters on planes striking N 40° E and N 130° E. The left column presents the data set chosen for relocation, while the right column shows the results of the relocation. The relocated earthquakes cluster together better and have been moved to shallower depths. As mentioned by Hoover and Dietrich (1969) the seismic activity during this time period was not at the disposal well. As a matter of fact, almost all of the relocated hypocenters are more than 3 km from the base of the well.

It is disconcerting that a definite fault plane is not apparent after all the relocation effort. The surface-wave studies indicate that the fault plane should strike in the direction of seismicity and dip either to the northeast or southwest. A tenuous argument can be made in favor of the southwest dipping fault plane. There seems to be a different spatial relationship between those earthquakes occurring above and below 5 km in depth, with the deeper ones occurring nearer to the well. Looking in the direction of strike, the shallower earthquakes do

seem to exhibit a southwestward dip. Unfortunately, we cannot be more precise.

## NEAR FIELD STUDIES

Twenty-five Wilmot seismoscopes were installed near the disposal well in 1966 in order to collect strong motion data ( Hollister et al, 1968). Seismoscope records are available from the April 10 and August 9 earthquakes. The numbered circles in Figures 6 and 7 are reproductions of the seismoscope traces due to the April 10 and August 9 earthquakes, respectively. The locations of the earthquakes with respect to the seismoscopes is given by the + sign ( Hollister et al, 1968).

Given this interesting data set, we were curious to see if we could model the observations. This was not an easy task since any errors in the focal mechanism, focal depth, source location or earth model would affect the particle motion a great deal. Because of this only the simplest model was used to synthesize the ground motions, that of a buried point source in a halfspace. A Cagniard-de Hoop program (Johnson, 1974) was used to generate ground motion time histories at the free surface for an earth model with compressional velocity 6.0 km/sec, shear velocity 3.45 km/sec and density 2.7 gm/cm$^3$ . The horizontal components of the ground motions were passed through a single degree of freedom oscillator with $T_n$ = 0.78 sec and $\eta$=10% ( Hudson and Cloud, 1967 ) to synthesize seismoscope traces. The source time function used was the parabolic pulse of Herrmann (1978) defined as

$$2Ts(t) = \begin{cases} 0 & t \leq 0 \\ 0.5(t/T)^2 & 0 \leq t \leq T \\ -0.5(t/T)^2+2(t/T)-1 & T \leq t \leq 3T \\ 0.5(t/T)^2-4(t/T)+8 & 3T \leq t \leq 4T \\ 0 & t \geq 4T. \end{cases}$$

This source pulse represents the velocity time history of the rupture.

Using the results of the surface wave study and the locations of the April 10 and August 9 earthquakes given by Hollister et al. (1968) as a starting point, many synthetic seismoscope traces were generated for different values of T, focal depth, focal mechanism, seismic moment and event location. The Hollister et al. (1968) locations provided the best fit. A good fit for the April 10 earthquake data was obtained using T = 0.24 sec, a source depth of 4 km, a seismic moment of 7.1 x $10^{22}$ dyne-cm and a focal mechanism characterized by a strike of $140^{\circ}$, a dip of $55^{\circ}$ and a slip of $80^{\circ}$. The predicted and observed traces are compared in Figure 6. The overall fit of shapes and amplitudes is quite good. Using the same focal depth and T values, a seismic moment of 2.1 x $10^{23}$ dyne-cm and a focal mechanism characterized by a strike of $135^{\circ}$, a dip of $55^{\circ}$ and a slip of $85^{\circ}$ yielded the best fit to the data of the August 9 earthquake. The observed and predicted traces are given in Figure 7.

The agreement between the observed and predicted traces is surprisingly good, indicating the appropriateness of the source parameters. The focal mechanisms used are just slightly different that those obtained from the surface wave analysis. The seismoscope simulation is really only a simplified test. Even though it is possible to generate time histories for a more realistic layered earth structure, the unknowns in structure and the earthquake process did not warrant the additional effort. On the other hand, this exercise reinforces the surface wave conclusions concerning the source depth and focal mechanism, and provides some constraints on the duration of the faulting process. This

exercise also places some confidence in the Hollister et al. (1968) locations, since data do not exist for the inclusion of these large events into the joint hypocenter determination.

## CONCLUSIONS

This detailed study of the three large Rocky Mountain Arsenal earthquakes of 1967 has yielded new information on the seismic moment and focal mechanisms of these earthquakes. The surface wave and P wave first motion support northwest striking normal faulting. Microearthquake data and simulation of seismoscope traces lend support to this conclusion. The seismic moment of the August 9 earthquake makes it one of the largest earthquakes east of the Continental Divide in the last 20 years (Herrmann, 1979). Even though this study has not dealt with the relationship of the earthquakes to the disposal well, it is hoped that these results lead to a better understanding of the causative process of these earthquakes.

From a scientific point of view, it is too bad these earthquakes occurred so long ago. The microearthquake data fortunately were still intact. They could easily have been lost. The sophistication of seismic instrumentation has improved substantially. Looking back, this earthquake sequence could have told us much more about the physics of an earthquake, in general, given modern instrumentation.

## ACKNOWLEDGMENTS

The efforts of Dr. Donald Hoover, USGS, Denver, in locating the microearthquake data is gratefully acknowledged. This work was

sponsored in part by the Department of the Interior, U. S. Geological Survey, under Contract 14-08-0001-16708 and by the U. S. Nuclear Regulatory Commission under Contract NRC-04-76-282. Dr. James W. Dewey provided a very enlightening review.

# REFERENCES

Bucher R. L. and R. B. Smith (1971). Crustal structure of the eastern Basin and Range province and in the northern Colorado Plateau from phase velocities of Rayleigh waves, in The Structure and Physical Properties of the Earth's Crust, Geophys. Monogr. Ser., vol 14, edited by J. G. Heacock, pp 59-70, American Geophysical Union, Washington, D.C.

Douglas, A. (1967). Joint hypocentre determination, Nature 215, 47-48.

Evans, D.M. (1966). The Denver area earthquakes and the Rocky Mountain disposal well, The Mountain Geologist 3, 23-36.

Healy, J.H., W.W. Rubey, D.T. Griggs and C.B. Raleigh (1968). The Denver Earthquakes, Science 161, 1301-1310.

Herrmann, R. B. (1978). A note on causality problems in the numerical solution of elastic wave propagation in cylindrical coordinate systems, Bull. Seism. Soc. Am. 68, 117-123.

Herrmann, R. B. (1979). Surface wave focal mechanisms for eastern North American earthquakes with tectonic implications, J. Geophys. Res. 84, 3543-3552.

Herrmann, R. B. and B. J. Mitchell (1975). Statistical analysis and interpretation of surface-wave anelastic attenuation data for the stable interior of North America, Bull. Seism. Soc. Am. 67, 209-218.

Hohn, F. E. (1964). Elementary Matrix Algebra, Macmillan Company, New York, 395pp.

Hollister, J.C. and Weimer, R.J., editors (1968). Geophysical and geological studies of the relationships between the Denver earthquakes and the Rocky Mountain Arsenal well, Quarterly of the Colorado School of Mines, 63, Golden, 251 pp.

Hoover, D.B. and J.A. Dietrich (1969). Seismic activity during the 1968 test pumping at the Rocky Mountain Arsenal disposal well, Geological Survey Circular 613, Washington, 35 pp.

Hudson, D. E. and W. K. Cloud (1967) An analysis of seismoscope data from the Parkfield earthquake of June 27, 1966, Bull. Seism. Soc. Am. 57, 1145-1159.

Johnson, L. R. (1974). Green's function for Lamb's problem, Geophys. J. 37, 99-131.

Lee, W.H.K.and J.C. Lahr (1972). HYPO71: A computer program for determining hypocenter, magnitude, and first motion patterns of local earthquakes, U.S. Geological Survey Open File Report 75-311.

Nuttli,O. W. (1969). Tables of angles of incidence of P wave at focus, calculated from 1968 P Tables, Earthquake Notes 40, 21-25

Nuttli, O. W. (1973). Seismic wave attenuation and magnitude relations for eastern North America, J. Geophys. Res. 78 , 876-885.

Nuttli, O. W., G. A. Bollinger, and D. W. Griffiths (1979). On the relation between modified Mercalli intensity and body-wave magnitude, Bull. Seism. Soc. Am. 69, 893-909.

Spencer, C. and D. Gubbins (1980). Travel-time inversion for simultaneous earthquake location and velocity structure determination in laterally varying media, Geophys. J. 63, 95-116.

van Poollen, H. K. and D. B. Hoover (1970). Waste disposal and earthquakes at the Rocky Mountain Arsenal, Derby, Colorado, J. Petroleum Technology 22, 983-993.

Department of Earth and Atmospheric Sciences
Saint Louis University
P. O. Box 8099 Laclede Station
St. Louis, MO 63156

## APPENDIX

As mentioned in the text, the application of joint hypocenter techniques to large numbers of earthquakes becomes difficult because of the large matrices which must be inverted. Without getting into the details of the joint hypocenter method, the normal equations to be solved are of the form

$$\begin{vmatrix} a_1 & 0 & \cdot & 0 & b_1 \\ 0 & a_2 & \cdot & 0 & b_2 \\ \cdot & \cdot & \cdot & \cdot & \cdot \\ 0 & 0 & \cdot & a_n & b_n \\ b_1^T & b_2^T & \cdot & b_n^T & c \end{vmatrix} \begin{vmatrix} x_1 \\ x_2 \\ \cdot \\ x_n \\ u \end{vmatrix} = \begin{vmatrix} y_1 \\ y_2 \\ \cdot \\ y_n \\ v \end{vmatrix} \qquad \text{(A-1)}$$

where the $a_i$ is the usual (4 x 4) matrix of the single event location problem, $y_i$ is a (4 x 1) matrix, $x_i$ is a (4 x 1 ) matrix given the adjustments to the spatial coordinates and origin time, $b_i$ is a (4 x M) matrix, c is an (M x M) matrix, v is (M x 1) and u is the (M x 1) matrix of adjustments to the station correction or earth model.

With the exception of the elements shown the large matrix of (A-1) is very sparse. Because of this, a solution by matrix partitioning is suggested. The first row of (A-1) can be written as

$$a_1 x_1 + b_1 u = y_1 \qquad \text{(A-2)}$$

or as

$$x_1 = a_1^{-1} y_1 - a_1^{-1} b_1 u.$$

Likewise,

$$x_2 = a_2^{-1} y_2 - a_2^{-1} b_2 u$$

through

$$x_n = a_n^{-1} y_n - a_n^{-1} b_n u.$$

Substituting these expressions for $x_k$ into the last row of (A-1), one obtains

$$\begin{vmatrix} c - b_1^T a_1^{-1} b_1 - b_2^T a_2^{-1} b_2 - \ldots - b_n^T a_n^{-1} b_n \end{vmatrix} u = \begin{vmatrix} v - b_1^T a_1^{-1} y_1 - b_2^T a_2^{-1} y_2 - \ldots - b_n^T a_n^{-1} b_n \end{vmatrix} \qquad \text{(A-3)}$$

(A-3) is a square matrix of dimensions (M x M). After solving (A-3) for u, the u can be back substituted into (A-2) to obtain $x_1$, etc. If disk or other storage media are used, the maximum array required to be stored in the computer at any one time is (M x M).

The above method is very efficient in solving for the source parameter and station correction perturbations. In order to estimate the confidence on the latest perturbation, the inverse of the left hand side of (A-1) is required. While the desired elements of the variance-covariance matrix could be obtained by making the right side of (A-1) the different columns of the identity matrix in succession, a matrix inversion by partitioning (Hohn, 1964) works very well.

Equation (A-1) can be written as

$$\begin{vmatrix} A & B \\ B^T & c \end{vmatrix} \begin{vmatrix} X \\ u \end{vmatrix} = \begin{vmatrix} Y \\ v \end{vmatrix} \qquad \text{(A-4)}$$

where A is the square matrix of the $a_i$'s, $B=\begin{vmatrix} b_1 & b_2 & \cdots & b_n \end{vmatrix}^T$, and similarly for X and Y.

The first equation of (A-4) can be manipulated to form

$$X = A^{-1}Y - A^{-1}Bu. \qquad \text{(A-5)}$$

Substituting this into the second equation, we get

$$[c-B^TA^{-1}B]u=[v-B^TA^{-1}Y]. \qquad \text{(A-6)}$$

Setting

$$D = A^{-1}B \text{ and}$$

$$E = c-B^TA^{-1}B = c-B^TD,$$

we have

$$u = (-DE^{-1})^TY + E^{-1}v,$$

where we have used the fact that the original square matrix and hence E are symmetric. Backsubstituting,

$$X = [A^{-1} + DE^{-1}D^T]Y+[-DE^{-1}]v$$

By examination, the inverse matrix for A-4 is

$$\begin{vmatrix} A^{-1}+DE^{-1}D^T & (-DE^{-1}) \\ (-DE^{-1})^T & E^{-1} \end{vmatrix}$$

which is symmetric.

Upon substituting the proper matrices from (A-1) into (A-4), we find that

$$E = c - B^T A^{-1} B \qquad (A\text{-}7)$$

$$= \left| c - b_1^T a_1^{-1} b_1 - \ldots - b_n^T a_n^{-1} b_n \right|$$

The right side is immediately recognized from (A-3). Since the inverse of E is routinely computed in order to get the perturbations, the information on the variances for the station corrections is already available. Since, we are only interested in the (4x4) covariance matrix for each event and not in the covariance between events or between the event and the station corrections, it can be shown that the (4x4) covariance matrix for the first event is just

$$\left| a_1^{-1} + a_1^{-1} b_1 E^{-1} b_1^T a_1^{-1} \right| . \qquad (A\text{-}8)$$

A paper just published by Spencer and Gubbins (1980) presents a similar development but extends it simply and elegantly to include stochastic and generalized inverses. The difference between this presentation and theirs lies in the way A-2 and A-3 are written. Given adequate disk storage, there is no program size limitation to the maximum number of events that may be studied, there is only a disk storage limitation.

TABLE 1
EARTH MODELS

| H(km) | $\alpha$(km/sec) | $\beta$(km/sec) | $\rho$(gm/cm$^3$) |
|---|---|---|---|
| | | Central United States | |
| 1 | 5.00 | 2.89 | 2.5 |
| 9 | 6.10 | 3.52 | 2.7 |
| 10 | 6.40 | 3.70 | 2.9 |
| 20 | 6.70 | 3.87 | 3.0 |
| | 8.15 | 4.70 | 3.4 |
| | | Colorado Plateau (Bucher and Smith, 1971) | |
| 2.5 | 3.00 | 1.73 | 2.4 |
| 24.5 | 6.20 | 3.58 | 2.83 |
| 13.0 | 6.80 | 3.87 | 2.99 |
| | 7.80 | 4.25 | 8.33 |
| | | Arsenal | |
| 0.38 | 2.17 | | |
| 0.82 | 3.05 | | |
| 1.15 | 3.22 | | |
| 0.45 | 4.10 | | |
| 0.15 | 4.60 | | |
| 0.69 | 4.87 | | |
| 1.06 | 5.80 | | |
| 10.30 | 5.90 | | |
| | 6.00 | | |

## FIGURE CAPTIONS

Fig. 1. Hypocenters determined from USGS array data. Epicenters and two vertical depth profiles are shown. The seismograph stations are indicated by triangles, with their names given on the base map. The position of the well is indicated on the epicenter maps and on the vertical depth projections.

Fig. 2. Focal mechanisms of the April 10, 1967, August 9, 1967 and November 27, 1967 earthquakes. The nodal planes satisfy surface-wave spectral amplitude data as well as the P-wave first motion data. Circles represent compressions, triangles, dilatations, and X's, uncertain arrivals of low amplitude. T and P are the intersections of the tension and pressure axes, respectively, with the lower hemisphere. An equal area lower hemisphere projection is used.

Fig. 3. Comparison between anelastic attenuation corrected observed and predicted Love-wave radiation patterns at selected periods, T, for the events studied. The scaling bars are spectral amplitudes in units cm-sec at a reference distance of $9^{\circ}$ from the source.

Fig. 4. Comparison between anelastic attenuation corrected observed and predicted Rayleigh-wave radiation patterns at selected periods for the events studied. The scaling bars are spectral amplitudes in cm-sec at a reference distance of $9^{\circ}$ from the source.

Fig. 5. The left column is the data set selected for joint hypocenter determination while the right column shows the relocated events. In each case the epicenters and two vertical depth profiles are shown. The well and seismographs stations, triangles, are indicated for reference. There is no vertical exaggeration.

Fig. 6. A comparison between the observed and predicted seismoscope records for the April 10, 1967 earthquake. The numbered, singly circled plots are the observed data while the doubly encircled plots are the predicted data. All plots are scaled such that the diameter of each circle represents 6 cm on the original trace. The centers of the double circles indicate the actual locations of the seismoscope and the + symbol indicates the earthquake location given by Hollister et al. (1968).

Fig. 7. A comparison between the observed and predicted seismoscope records for the August 9, 1967 earthquake. See Fig. 6 for a description of the figure.

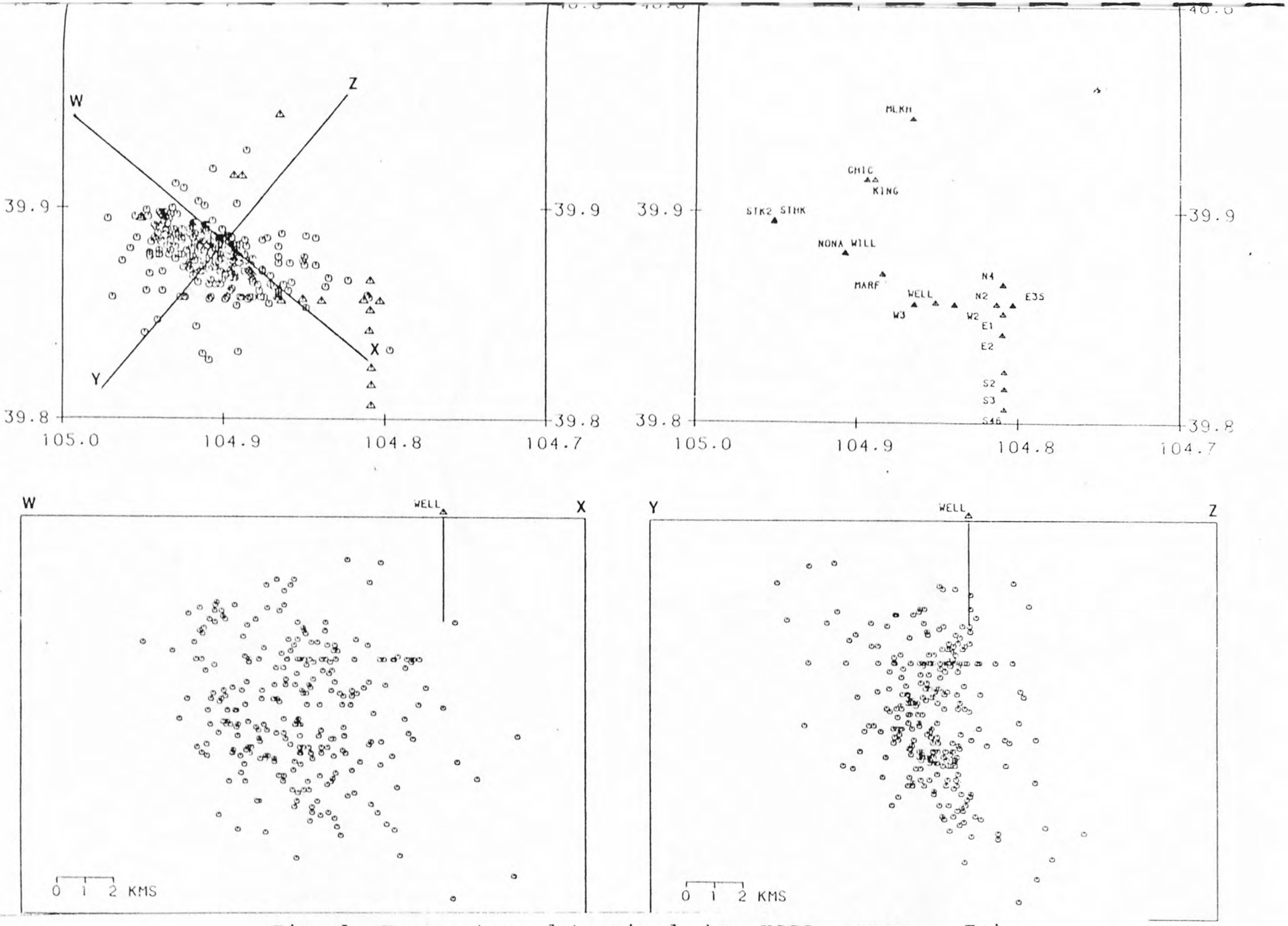


Fig. 1. Hypocenters determined by USGS array. Epicenters and two vertical depth profiles are shown. The seismograph stations are indicated by triangles, with their names given on the base map. The position of the well is indicated on the epicenter maps and on the vertical depth

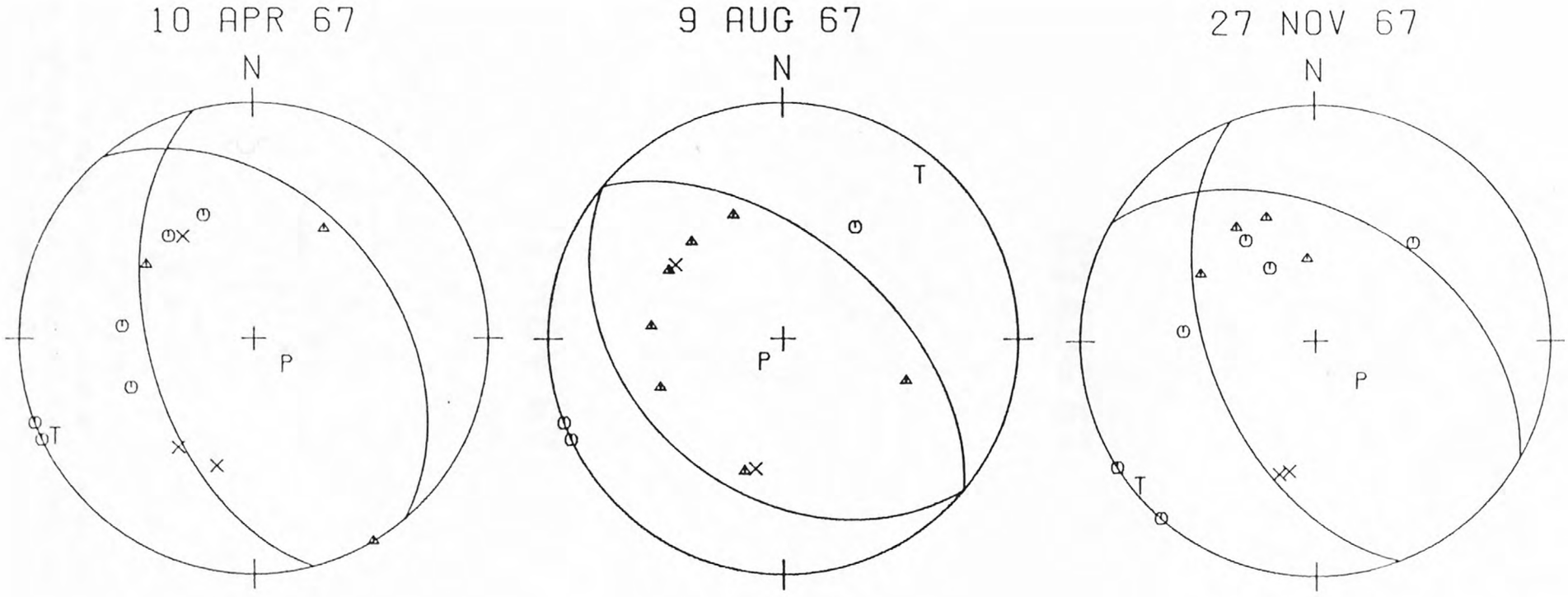


Fig. 2. Focal mechanisms of the April 10, 1967, August 9, 1967 and November 27, 1967 earthquakes. The nodal planes satisfy surface-wave spectral amplitude data as well as the P-wave first motion data. Circles represent compressions, triangles, dilatations, and X's, uncertain arrivals of low amplitude. T and P are the intersections of the tension and pressure axes, respectively, with the lower hemisphere. An equal area lower hemisphere projection is used.

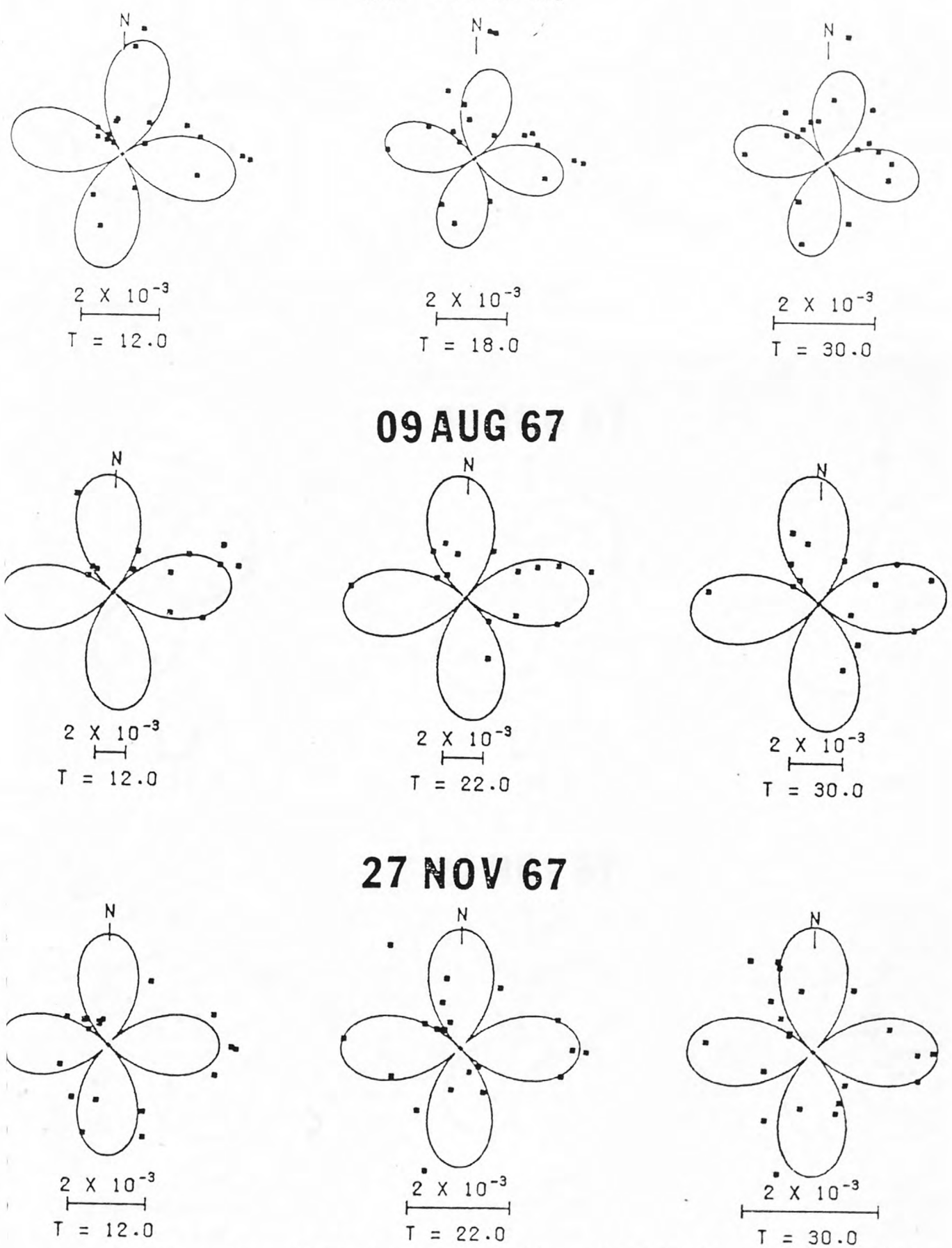


Fig. 3. Comparison between anelastic attenuation corrected observed and predicted Love-wave radiation patterns at selected periods, T, for the events studied. The scaling bars are spectral amplitudes in units cm-sec at a reference distance of $9^{\circ}$ from the source.

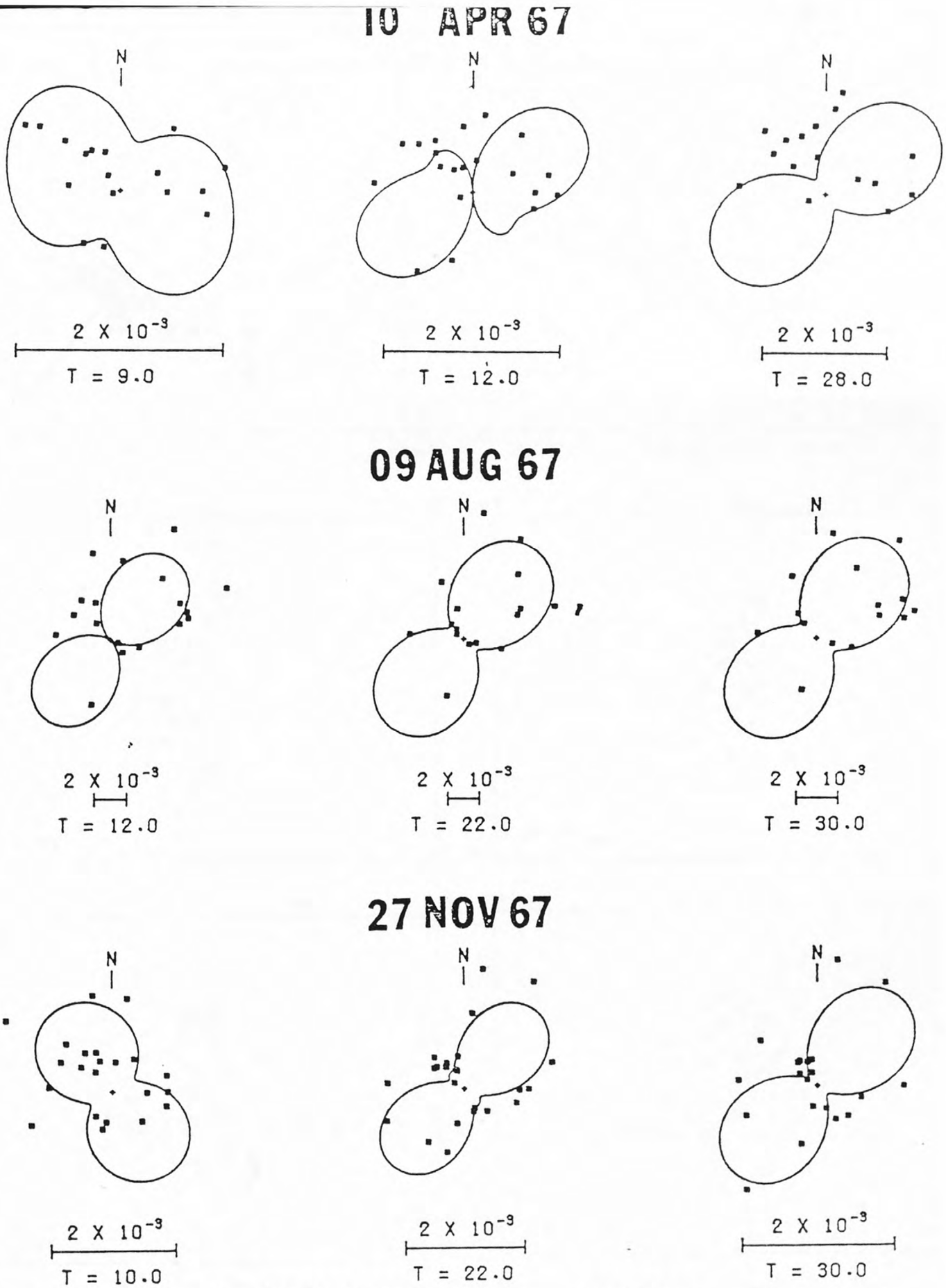


Fig. 4. Comparison between anelastic attenuation corrected observed and predicted Rayleigh-wave radiation patterns at selected periods for the events studied. The scaling bars are spectral amplitudes in cm-sec at a reference distance of $9^{o}$ from the source.

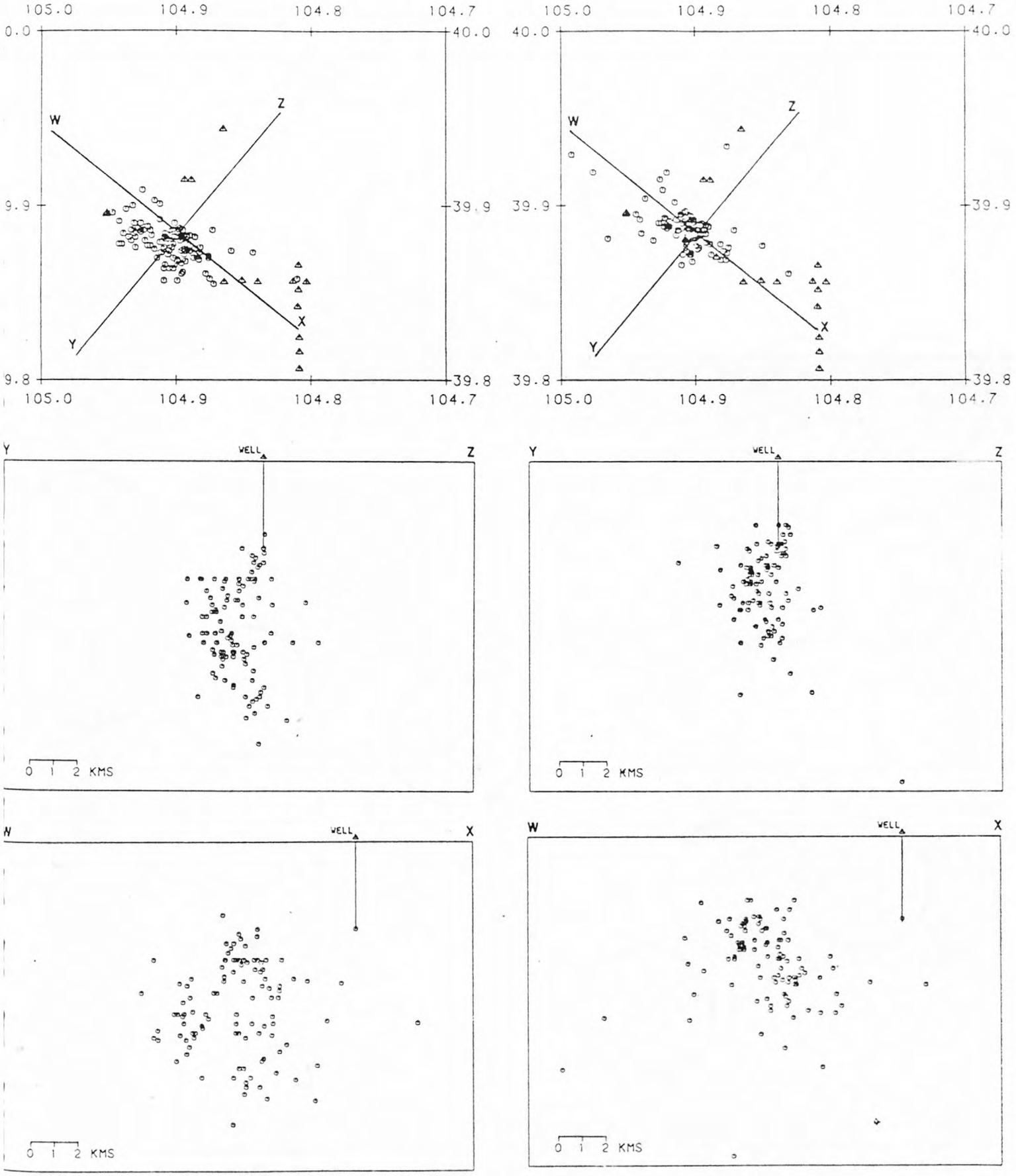


Fig. 5. The left column is the data set selected for joint hypocenter determination while the right column shows the relocated events. In each case the epicenters and two vertical depth profiles are shown. The well and seismographs stations, triangles, are indicated for reference. There is no vertical exaggeration.

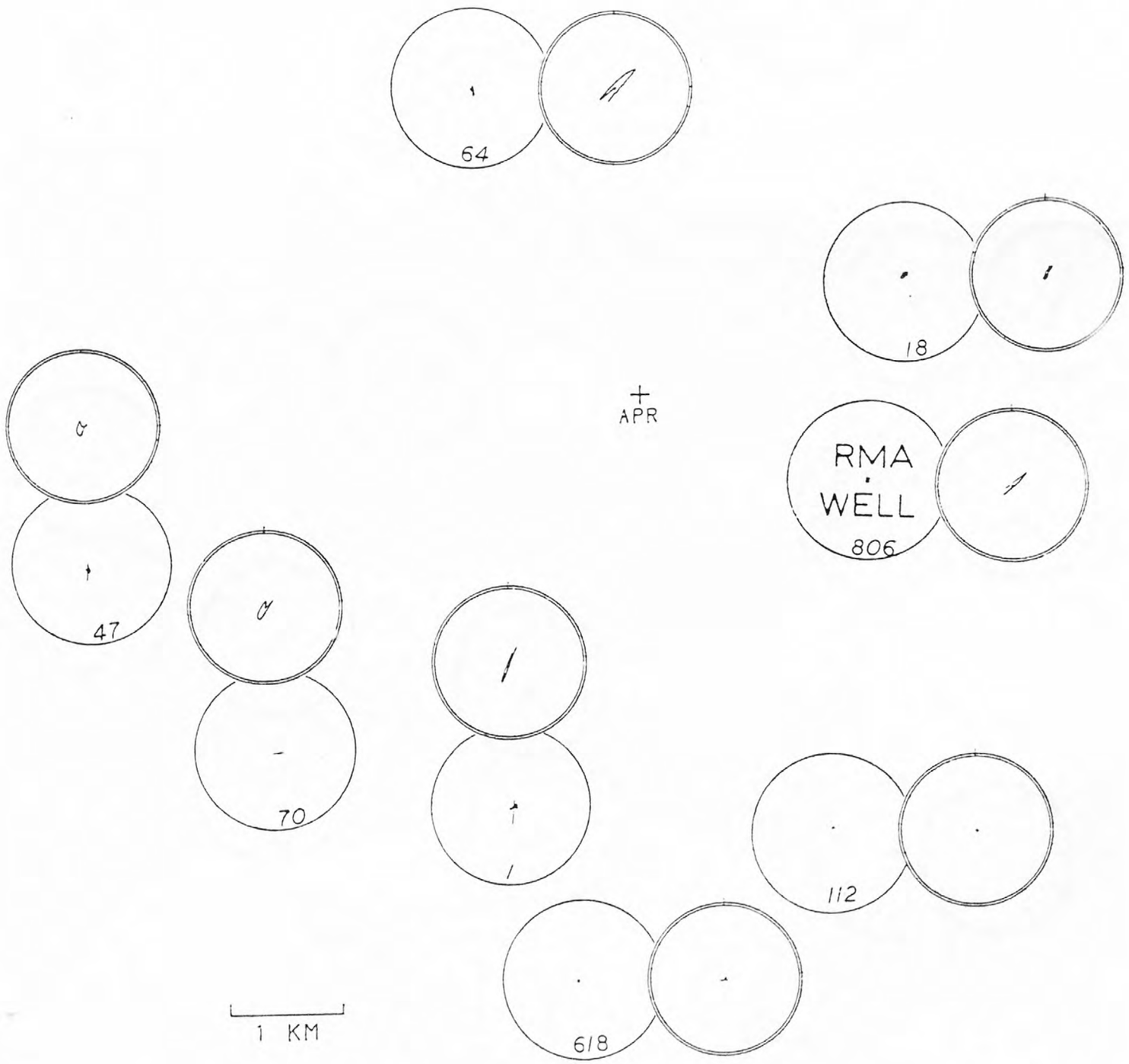


Fig. 6. A comparison between the observed and predicted seismoscope records for the April 10, 1967 earthquake. The numbered, singly circled plots are the observed data while the doubly encircled plots are the predicted data. All plots are scaled such that the diameter of each circle represents 6 cm on the original trace. The centers of the double circles indicate the actual locations of the seismoscope and the + symbol indicates the given earthquake location.

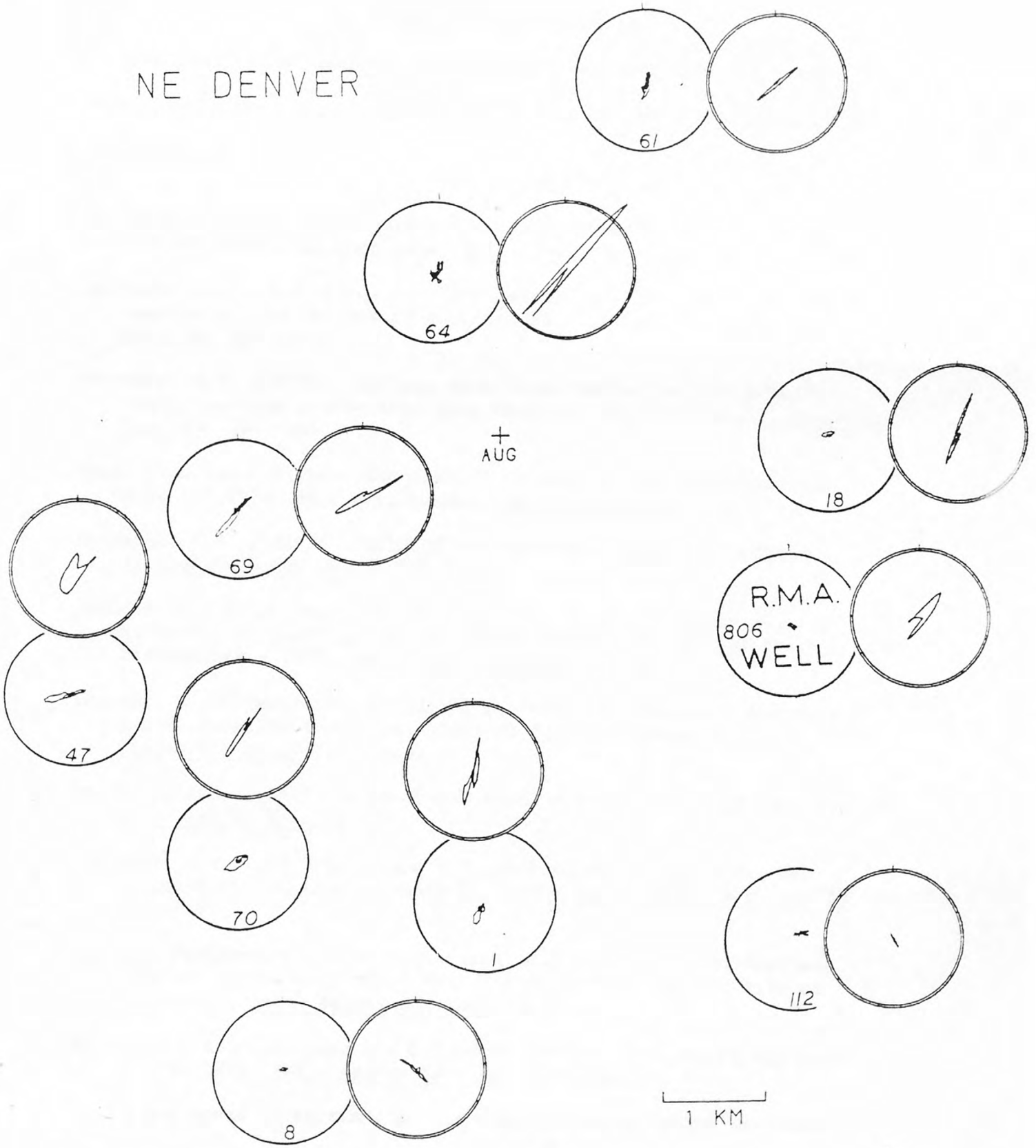


Fig. 7. A comparison between the observed and predicted seismoscope records for the August 9, 1967 earthquake. See Fig. 6 for a description of the figure.

## 3. Research Accomplishments

The past three years of effort under this contract have been very productive. This is evidenced in part by the following list of publications:


Herrmann, R.B. and J.A. Canas (1978). Focal mechanism studies in the New Madrid seismic zone, Bull. Seism. Soc. Am. 68, 1095-1102.

Herrmann, R.B., S.H. Cheng, and O.W. Nuttli (1978). Archaeseismology applied to the New Madrid earthquakes of 1811-1812, Bull. Seism. Soc. Am. 68, 1751-1759.

Herrmann, R.B. (1978). Surface wave focal mechanisms for Eastern North American earthquakes with tectonic implications, J. Geophys. Res. 84, 3543-3552.

Voss, J.A. and R.B. Herrmann (1980). A surface wave study of the June 16, 1978 Texas earthquakes, Earthquake Notes 51, 3-14.

Herrmann, R.B. (1979). FASTHYPO - A hypocenter location program, Earthquake Notes 50, 25-37.

Stauder, W., R. Herrmann, C. Nicholson, S. Singh, M. Woods, C. Kim, R. Perry, S. Morrissey and E. Haug, Central Mississippi Valley Earthquakes - 1978, Earthquake Notes 51, 22-24.

Stauder, W., R. Herrmann, S. Singh, D. Reidy, R. Perry, S. Morrissey and E. Haug, Central Mississippi Valley Earthquakes - 1979, Earthquake Notes (in press).

Herrmann, R.B. (1980). Q estimates using the coda of local earthquakes, Bull. Seism. Soc. Am. 70, 447-468.

Herrmann, R.B., J.W. Dewey, and S.K. Park (1980). The Dulce, New Mexico earthquakes of January 23, 1966, Bull. Seism. Soc. Am. 70, 2171-2183.

Eberhart-Phillips, D., R.M. Richardson, M.L. Sbar and R.B. Herrmann (1981). Analysis of the 4 February 1976 Chino Valley, Arizona earthquake, Bull. Seism. Soc. Am. (in press).

Herrmann, R.B., S.K. Park and C.Y. Wang (1981). The Denver earthquakes of 1967-1968, Bull. Seism. Soc. Am. (in press).


As mentioned in section 2a, the computer installation represents a quantum jump in the research being performed, both in quality and quantity. The computer system should meet the research needs for the next few years.

Future research directions include a study of the three dimensional seismicity patterns in the New Madrid Seismic Zone, a more detailed examination of faulting mechanics by performing composite focal mechanism studies and a study of the uses of the digital data arising from the network.